Structural and biochemical characterisation of the C-type lectin receptor DNGR-1 and its binding to F-actin

Pavel Hanč

University College London

and

Cancer Research UK London Research Institute

PhD Supervisor: Caetano Reis e Sousa, DPhil, FMedSci

A thesis submitted for the degree of

Doctor of Philosophy

University College London

September 2015

Declaration

I, Pavel Hanč, confirm that the work presented in this thesis is my own. Where information has been derived from other sources, I confirm that this has been indicated in the thesis.

Abstract

DNGR-1 is a C-type lectin receptor that has been implicated in the regulation of endocytic trafficking and cross-presentation of dead cell-associated antigens. Dendritic cells deficient in DNGR-1 are impaired in priming effector T-cell responses against cytopathic viruses and other dead cell-associated antigens. The ligand for DNGR-1 is the polymerized form of actin (F-actin) revealed in dead cells upon loss of membrane integrity.

In this study we set out to determine biophysical, biochemical, and structural properties of DNGR-1 and its interaction with F-actin.

First, we describe a conformational change that occurs in the neck region of the receptor in a pH- and ionic strength-dependent manner. Notably, the conformational change happens between conditions corresponding to the extracellular environment and the environment present in the vesicles of the endosomal pathway respectively, suggesting a possible role in the spatial regulation of the DNGR-1 function.

Second, in collaboration with Keichii Namba and Takashi Fujii (RIKEN Quantitative Biology Center, Osaka, Japan) we used electron cryomicroscopy to solve the structure of DNGR-1 bound to F-actin at 7.7 Å resolution. Interestingly, DNGR-1 binds into the groove between actin protofilaments, making contacts with three actin subunits that are helically arranged in the F-actin structure. We identify the residues directly involved in the interaction, confirm their contribution to the binding and demonstrate the importance of avidity of the multivalent interaction between DNGR-1 and F-actin. Additionally, in collaboration with David Sancho and Salvador Iborra (Centro Nacional de Investigaciones Cardiovasculares, Madrid, Spain) we formally demonstrate that ligand recognition is prerequisite for the biological function of DNGR-1 in dendritic cells.

Third, by using heterodimeric DNGR-1 proteins in which one half of the dimer is incapable of binding to ligand, we demonstrate that DNGR-1 can bind with both ligand-binding domains to a single actin filament, suggesting an exceptional flexibility of the neck region, and demonstrating an absence of rigid dimerization interface between the ligand-binding domains.

In summary, we provide a comprehensive description of the structural and biophysical properties of DNGR-1, offering novel insights into its function and shedding light into innate immune mechanisms involved in recognition of cell death.

Acknowledgement

First and foremost, I would like to thank my supervisor, Caetano Reis e Sousa, for giving me the chance to carry out this work in his lab, for giving me his guidance when needed and at the same time allowing me to develop my independence and learn from my mistakes, for showing me how to be a better scientist in myriad ways both small and large, and for always being supportive and encouraging, even when the data were not.

Many thanks go out to my thesis committee, Facundo Batista and Erik Sahai, for all the helpful advice I've received from them over the years and their supportive attitude during our meetings.

None of my work would have been possible without our numerous collaborators. Namely, I'd like to thank Keiichi Namba and Takashi Fujii for lending their Cryo-EM expertise, David Sancho and Salvador Iborra for helpful discussions and indispensable assistance with antigen-presentation assays, Steve Martin for his help with circular dichroism measurements, Thomas Surrey and Christian Duellberg for their assistance with TIRF-based experiments, Svend Kjær for numerous size exclusion chromatography purifications as well as many helpful discussions about anything "protein-related," and last but not least Michael Way for all his advice regarding the properties and behaviour of actin.

I'm truly grateful for the great time I've had in the Immunobiology lab during the last four years, for the friendly, helpful and supportive, yet stimulating and highly productive environment, and for all the things that I've had a chance to learn. In one way or another I'm indebted to all members of the lab, past and present, but in particular to Oliver Schultz for showing me the ropes when I joined the lab and for many helpful discussions over the years, to the other members of the "DNGR-1 team," Jatta Huotari and formerly Susan Ahrens for all their help, to Santiago Zelenay for insightful comments and plentiful DNGR-1 (and otherwise) centred lunch-time conversations, to Janneke, Kat, Oliver, Naren and Jan for making Friday evenings worth having, and to everyone else for making the lab a place where one can not only work but also have fun!

Outside of the lab, I'd like to thank my family and friends for their continual support during what was an exciting, but not always an easy time. And finally, special

thanks to Kristyna for having endless patience with me, for listening to my moaning and complaining when things went wrong without ever telling me to be quiet, for always being there, and last but not least, for proof-reading this thesis and finding all the little details that I have no eye for.

Table of Contents

Table of figures

List of tables

Abbreviations

ABP	actin-binding protein
AIM2	absent in melanoma 2
AMP	antimicrobial peptide
APC	antigen-presenting cell
β-ME	beta-mercaptoethanol
BIR	baculovirus inhibitor of apoptosis protein repeat
BLI	biolayer interferometry
BCR	B cell receptor
CARD	caspase activation and recruitment domain
CD	cluster of differentiation
cDC	conventional dendritic cell
CDP	common DC precursor
CLIP	Class-II-associated invariant chain peptide
CLR	C-type lectin receptor
CRD	carbohydrate recognition domain
CTL	cytotoxic T-lymphocyte
CTLD	C-type lectin-like domain
C2TA	MHC class 2 transcription activator
DAMP	damage-associated molecular pattern
DAPI	4',6-Diamidino-2-Phenylindole
DC	dendritic cell
DNGR-1	DC, NK lectin group receptor 1
DTT	dithiothreitol
ECD	extracellular domain
EMBP	eosinophil major basic protein
ER	endoplasmic reticulum
FACS	fluorescence-activated cell sorting
FCS	foetal calf serum
GFP	green fluorescent protein
GPCR	G-protein coupled receptor
HET-E	incompatibility locus protein from Podospora anserina

HMGB-1	high-mobility group protein B-1
HSP	heat shock protein
IL	interleukin
IFI16	interferon-inducible protein 16
IFN	interferon
ILC	innate lymphoid cell
ITAM	immunoreceptor tyrosine-based activatory motif
ITIM	immunoreceptor tyrosine-based inhibitory motif
LDL	low-density lipoprotein
LOX-1	LDL receptor-1
LPS	lipopolysaccharide
MALS	multi-angle light scattering
MAVS	Mitochondrial antiviral-signalling protein
MBP	mannose binding protein
MDP	macrophage, dendritic cell progenitor
MFI	mean fluorescence intensity
MHC	major histocompatibility complex
MyD88	myeloid differentiation primary response gene 88
NACHT	NAIP, C2TA, HET-E, TP1
NAIP	neuronal apoptosis inhibitor protein
NFAT	nuclear factor of activated T-cells
NF-κB	nuclear factor kappa-light-chain-enhancer of activated B cells
NLR	NOD-like receptor
NOD	nucleotide-binding oligomerization domain
PAMP	pathogen-associated molecular pattern
PCR	polymerase chain reaction
pDC	plasmacytoid dendritic cell
PH	pleckstrin homology
PLC	Phospholipase C
PNGase F	peptide-N-Glycosidase F
PRR	pattern recognition receptor
PSP	pulmonary surfactant protein
RAG	recombination-activating gene
RIPK	receptor-interacting protein kinase

RIG-I	retinoic acid-inducible gene 1
RLR	RIG-I-like receptor
RNS	reactive nitrogen species
ROS	reactive oxygen species
SH2	Src-homology 2
SHP	SH2 domain-containing phosphatase
SHIP	SH2 domain-containing inositol 5'-phosphatase
Syk	spleen tyrosine kinase
TAP	transporter associated with antigen processing
TCR	T cell receptor
TGF	transforming growth factor
T_H	T-helper cell
TIR	Toll/interleukin-1 receptor domain
TIRAP	Toll/interleukin-1 receptor domain-containing adapter protein
TLR	Toll-like receptor
TP1	telomerase-associated protein
TRAM	TRM2 and miaB domain
TRIF	TIR-domain-containing adapter-inducing interferon-β
YFP	yellow fluorescent protein

Chapter 1. Introduction

1.1 Brief overview of the conceptual development of immunology

Immune system is one of the basic mechanisms involved in the maintenance of homeostasis, and although some of its underlying features had been known for thousands of years, the beginning of the field of immunology as a science can be dated to the late 18th and early 19th century, and the experiments of Edward Jenner (Riedel, 2005). Like others before him, Jenner had noted that once recovered, cowpox patients appeared resistant to smallpox. Unlike his predecessors, however, Jenner set out to test the concept experimentally. By means of infecting a young boy with cowpox, followed by a challenge with smallpox, Jenner at the same time introduced the concept of vaccination and demonstrated the protection against smallpox infection, which eventually led to the eradication of the disease in the 20th century (Riedel, 2005).

Jenner's experiments, however, rested only on empirical findings and lacked all understanding of mechanisms underlying the observed phenomena. It was not until late 19th century that Robert Koch demonstrated the causal link between pathogenic microorganisms and human disease (Blevins and Bronze, 2010) and Elie Metchnikoff and Paul Ehrlich showed the involvement of phagocytes and antibodies, respectively, in their clearance (Gordon, 2008, Silverstein, 1999).

The principal milestone in the development of the field of immunology as we understand it today only came in the second half of the 20th century with the formulation and development of the "self" and "non-self" hypothesis by MacFarlane Burnet and Peter Medawar, whereby they postulated that the immune system differentiates between endogenous and exogenous molecules, initiating a response against the latter, while maintaining tolerance to the former (Billingham et al., 1953, Burnet and Fenner, 1949).

The last great conceptual leap in our understanding of the immune system came with the infectious non-self model originally proposed by Charles Janeway Jr. (Janeway, 1989). Building on the concept of antigen presenting cell (APC) introduced by Lafferty and Cunningham (Lafferty and Cunningham, 1975), Janeway suggested that APCs are able to recognize characteristic molecular

patterns conserved between pathogens (PAMPs, pathogen-associated molecular patterns), thereby sensing infection, and in turn activate the adaptive immune system (Janeway, 1989). Abundant evidence in support of this model has accumulated over the last decades; however, certain phenomena such as transplant rejection, anti-tumour immunity or autoimmunity where no overt signs of infection could be detected still posed a conceptual problem. In attempt to explain these, danger theory was suggested by Polly Matzinger, according to which APCs could respond to specific endogenous signals released by stressed, damaged or dead cells (later termed DAMPs, damage-associated molecular patterns) (Matzinger, 1994).

While controversies have arisen over the usefulness of the danger model, as well as over whether there can be a single “unifying theory” of how the immune system operates (Vance, 2000), clearly our understanding of the immune system has expanded explosively over the last decades, and the theories and models suggested previously have served us well thus far.

1.2 Innate and adaptive immune system and their roles in homeostasis maintenance

Historically, the immune system has been divided into two major parts – the innate and the adaptive. The innate immune system is evolutionarily older, appears to be present in some form in all animal and plant phyla, and its cells express only a limited set of germ line-encoded receptors specific for a limited set of molecules (Iwasaki and Medzhitov, 2015). The adaptive immune system, on the other hand, is generally considered to be present only in vertebrates and is characterised by the ability to somatically generate receptors of broad specificity, and by immunological memory (Hoffmann et al., 1999). It is getting increasingly clear, however, that albeit useful, this division is somewhat arbitrary (Borghesi and Milcarek, 2007), as certain subsets of B- and T-lymphocytes, the prototypical cells of the adaptive immune system, share multiple properties with innate cells (Bendelac et al., 2001), and certain innate cells show traits of the adaptive responses, such as memory-like activity reported in natural killer (NK) cells (O'Leary et al., 2006). Furthermore, certain features of “adaptivity” have been observed in organisms that are generally

considered as having only the innate immune system, such as earthworms (Cooper, 1968), freshwater snails (Zhang et al., 2004) or sea urchins (Rast et al., 2006), or as having no immune system at all, such as bacteria, and their newly-discovered ability to mount specific response to bacteriophages using the CRISPR Cas9 system (Barrangou and Marraffini, 2014). Regardless of the exact definition, it is, however, still useful to think of the two systems in terms of their role and function in the maintenance of homeostasis.

1.2.1 Innate immune system

In the classical model, the cells and effector molecules of the innate immune system serve as the first line of defence against pathogens. Their responses are rapid to instantaneous, their ability to differentiate between self and non-self (or modified/missing self in the case of NK cells) is near absolute, and they can activate and instruct the adaptive immune system. On the other hand, barring certain exceptions, the innate immune system lacks the ability to generate diversity of receptor specificities, and immunological memory (Janeway and Medzhitov, 2002).

Low energy-cost and low threat-to-self potential combined with their fast mode of action make it possible for certain molecules of the first-line defences to be expressed and active constitutively (Iwasaki and Medzhitov, 2015). These include the antimicrobial peptides (AMPs) produced by many diverse tissues and cell types (Brogden, 2005), natural antibodies produced by the B1 cells (Schwartz-Albiez et al., 2009), or the serum complement system (Carroll, 2004), all of which are designed to clear the potential pathogen at minimal fitness cost to the host. If these turn out to be insufficient, cellular defences including cells of the polymorphonuclear and mononuclear phagocyte system as well as dendritic cells (DCs) placed at strategic sites throughout the body can be activated by microbial PAMPs, resulting in the phagocytosis of the invading pathogens as well as rapid production of cytokines and chemokines to activate and recruit other immune cells. Additionally, DCs migrate to lymphatic tissues such as lymph nodes and spleen and present microbial antigens to the adaptive immune system (Iwasaki and Medzhitov, 2015). Finally, at increased fitness cost, cells of the polymorphonuclear

system including neutrophils, basophils and eosinophils can be activated. Activated neutrophils in particular are extremely potent in clearance of extracellular pathogens, but at the same time their activation can result in significant collateral damage to the surrounding tissues due to release of reactive oxygen and nitrogen species (ROS and RNS) (Fialkow et al., 2007, Iwasaki and Medzhitov, 2015).

In addition to the "classical" myeloid cells of the innate immune system mentioned above, innate lymphoid cells (ILCs) form a relatively newly recognised heterogeneous group of cells of the lymphoid lineage with diverse functions ranging from direct lysis of virus-infected or transformed cells to regulation of the development of lymphoid tissues to orchestrating the interplay between the immune system and commensal microbiota. It is becoming increasingly clear that, although rare, these cells play indispensable roles in the regulation of the immune system, and the field of ILC research is rapidly evolving (Walker et al., 2013).

In sum, the function of the innate immune system is to hold off potential pathogens and where needed to activate and instruct the adaptive immune system (Iwasaki and Medzhitov, 2015). Based on the type of pathogen recognised and the cell initiating the response, different types of adaptive responses can be activated – cytotoxic T-lymphocytes (CTLs) and T helper type-1 (T_H1) lymphocytes for elimination of intracellular pathogens, T_H17 cells for elimination of extracellular bacteria and fungi, or T_H2 cells for immunity against macroscopic parasites and venoms, underscoring the role of the innate immune system as the master controller of the immune response (Iwasaki and Medzhitov, 2015).

1.2.2 Adaptive immune system

In stark contrast to the innate immune system, the cells of the adaptive immune system are able to generate a diverse repertoire of antigen-specific receptors as well as immunological memory, allowing enhanced response towards the same antigen on the next encounter. The adaptive immune responses, however, take days to develop, for most part they need to be activated by the innate immune system, and the broad range of receptor-specificities brings about the risk of self-reactive clones (Boehm, 2011).

Traditionally T- and B-lymphocytes are considered the prototypical cells of the adaptive immune system, and in both cases they somatically generate diversity of their receptor-specificities by recombination-activating gene (RAG)-mediated rearrangement and recombination of genes coding for their T-cell receptors (TCRs) and B-cell receptors (BCRs) respectively (Fugmann et al., 2000, Tonegawa, 1983). This process results in generation of an immensely diverse anticipatory repertoire with, for example, up to 10^{15} possible canonical αβ TCR specificities predicted (Davis and Bjorkman, 1988). Of those, however, only a fraction gets expressed and, at least in the case of human, the lower limit has been estimated at 25 x 10^6 distinct TCRs in blood, although this might be an underestimate (Arstila et al., 1999, Nikolich-Zugich et al., 2004). Such a degree of diversity brings about a significant risk of self-reactivity, and consequently sophisticated mechanisms for elimination or functional inactivation of self-reactive clones have evolved, collectively termed central and peripheral tolerance (Nemazee et al., 2000, Piccirillo and Shevach, 2004, Starr et al., 2003).

In addition to the potential for autoreactivity, the high number of potential TCR and BCR specificities also means that of the several billion T- or B-cells present in the body, only several hundred are specific for any given antigen (Masopust and Schenkel, 2013). In order to mount an effective immune response, these are consequently the cells that need to be activated and rapidly expanded, while activation of all the other, non-cognate, cells is largely undesirable. This explains why it takes adaptive immune system significant amount of time to mount an effective response, but at the same time it brings to light an obvious conundrum of how the few antigen-specific cells are to find their cognate antigen in time (Masopust and Schenkel, 2013). As alluded to in the previous paragraphs, the innate immune system provides the solution to this problem in the form of the antigen presenting cells (APCs), the most prominent of which are the DCs. While lymphocytes circulate through lymphatic vessels and blood, APCs are stationed at strategic places throughout the body, and upon recognition of pathogens, they rapidly migrate to the nearest secondary lymphatic tissue – lymph nodes or spleen, where they can present the antigens to the lymphocytes that steadily circulate through these organs (Guermonprez et al., 2002, Masopust and Schenkel, 2013).

After activation, T-cells undergo rapid proliferation, and based on their subtype, $CD4^+$ T-cells become effector T helper cells (T_H), specialised in production of

cytokines and helping other immune cells, while $CD8^+$ T-cells become activated cytotoxic T-cells (CTLs) specialised in direct lysis of infected cells. After resolution of the infection and removal of the antigen, a “clonal contraction” phase ensues, when most of the T-cells undergo apoptosis, while a subset survives to become long-lasting memory T-cells. These cells exhibit remarkable heterogeneity with respect to their phenotype, localization, and functional potential, but they share the ability to rapidly respond to restimulation (Pulendran and Ahmed, 2006, Masopust and Schenkel, 2013).

Unlike T-cells, B-cells can form germinal centres upon activation, and in addition to proliferation they undergo further rounds of genetic rearrangements, namely somatic hypermutation and class switch processes aimed at increasing the affinity of their BCRs for the presented antigens, and production of different classes of antibodies (Wagner and Neuberger, 1996). Germinal centre-selected B-cells then become short-lived antibody-producing cells, some of which have the potential to become long-lived plasma cells and constitutively produce lower amounts of antibodies for prolonged periods of time, or become long-lived memory B-cells, which, like their T-cell counterparts, are ready to be reactivated by next exposure to the same antigen (Radbruch et al., 2006).

In sum, the adaptive immune system in the form briefly outlined above is an evolutionary novelty, present only in jawed vertebrates, and has evolved as an addition to the innate immune system. Given its mechanism of receptor specificity generation combined with its highly protective, but at the same time highly destructive potential, its activation and function needs to be tightly regulated. Taking into account both of the above, it is not surprising that the adaptive immune system is largely under control of the evolutionarily older, less error-prone innate immune system, and defects in any of the many regulatory mechanisms often result in immunopathologies including autoimmune diseases, allergies or immunodeficiencies (Milner and Holland, 2013, Waldner, 2009).

1.3 Dendritic cells

Dendritic cells were originally described by Steinman and Cohn in the spleen of mice based on their distinct morphology (Steinman and Cohn, 1973, Steinman and

Cohn, 1974). In the following decades, DCs were shown to be cells of the myeloid lineage, crucial for the initiation and regulation of adaptive immune responses, in particular due to their superior ability to present antigens and activate T-lymphocytes (Steinman and Idoyaga, 2010).

The basis of the current, broadly accepted definition of DCs is their high expression level of integrin CD11c and major histocompatibility complex (MHC) class II molecules (Metlay et al., 1990, Nussenzweig et al., 1981) and their ability to prime T-cells (Heath and Carbone, 2009). This definition, however, is ambiguous, as other cell-types have been shown to express CD11c and MHC II, and even prime T-cell responses, making the definition of a DC context-dependent and open to multiple interpretations (Hume, 2008, Schraml and Reis e Sousa, 2015). This disparity has even led to suggestions that “DCs as a separate cell type with unique capacity or destiny do not actually exist” and that “they are simply a heterogeneous subset of mononuclear phagocytes” (Hume, 2008).

Our current understanding of DC development is largely based on the mouse model, where a common precursor of both macrophage and DC lineages (MDP) has been defined (Fogg et al., 2006). MDP can further differentiate into a common DC precursor (CDP), which in turn can give rise to all DC subsets including plasmacytoid (pDC) and conventional (cDC) dendritic cells (Onai et al., 2007). Given this lineage specificity, it has been proposed that ontogeny-based definition of DCs rather than one based on phenotypical or functional properties should be used in order to resolve the ambiguity of DC definition (Guilliams et al., 2014, Schraml and Reis e Sousa, 2015). In this view, any cell derived from the CDP should be considered a DC, and conversely, no cell that derives from a different precursor should be called one, regardless of its functional or phenotypical properties (Guilliams et al., 2014).

1.3.1 Function of dendritic cells

DCs act as immunological sentinels, located throughout the body in an immature state (Stockwin et al., 2000). Upon recognition of PAMPs and certain DAMPs, DCs get activated and migrate from peripheral tissue where they encountered the pathogen into the secondary lymphoid tissues where they can in turn activate

T-cells. Upregulation of co-stimulatory molecules (CD80, CD86) together with MHC molecules, as well as production of cytokines are the characteristic hallmarks of an activated DC (Banchereau and Steinman, 1998).

Exposure of DCs to PAMPs results in the production of many cytokines and chemokines, which serve to activate other innate immune cells including NK cells and neutrophils as well as to attract them to the sites of infection (Steinman and Hemmi, 2006). The main function of DCs, however, is presentation of antigens to T-lymphocytes, and this together with delivering the co-stimulatory signals results in activation of cognate T-cells and activation of the effector arm of the immune system (Hubo et al., 2013). In particular, DCs can present exogenous antigens on MHC class II molecules to $CD4^+$ T-helper lymphocytes and, like any other cell, endogenous antigens on MHC class I molecules to $CD8^+$ cytotoxic T lymphocytes (Blum et al., 2013, Steinman and Hemmi, 2006).

The classical mode of presentation on MHC-I molecules involves predominantly 26S proteasome-derived peptides of cytoplasmic proteins, which are translocated into the endoplasmic reticulum (ER) by the transporter associated with antigen processing (TAP) complex. Once inside the ER, the peptides can be loaded onto empty MHC-I molecules stabilised in a complex with tapasin, calreticulin and ERp57. Peptide binding then results in disassembly of the complex and export of the peptide-bound MHC-I to the cell membrane (Blum et al., 2013).

MHC-II molecules are also assembled within the ER, together with the invariant chain. Invariant chain structurally stabilises the MHC-II molecule during the folding process, and prevents binding of ER-resident peptides. Functional maturation of MHC-II then takes place in an endosomal compartment, where the invariant chain is progressively degraded, leaving only a short peptide termed CLIP (class-II-associated invariant chain peptide) bound within the peptide-binding pocket. Finally, release of CLIP and binding of peptides derived from endocytosed proteins is mediated by MHC-related molecules DM and DO within late endosomes (Blum et al., 2013).

In addition to the classical mode of MHC-I antigen presentation, exogenous antigens can also be presented on MHC-I in a process known as cross-presentation (Joffre et al., 2012). This pathway ensures that peptides derived from sources like viruses that do not infect DCs or from tumour cells can still be presented to cytotoxic T-lymphocytes (Zelenay and Reis e Sousa, 2013). In

principle the process of cross-presentation can be achieved in two ways – by endosome-to-cytosol translocation of endocytosed material followed by cytoplasmic degradation and loading of the peptides onto MHC-I in the classical pathway (Ackerman et al., 2006), or by means of direct loading of endocytosed material-derived peptides onto recycling MHC-I within the endocytic pathway (Shen et al., 2004). Of the two, the former appears to be more important (Rock and Shen, 2005) and a molecular mechanism explaining the process of cytosol release through the translocon Sec61 has recently been reported (Zehner et al., 2015).
Finally, as a counterpart to presentation of exogenous antigens on MHC-I, cytoplasmic and nuclear antigens can be presented on MHC-II through the process of autophagy, a mechanism useful for immunity against intracellular pathogens like viruses or certain bacteria (Crotzer and Blum, 2009).

1.3.2 DC subsets and their roles within immune system

DCs comprise of two major subsets – conventional DCs (cDCs) and plasmacytoid DCs (pDCs). pDCs significantly differ from the cDCs in that they express low levels of MHC-II and co-stimulatory molecules, and only a narrow range of pattern recognition receptors (PRRs). The characteristic PRRs include TLR 7 and 9, which allow pDCs to recognize foreign nucleic acids, to which they respond by strong production of type I interferons (IFNs). As such, pDCs are involved in anti-viral immunity (Reizis et al., 2011).
cDCs can broadly be divided into lymphoid tissue-resident and migratory DCs. These can then be further subdivided based on their expression of integrin CD11b into $CD11b^+$ and $CD11b^-$ DCs (Merad et al., 2013). $CD11b^+$ DCs form a heterogeneous group of cells dependent on the transcription factor IRF4 in both lymphoid and non-lymphoid tissues (Suzuki et al., 2004). Lack of a specific model for $CD11b^+$ DC depletion has made it difficult to assess the precise contribution of these cells (Merad et al., 2013), however, their superior expression of genes involved in MHC-II presentation suggests their involvement largely in activation of $CD4^+$ T-helper cells (Dudziak et al., 2007). Recently the $CD11b^+$ DCs were also shown to play an important role in T follicular helper (Tfh) cell induction, resulting in generation of humoural immune responses (Shin et al., 2015).

The CD11b$^-$ group of DCs is often referred to as "CD8α$^+$-like" DCs and is characteristic by its CD8α expression in lymphoid organs, and CD103 expression in the case of the DCs in the tissues (Merad et al., 2013). In both cases, the cells share their dependence on IRF8 and Batf family transcription factors, and the ability to cross-present exogenous antigens to cytotoxic T-cells (Miller et al., 2012). In addition, CD8α$^+$-like DCs show increased potential to activate cytotoxic T-cells regardless of their ability to cross-present, mainly due to higher expression of genes related to MHC-I presentation (Dudziak et al., 2007) and production of IL-12 (Hochrein et al., 2001) and IL-15 (Mattei et al., 2001), two cytokines involved in differentiation of CTLs. CD8α$^+$-like DCs express high levels of DNGR-1 in mouse (Caminschi et al., 2008, Sancho et al., 2008), and this pattern of expression appears to be shared between mouse and human where DNGR-1 identifies DC subset equivalent to murine CD8α$^+$ DCs (Poulin et al., 2010). The expression of XCR1 marker is also restricted to the CD8α$^+$-like family of DCs across species, and consequently, these cells are now often called XCR1$^+$ DCs (Vu Manh et al., 2015).

1.4 PAMP and DAMP recognition

As postulated by Janeway in 1989, in order for an immune response to be initiated, innate immune system needs to detect presence of pathogens (Janeway, 1989). Specific receptors aimed at recognising PAMPs, broadly termed pattern recognition receptors (PRRs) are consequently expressed by a diverse range of cells of both innate and adaptive immune system as well as epithelial and other cell types. PRRs allow these cells to screen their environment for the presence of pathogens, and ligation of different classes of PRRs expressed by different cell types can gives the immune system detailed information about what kind of pathogen it faces (Iwasaki and Medzhitov, 2015).

In addition to pathogen recognition by PRRs, immune system can also sense damage. When cells die by necrosis, they lose their membrane integrity, and as a consequence, proteins that are normally sequestered in the cytoplasm become exposed to the extracellular milieu (Zelenay and Reis e Sousa, 2013). Similar situation can occur if cells undergo apoptosis in numbers exceeding the capacity of scavenger cells to take up the apoptotic cell corpses. If not phagocytosed in a

timely fashion, apoptotic cells undergo secondary necrosis, which also results in the release of their cytosol components into the extracellular milieu (Silva, 2010). Thus expression of DAMP receptors on immune cells enables the immune system to sense the presence of damaged cells or excessive cell death. Interestingly though, while PAMP recognition almost universally results in activation of the PRR-expressing cell, and is often on its own sufficient for induction of inflammatory responses, DAMP recognition is significantly less potent and often results in regulation of other cellular functions, such as antigen handling by APCs (Zelenay and Reis e Sousa, 2013).

1.4.1 PRRs and PAMP recognition

Both PRR and PAMP are somewhat loosely defined terms. Any conserved molecule of pathogen origin that can be directly recognised by the innate immune system is usually referred to as a PAMP, and at the same time any receptor that recognizes a PAMP is considered a PRR. Regardless of the above, however, PAMPs generally are conserved molecules, often shared between multiple pathogenic agents, but absent from host cells (Akira et al., 2006). Notable exception from this rule are the nucleic acids, which are shared between the pathogen and the host, and their recognition as PAMPs is compartment-specific – for example DNA is recognised as a PAMP in the cytoplasm, but not in the nucleus (Barber, 2011). As a rule, PAMPs in their physiological role are of vital importance for the pathogen and its ability to infect the host, and their loss or modification usually results in a significant decrease in virulence or viability, or is impossible altogether. As such, escape strategies, often seen in the context of adaptive immune responses are not common, and PAMP recognition by PRRs provides an unambiguous way of detecting presence of pathogens (Akira et al., 2006).

PRRs constitute several major groups of proteins, most prominently the transmembrane Toll-like receptors (TLRs) and C-type lectin receptors (CLRs), and cytosolic NOD-like receptors (NLRs) and RIG-I-like receptors (RLRs). The expression of many of these genes is not restricted to the innate immune system, and some are expressed universally by most, if not all cell types (Takeuchi and Akira, 2010).

TLRs are probably the best-known group of PRRs (O'Neill et al., 2013). The founding member of the family, Toll, was originally described in *Drosophila melanogaster* as a gene involved in embryogenesis, and only later its importance for the fly's immune response was also recognised (Lemaitre et al., 1996). In a triumph of comparative immunology, shortly thereafter its mammalian homologue, later classified as Toll-like receptor 4 (TLR-4), was cloned and shown to induce activation of the immune system in response to bacterial lipopolysaccharide (LPS) (Medzhitov et al., 1997, Poltorak et al., 1998). Since then, thirteen members of the TLR family have been described (TLR-1 – 13) and shown to reside on the plasma membrane (TLR-1, 2, 4, 5, 6, 11, 12) or in the endosomes (TLR-3, 7, 8, 9, 10 and 13). Broad spectrum of PAMP ligands for various TLRs have been identified, ranging from bacterial cell-wall constituents, to viral nucleic acids, to bacterial ribosomal RNA (O'Neill et al., 2013). The signalling pathways induced by various members of the TLR family are largely shared, and most TLRs signal either through MyD88 or TIRAP adapters towards NF-κB activation, resulting in production of proinflammatory cytokines, or through TRIF or TRAM adapters towards IRF3 activation and resultant production of type I IFNs. Uniquely among TLRs, TLR4 appears to utilise both of these pathways (Akira and Takeda, 2004).

CLRs form the second large group of trans-membrane PRRs, and they will be discussed in greater detail in the following sections.

Of all the main groups of PRRs, the cytosolic RLR family is the smallest with only three members – RIG-I, MDA5 and LGP-2 – and also exhibits the narrowest range of ligand-specificities. Both RIG-I and MDA5 have been shown to primarily recognise viral RNAs, while LGP-2 appears to be an accessory protein modulating signalling by the other two, although its exact function is not yet entirely clear (Goubau et al., 2013). Ligation of both RIG-I and MDA-5 results in their oligomerization-induced activation and binding to mitochondrial adapter MAVS, in turn activating the NF-κB as well as IRF3 and IRF7 transcription factors (Goubau et al., 2013).

Finally, NLRs constitute a diverse family of cytoplasmic proteins, which are often considered PRRs, even though many of them show no direct binding to any known PAMPs (Franchi et al., 2006). Twenty three NLR genes have so far identified in human and thirty four in mouse (Rathinam et al., 2012). Based on the type of their N-terminal domain, four groups are currently recognised – NLRA (acid domain-

containing), NLRB (BIR domain-containing), NLRC (CARD domain-containing) and NLRP (pyrin domain-containing), with a single uncategorised NLRX protein with no homology to the N-terminal domains of all the other NLRs (Ting et al., 2008). NLRs can be activated by diverse stimuli ranging from cytosolic dsDNA (through recognition by AIM2 and IFI16) (Hornung and Latz, 2010) to bacterial flagellin (through recognition by NAIP 5 and 6) (Kofoed and Vance, 2011) to multitude of disparate entities including extracellular ATP, pore-forming toxins or various crystals (through incompletely understood NLRP3-mediated mechanism) (Latz, 2010). Upon activation, the NLRs oligomerize through their NACHT domains, forming large multi-protein complexes termed inflammasomes. The main role of inflammasomes is activation of caspase-1 from its inactive precursor pro-caspase-1. Pro-caspase-1 molecules are recruited to the inflammasome via direct CARD-CARD interaction or through interaction with additional adapter proteins, resulting in their proximity-induced autoproteolytic activation (Martinon et al., 2002). Finally, active caspase-1 mediates cleavage of pro-IL-1β and pro-IL-18 to their biologically active forms and their release, as well as induction of proinflammatory cell death termed pyroptosis (Davis et al., 2011, Rathinam et al., 2012).

1.4.2 DAMP recognition by innate immune receptors

Under steady-state conditions, cell death within a multicellular organism is a highly regulated process allowing for turnover of cells within tissues as well as removal of excess or no longer required cells and physiological structures during development. Such organised modality of cell death is called apoptosis, and its hallmark is activation of a class of cysteine proteases called caspases, resulting in the cleavage of various cellular substrates and easily recognizable cellular morphology with plasma membrane blebbing and separation of cell fragments into apoptotic bodies (Elmore, 2007). Under normal conditions, the apoptotic cell corpses are disposed of quickly and efficiently by phagocytic cells, usually macrophages and immature DCs, but in some cases also by the neighbouring cells (Hochreiter-Hufford and Ravichandran, 2013). Soluble mediators known as “find-me” signals, as well as surface molecules referred to as “eat-me” signals have been shown to direct phagocytes to apoptotic corpses and to help distinguish them from

surrounding healthy cells (Hochreiter-Hufford and Ravichandran, 2013). Importantly, apoptosis is an immunologically silent process, and phagocytosis of apoptotic cells can even dampen inflammation by induction of anti-inflammatory cytokine production including TGF-β and IL-10 in macrophages (Chung et al., 2007, Fadok et al., 1998).

In direct contrast to the "tidy" and controlled apoptosis, stands necrosis, the prototypical lytic form of cell death characterised by loss of membrane integrity and efflux of cytoplasmic components into the extracellular milieu. Classically, physical or chemical insults as well as lytic virus replication can directly cause necrosis (Krysko et al., 2008). In addition to the uncontrolled necrosis, a controlled lytic form of cell death termed necroptosis can be induced, most prominently, by signalling through the "death receptors" (Guicciardi and Gores, 2009) but also by engagement of various PRRs (Han et al., 2011). Recruitment of RIPK1 and RIPK3 together with inhibition, often mediated by viral inhibitors, of apoptosis-inducing caspase-8, is essential for necroptosis induction (Moriwaki and Chan, 2013).

Death by necrosis, necroptosis, or pyroptosis all result in the release of DAMPs (Kaczmarek et al., 2013). DAMPs themselves constitute a heterogeneous group of entities with no shared property other than their absence from extracellular milieu in steady state conditions (Table 1). Some of the DAMPs can be recognised by certain receptors that also function as PRRs mentioned in the previous section, while other DAMPs have dedicated, specific DAMP-receptors. In addition, surprising degree of promiscuity exists, and in many cases, one DAMP can be recognised by multiple DAMP-receptors, while one DAMP-receptor can often bind multiple DAMPs (Table 1) (Zelenay and Reis e Sousa, 2013). The fact that some DAMPs and PAMPs bind to the same receptors could suggest that the mode of action of, at least, certain DAMPs is equivalent to that of PAMPs, i.e. induction of inflammatory responses. Surprisingly though, this does not appear to be the case, and consequently, extra regulatory mechanisms must exist, allowing the differentiation between PAMP and DAMP recognition (Liu et al., 2009). For example, as mentioned in the previous section, TLR-4-mediated recognition of LPS leads to a potent NF-κB activation (Medzhitov et al., 1997, Poltorak et al., 1998). On the other hand, HMGB1 (Andersson and Tracey, 2011) or heat shock protein (HSP) (Quintana and Cohen, 2005) recognition by the same receptor is accompanied by the ligation of CD24, which in turn activates Siglec G (mouse) or

Siglec 10 (human), bringing activated phosphatases to close proximity of TLR-4 and dampening the response (Liu et al., 2009). Consequently, it remains to be conclusively established whether the DAMP-induced responses are, at least in some cases, identical to those induced by PAMPs (Zelenay and Reis e Sousa, 2013).

DAMP	Receptor	Reference
ATP	P2X7	(Jarvis and Khakh, 2009)
β-amyloid	CD36, TLR-4, TLR-6, RAGE, NLRP3	(Stewart et al., 2010), (Yan et al., 1996), (Halle et al., 2008)
Biglycan	TLR-2, TLR-4	(Schaefer et al., 2005)
Calreticulin	CD91	(Obeid et al., 2007)
DNA	TLR-9, AIM2	(Boule et al., 2004), (Hornung et al., 2009)
Granulysin	TLR-4	(Tewary et al., 2010)
Heparan sulfate	TLR-4	(Johnson et al., 2002)
HMGB-1	TLR-4, CD24, RAGE	(Andersson and Tracey, 2011), (Liu et al., 2009)
HMGN-1	TLR-4	(Yang et al., 2012)
HSPs	TLR-2, TLR-4, CD24, CD14	(Vabulas et al., 2001), (Fang et al., 2011), (Liu et al., 2009), (Kol et al., 2000)
Hyaluronan	TLR-2, TLR-4	(Jiang et al., 2005)
H_2O_2	Lyn	(Yoo et al., 2011)
IL-1α	IL-1R	(Eigenbrod et al., 2008)
IL-33	ST2	(Bonilla et al., 2012)
RNA	TLR-7, TLR-8	(Vollmer et al., 2005)
SAP130	Mincle	(Yamasaki et al., 2008)
S100	RAGE	(Hofmann et al., 1999)

Table 1 Examples of previously described DAMPs and their receptors

1.5 C-type lectin receptors

1.5.1 C-type lectin terminology

Historically, lectins were defined as carbohydrate-binding proteins, and currently they are divided into at least twelve large, structurally distinct groups, of which the C-type and S-type lectins are the largest (Kilpatrick, 2002). C-type lectins can then be further divided into seventeen groups (I – XVII) based on their structure and phylogeny (Zelensky and Gready, 2005).

C-type lectins were originally described as extracellular, Ca^{2+}-dependent carbohydrate binding proteins structurally similar to the asialoglycoprotein receptor (Drickamer, 1988). The structural unit responsible for carbohydrate binding was termed carbohydrate recognition domain (CRD) and was shown to be conserved among members of the C-type lectin family (Drickamer, 1989). As new members of the family were described, however, it became clear that not all C-type CRD-containing proteins bind carbohydrates, or even Ca^{2+}, and so in order to resolve the inconsistency, the term C-type lectin-like domain (CTLD) was introduced (Drickamer, 1999). Somewhat confusingly, the term now tends to be used interchangeably to describe either the whole group of domains with similarity to the C-type CRD regardless of their ability to bind carbohydrates, or as a term complementary to CRD, describing domains related to it but lacking carbohydrate-binding capacity (Zelensky and Gready, 2005).

1.5.2 Structural features of C-type lectins

The CTLDs of C-type lectins share a highly conserved fold consisting of two anti-parallel β-sheets and two α-helices (Figure 1.1). Typically, the β2 strand divides the structure into two lobes, the lower and the upper. The upper lobe is formed by the long loop region (LLR) and a β-sheet consisting of β2, β3 and β4 strands, while the lower lobe contains both α-helices and a vertical β-sheet consisting of β1, β5 and β1' strands (Zelensky and Gready, 2003). The presence of LLR further divides CTLDs into two large families – the canonical and the compact, of which the latter lacks the LLR. The LLR is classically involved in Ca^{2+}-mediated

carbohydrate binding, even though some CTLDs of the compact family can still bind carbohydrates in Ca^{2+}-independent manner (Zelensky and Gready, 2003).

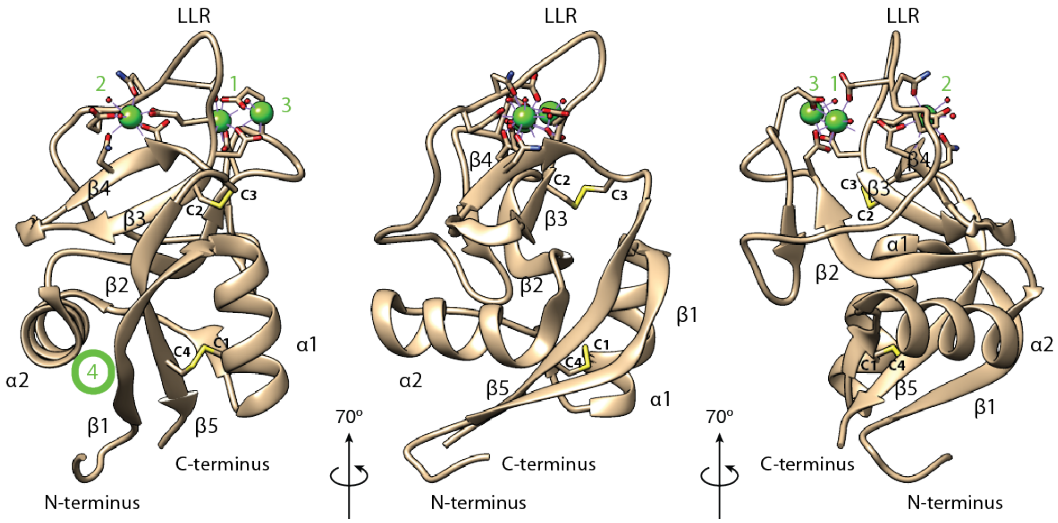

Figure 1.1 Structure of a prototypical CTLD from rat mannose binding protein A

Structure of mannose binding protein (MBP) CTLD (PDB ID 1KWT)(Ng et al., 2002) as a prototypical C-type lectin with elements of secondary structure discussed in the text highlighted (α1, α2 and β1-β5). Green balls with green numbers correspond to Ca^{2+}-binding sites occupied with Ca^{2+} ions and green circle corresponds to site 4, which is not occupied in MBP. C1 – C4 mark conserved cysteines forming intramolecular disulphide bonds. LLR = long loop region.

The typical CTLD fold is stabilised by at least two disulphide bonds formed by four cysteines, which are also the most conserved CTLD residues, present in virtually all members of the C-type lectin family. C1 and C4 connect β5 and α1, helping stabilise the characteristic end-to-end structure where the C- and N-termini come into close proximity, and C2 and C3 link β3 and β5, providing stabilization to the upper part of the CTLD (Fig 1.1)(Drickamer and Dodd, 1999, Zelensky and Gready, 2003, Zelensky and Gready, 2005). In addition, four other disulphide bonds have been described in various CTLDs, providing further stabilization of the structure (Drickamer and Dodd, 1999).

Four Ca^{2+}-binding sites appear within the CTLD fold, and their occupancy depends on the identity of the CTLD as well as on the crystallization conditions (Weis et al., 1992, Weis et al., 1991). Of the four sites, three (1 – 3) are located in the upper lobe of the CTLD structure and one (4) between α2 helix and β1/5 sheet (Fig 1.1). Ca^{2+}-binding residues within site 2 as well as the ion itself are involved in carbohydrate binding, while none of the other sites have been shown to play a role

in ligand recognition, and their function appears to be purely structural (Zelensky and Gready, 2005). Within site 2, a central role in carbohydrate binding is mediated by a conserved proline residue, the flanking residues of which dictate specificity of carbohydrate recognition – amino acid sequence EPN confers specificity for mannose, while QPD sequence is responsible for specificity for galactose. Consistently, switching motifs is enough, for example, to change the specificity of mannose binding protein A to galactose (Drickamer, 1992).

As mentioned previously, not all members of the C-type lectin superfamily bind carbohydrates, and CTLDs have been described that bind proteins (Natarajan et al., 2002), lipids (Sano et al., 1998) as well as inorganic compounds (Geider et al., 1996). Unlike in the case of carbohydrate recognition, however, no conserved motifs responsible for the non-carbohydrate specificity have been described.

1.5.3 C-type lectins in the immune system

C-type lectins are divided into seventeen groups (I – XVII) of which at least six (II, III, IV, V, VI and XII) include proteins that play various roles in the immune system (Zelensky and Gready, 2005). Notably, group II includes receptors expressed by myeloid cells of both DC and macrophage lineage such as DC-SIGN and DC-SIGNR (Park et al., 2001), Mincle (Matsumoto et al., 1999), DCIR (Bates et al., 1999) or MCL (Balch et al., 1998). Structurally its members are type II transmembrane proteins containing a short cytoplasmic tail, single carbohydrate and Ca^{2+}-binding CTLD, and a neck region involved in oligomerization of the receptors (Sancho and Reis e Sousa, 2012, Zelensky and Gready, 2005).

Group III, also known as collectins, includes serum mannose-binding proteins (MBPs) and pulmonary surfactant proteins (PSPs) involved in recognition of carbohydrate PAMPs and complement activation as well as activation of phagocytosis (Wright, 2004, van de Wetering et al., 2004). Characteristic organization of CTLDs into oligomeric complexes helps collectins recognise ordered arrays of carbohydrates, such as on the surface of pathogens (Zelensky and Gready, 2005).

Members of group IV, collectively known as selectins, play crucial roles in cell migration and recruitment of immune cells to the sites of inflammation by mediating

both their initial attachment as well as the subsequent rolling movement. Universally, selectins bind carbohydrate sialyl Lewis^X moiety with low affinity, and additionally, different high-affinity glycoprotein ligands were identified for different members of the family (Somers et al., 2000).

Group V, also known as NK-cell receptors includes several large receptor families including Ly49 (Anderson et al., 2001), NKG2 (Gunturi et al., 2004) and NKrp1 (Plougastel and Yokoyama, 2006) as well as the Dectin family and CLEC2 (Sancho and Reis e Sousa, 2012). Most of the proteins are expressed on NK cells but some also on T-cells (Voehringer et al., 2002) and cells of the myeloid lineage (Tian et al., 2005, Sancho and Reis e Sousa, 2012). The proteins are mostly dimeric, and bind protein ligands (Zelensky and Gready, 2005), although in some cases binding to carbohydrates has been described. Most prominent example of the latter is Dectin-1, binding of which is Ca^{2+}-independent, and involves an atypical carbohydrate-recognition site (Adachi et al., 2004, Brown, 2006).

Group VI is characteristic by its members expressing multiple CTLDs, and includes macrophage mannose receptor (MManR) and DEC205 (East and Isacke, 2002). Oligomeric nature of the proteins results in a high-affinity binding of polymeric ligands, even though most members of the group lack the residues involved in Ca^{2+}-binding site 2 (Zelensky and Gready, 2005).

Finally, group XII has a single member, eosinophil major basic protein (EMBP), which functions as a cytotoxic agent against macroscopic parasites. Its ligand-binding function is currently unclear, although binding to heparin has been reported (Swaminathan et al., 2001).

1.5.4 Signalling by C-type lectins

C-type lectins, like most other transmembrane receptors utilise conserved motifs to translate ligand recognition into a functional output. Based on the outcome of their signalling and the type of cytoplasmic signalling motifs, C-type lectins can be divided into four large groups: ITAM-coupled, ITIM-containing, hemITAM-containing and ITAM/ITIM-independent (Fig 1.2) (Sancho and Reis e Sousa, 2012).

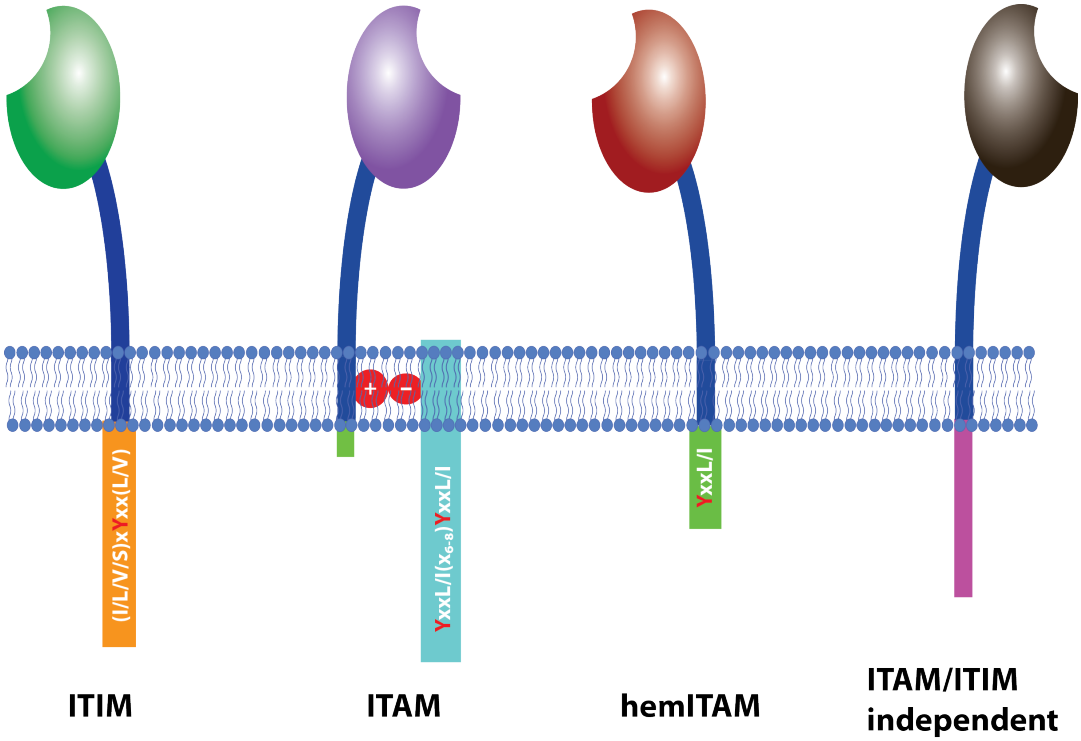

Figure 1.2 Schematic depiction of C-type lectins and their signalling motifs

Sequences of conserved signalling motifs are in white; tyrosine residues amenable to phosphorylation are highlighted in red. Charged residues mediating interaction between ITAM-bearing adapter and ITAM-coupled receptor are depicted as red circles with their charges in white.

ITIM (immunoreceptor tyrosine-based inhibitory motif) containing receptors are characterised by the intracellular sequence (I/L/V/S)xYxx(L/V), which upon tyrosine phosphorylation allows recruitment of SH2 domain-containing phosphatases (SHP-1, SHIP, and in some cases also SHP-2) (Billadeau and Leibson, 2002). When activated by Src family kinases, the phosphatases can directly reverse activatory phosphorylation of other proteins (SHP-1/2) (Binstadt et al., 1996) or catalyse hydrolysis of membrane phosphoinositide triphosphate (SHIP), facilitating release of pleckstrin homology domain-containing proteins from the membrane, in turn blocking influx of extracellular calcium (Ravetch and Lanier, 2000).

Unlike the ITIM, which is an integral part of the cytoplasmic domain of the receptors, the ITAM (immunoreceptor tyrosine-based activation motif), characterised by the YxxL/I(x_{6-8})YxxL/I sequence, is not expressed as a constituent part of C-type lectin receptors. Consequently, in order to signal through ITAM, the receptors need to be able to associate with ITAM-containing adapter proteins such as DAP12 or FcRγ (Billadeau and Leibson, 2002, Sancho and Reis e Sousa, 2012). The interaction is

mediated by charged residues within the transmembrane regions of both molecules – aspartate in the adapter protein and a conserved basic residue (arginine or lysine) in the receptor (Feng et al., 2005). Phosphorylation of both tyrosine residues within the ITAM of the adapter protein by Src family kinases then leads to recruitment of tandem SH2 domain-containing spleen tyrosine kinase (Syk), which in turn results in its autophosphorylation-mediated activation, and consequent induction of the downstream pathways including NF-κB, NFAT and others (Billadeau and Leibson, 2002, Sancho and Reis e Sousa, 2012, Mocsai et al., 2010).

As the name suggests, the hemITAM motif contains a single tyrosine residue within an YxxL motif, hence forming a "half" of the consensus ITAM. Unlike ITAM, hemITAM motifs are a part of the cytoplasmic domain of receptors (Rogers et al., 2005). Like the full ITAM, however, hemITAM phosphorylation also creates a docking site for Syk recruitment, which results in its activation (Sancho and Reis e Sousa, 2012, Rogers et al., 2005, Kerrigan and Brown, 2010). It is currently not entirely clear how does single tyrosin-containing hemITAM motif support recruitment of the two SH2 domains of Syk, but it has been speculated that dimeric status of the hemITAM-bearing receptors can make the two hemITAMs serve as one "complete" ITAM (Sancho and Reis e Sousa, 2012, Kerrigan and Brown, 2010, Hughes et al., 2010). It remains to be established whether the modes of Syk activation by ITAM and hemITAM motifs are equal, but at least in the case of platelets this does not appear to be the case, as Syk activation by hemITAM-containing receptor CLEC-2 and ITAM-coupled receptor GPVI resulted in distinct functional outcomes (Manne et al., 2015). Whether this is a direct result of differential mode of Syk recruitment or if other mechanisms and molecules are involved will, however, need to be confirmed.

The "ITAM/ITIM-independent receptors" is an umbrella term under which many of the receptors not fitting into any of the previous categories are grouped. As such, they have little in common apart from the fact that they can serve as endocytic receptors, and some have the potential to modulate signalling of other receptors, even though their stimulation alone does not result in any signs of cell activation. Examples include DEC205, LOX-1, langerin or CLEC-1 (Sancho and Reis e Sousa, 2012).

1.5.5 HemITAM containing C-type lectins

HemITAM containing C-type lectins form a small group of receptors with only four members: Dectin-1 (CLEC7A), CLEC-2 (CLEC1B), DNGR-1 (CLEC9A) and murine SIGNR3 (Sancho and Reis e Sousa, 2012, Kerrigan and Brown, 2010).

Dectin-1 is often considered to be the prototypical example of hemITAM-bearing C-type lectins (Sancho and Reis e Sousa, 2012, Kerrigan and Brown, 2010, Brown, 2006). It was originally described by subtractive cloning as a dendritic cell-associated molecule (Ariizumi et al., 2000), and shortly thereafter it was identified to be the β-glucan receptor expressed by macrophages (Brown and Gordon, 2001). The expression pattern of Dectin-1 includes myeloid cells as well as a subset of γδ T-cells in mouse and also B-cells and eosinophils in human (Brown, 2006). As mentioned elsewhere, Dectin-1 binds carbohydrates through a Ca^{2+}-independent mechanism (Adachi et al., 2004), however, the original report also suggested binding to an unidentified self-ligand on T-cells (Ariizumi et al., 2000). On the cell membrane, Dectin 1 is expressed as a monomer and binding to ligand is thought to induce its dimerization and translocation into lipid rafts, which in turn results in phagocytosis as well as NF-κB and NFAT activation (Goodridge et al., 2007, Hernanz-Falcon et al., 2009, Xu et al., 2009, Reid et al., 2009). NF-κB and NFAT are important proinflammatory programs in myeloid cells, and consequently, Dectin-1 signalling leads to production of cytokines including IL-2, IL-6, IL-10 and TNF-α as well as to DC maturation and subsequent activation of T-cells (LeibundGut-Landmann et al., 2007, Leibundgut-Landmann et al., 2008). Consistent with its activatory function and binding to β-1,3-linked glucans present in the cell wall of fungi and certain bacteria (Palma et al., 2006), Dectin-1 plays an important role in immunity against fungal pathogens, and Dectin-1-deficient mice showed impaired immune responses during fungal infection *in vivo* (Taylor et al., 2007, Saijo et al., 2007).

CLEC-2, the second hemITAM-containing receptor is expressed by multiple myeloid cell-types (Colonna et al., 2000) as well as by platelets (Suzuki-Inoue et al., 2006) in both mouse and human. CLEC-2 is the target of snake venom rhodocytin, which activates CLEC-2, leading to Syk, Src, Tec and PLCγ2 activation and platelet aggregation. Additionally, an endogenous ligand for CLEC-2 exists – a cell-surface glycoprotein podoplanin (Suzuki-Inoue et al., 2006). Podoplanin-mediated

activation of CLEC-2 on DCs induces DC motility (Acton et al., 2012), while at the same time CLEC-2-mediated activation of podoplanin results in expansion of fibroblastic network within lymph nodes (Acton et al., 2014). Even though CLEC-2 signals through Syk just as Dectin-1, its cross-linking results in NFAT but not NF-κB activation. Consequently, CLEC-2 signalling does not induce DC activation and only augments production of IL-2 and IL-10 when combined with TLR stimuli (Mourao-Sa et al., 2011). The reasons for this difference are not currently understood.

Mouse SIGNR3 has an YxxL/I motif in the cytoplasmic domain just as its human homolog DC-SIGN, however only SIGNR3 has been shown to couple to Syk, and induce inflammatory cytokines in macrophages in response to mannosylated lipoarabinomannan, a component of *Mycobacterium tuberculosis* cell wall (Tanne et al., 2009). Human DC-SIGN does not couple to Syk, and consequently is not considered a hemITAM-containing receptor (Sancho and Reis e Sousa, 2012).

Finally, DNGR-1 is the last example of hemITAM-containing C-type lectin receptors (Huysamen et al., 2008, Sancho et al., 2008) and will be discussed in greater detail in the following section.

1.6 DNGR-1

1.6.1 Discovery of DNGR-1

DNGR-1 (DC, NK lectin group receptor 1), also known as CLEC9A or CD370 was independently reported by several groups (Caminschi et al., 2008, Huysamen et al., 2008, Sancho et al., 2008) as a novel C-type lectin expressed on dendritic cells. While Sancho et al. and Caminschi et al. discovered DNGR-1 in screens designed to identify genes differentially expressed in different DC subsets (Caminschi et al., 2008, Sancho et al., 2008), Huysamen et al. characterized it as a part of a systematic effort (Marshall et al., 2004, Huysamen et al., 2008) to analyse C-type lectins found in the NK gene complex, telomeric of CD94 (Sobanov et al., 2001).

In both Sancho et al. and Huysamen et al. reports, DNGR-1 was shown to be a type II transmembrane protein with an intracellular signalling domain, and a single extracellular CTLD. In human, DNGR-1 is encoded by the *Clec9a* gene consisting of 6 exons with a single splice-variant (exons 1 – 6) described, while in the case of

the murine *Clec9a* gene seven exons were described (Huysamen et al., 2008, Sancho et al., 2008). Disparately, Sancho et al. number the murine exons 1 – 7, while Huysamen et al. refer to the fourth and fifth exon as exons 4' and 4 respectively. In all, five splice variants of murine DNGR-1 have been reported (Fig 1.3). Sancho et al. describe three isoforms, which they term *long* (containing all seven exons), *short* (lacking exon 4) and *very short* (containing only exons 1 – 3 and 7). In addition to these, Huysamen et al. describe two more isoforms – one lacking exon 2, and the other lacking exons 4 and 6 and containing a premature stop codon in exon 7 (Fig 1.3). For clarity, I will use the exon and splice variant notation as per Sancho et al. throughout.

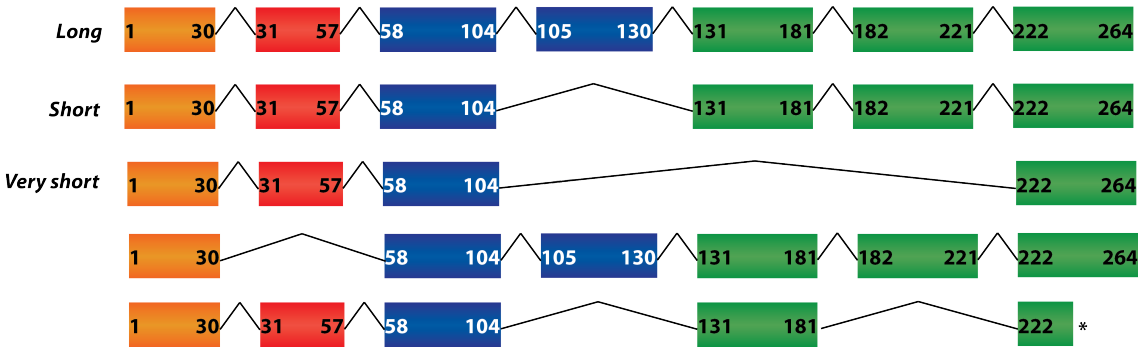

Figure 1.3 Schematic depiction of mouse DNGR-1 splice variants

Each rectangle corresponds to one exon. Intracellular domain in yellow, transmembrane region in red, extracellular neck region in blue and CTLD in green.

1.6.2 Genomic arrangement and isoforms of DNGR-1

The genomic structure of DNGR-1 remains conserved between mouse and human, and in both cases exon 1 corresponds to a short cytoplasmic domain containing the hemITAM signalling motif, exon 2 to the transmembrane domain and exons 3 – 6 or 7 in the case of the murine isoforms, to the extracellular domain composed of a C-type lectin-like domain (CTLD) and a membrane-proximal neck region (Fig 1.3). The neck region contains a conserved cysteine residue at position 94 (mouse) or 96 (human), which is thought to be involved in covalent dimerization via formation of an intermolecular disulphide bond (Huysamen et al., 2008, Sancho et al., 2008). The CTLD of DNGR-1 contains six canonical cysteine residues stabilizing the CTLD fold by forming three disulphide bonds, but it lacks the conserved residues

involved in calcium coordination and carbohydrate binding (Huysamen et al., 2008, Sancho et al., 2008).

The murine isoform that most closely resembles the human receptor is the *short* isoform. However, while human DNGR-1 (hDNGR-1) is expressed as glycosylated disulphide-bonded homodimer, the *short* mouse isoform was reported to be expressed as a non-glycosylated monomer (Huysamen et al., 2008). This observation appears counterintuitive, given that the *long* mouse isoform was reported to be a glycosylated, disulphide-bonded homodimer (Sancho et al., 2008), and the *short* isoform still contains the putative dimerization cysteine, as well as all the glycosylation sites, and also shows high degree of homology to the dimeric human variant.

1.6.3 Structure of hDNGR-1 CTLD

Crystal structure of glycosylation deficient S225D mutant CTLD of human DNGR-1 was reported in 2012 (PDB ID 3VPP). It covers residues S111 – L236 with a stretch of five amino acids between E202 and N208 missing, presumably due to disordered nature of this region. A calcium ion involved in the formation of a salt bridge between α2 helix and β1/β5 sheet was observed coordinated within the structure (Fig 1.4) (Zhang et al., 2012), in the region corresponding to the calcium coordination site 4 as per Zelensky and Gready (Zelensky and Gready, 2005). This is consistent with the ion helping stabilize the fold of the CTLD, but not being involved in ligand binding (Zhang et al., 2012).

In the crystal, the asymmetric unit contained a dimer of two CTLDs (Zhang et al., 2012). The dimeric interface was, however, highly fenestrated and buried in it was a loop that is under normal conditions accessible to antibodies, suggesting that the interface was likely an artefact of crystal packing (Zhang et al., 2012). Structural homology of DNGR-1 to lectin-like oxidized low-density lipoprotein (LDL) receptor-1 (LOX-1), also known as CLEC8A (PDB ID 1YPU, (Park et al., 2005)), led Zhang et al. to make a model of LOX-1-like dimer of DNGR-1 and to propose that the dimeric interface inferred from the model is more reflective of the form DNGR-1 takes under physiological conditions (Zhang et al., 2012). A subsequent study has, however, shown that a tryptophan residue in LOX-1 (W150), which is not

conserved between LOX-1 and DNGR-1, is crucial for maintaining the proper dimeric interface of LOX-1, and its loss results in abrogation of all inter-domain interactions between the two CTLDs even in the presence of the dimerization cysteine (Nakano et al., 2012). In light of these observations, the validity of the LOX-1-like model of DNGR-1 dimerization is questionable, and further work will be needed to confirm which form, if any, does the dimerization interface of DNGR-1 take.

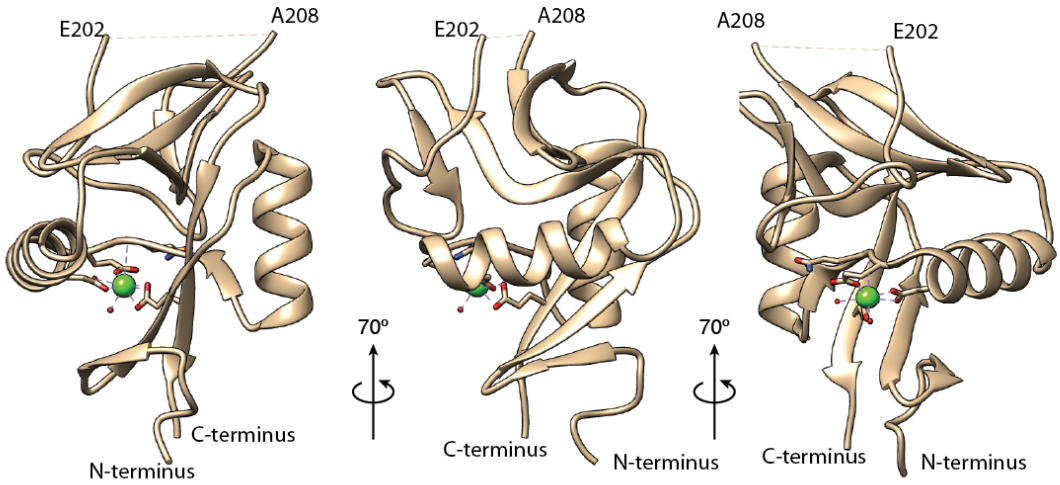

Figure 1.4 Structure of hDNGR-1 CTLD

Structure of hDNGR-1 CTLD (PDB ID 3VPP, (Zhang et al., 2012)) with the C- and N-termini as well as the missing region (dashed line) labelled. Ca^{2+} ion (green ball) and Ca^{2+}-coordinating residues (sticks) are highlighted.

1.6.4 DNGR-1 is involved in cross-presentation of dead cell-associated antigens

The intracellular portion of DNGR-1 contains a hemITAM motif, which led to the assumption that DNGR-1 is an activatory receptor (Huysamen et al., 2008). DNGR-1 hemITAM bears resemblance to those of related C-type lectin receptors Dectin-1 and CLEC-2, both of which can serve as activatory receptors in DCs and platelets respectively (Sancho and Reis e Sousa, 2012). Antibody or ligand-mediated cross-linking of DNGR-1, however, did not lead to DC activation (Sancho et al., 2008), even though it could activate reporter cells co-expressing DNGR-1 and Syk (Sancho et al., 2009). The reasons for different ability of DNGR-1

to activate DCs and reporter cells are currently unclear, but can have to do with different levels of Syk expression or presence of other interacting molecules.

Interestingly, the hemITAM of DNGR-1 differs from those of Dectin-1 and CLEC-2 in that the DEDG sequence immediately upstream of the tyrosine, which was previously shown to be involved in signalling (Fuller et al., 2007) is substituted by AEEI or EEEI sequence in mouse and human DNGR-1 respectively (Fig 1.5) (Zelenay et al., 2012). This places a bulky hydrophobic isoleucine residue in the place where a small glycine is found in the other receptors, possibly creating a sterical hindrance that may result in a different mode of Syk recruitment and consequent attenuation of DNGR-1 signalling when compared with Dectin-1. In agreement with this notion, mutating the isoleucine to glycine improved the ability of DNGR-1 hemITAM to activate DCs upon ligand recognition in the context of chimeric receptors comprising the extracellular domain of Dectin-1 and intracellular domain of DNGR-1. Mutant generated by substituting the alanine present in murine isoform of DNGR-1 with aspartic acid on the other hand showed no phenotype (Zelenay et al., 2012).

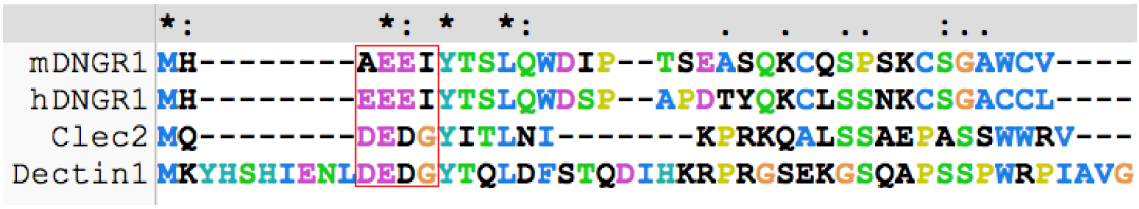

Figure 1.5 Alignment of DNGR-1, Clec2 and Dectin-1 intracellular domains

Sequences of intracellular domains of human and mouse DNGR-1, Clec2 and Dectin-1 aligned using Clustal X software. Conserved DEDG motif is highlighted by red rectangle.

DNGR-1 was shown to function as an endocytic receptor (Huysamen et al., 2008, Sancho et al., 2008) binding to a ligand revealed in cells that have lost their membrane integrity (Sancho et al., 2009). While DNGR-1 is not an activatory receptor, and its loss does not affect the ability of DCs to take up necrotic cell material, mice deficient in DNGR-1 (DNGR-1 KO) showed impairment in cross-presentation of dead cell-associated antigens. This resulted in a defect in activation of cytotoxic T-cell responses against model antigens carried by dead cells in a model of sterile immunity (Sancho et al., 2009). Subsequently, the phenotype was also extended to infection with viruses *in vivo*, where DNGR-1 KO

animals showed weakened CTL responses to HSV-1 and Vaccinia viruses, as well as impairment in memory responses after vaccination (Iborra et al., 2012, Zelenay et al., 2012).

1.6.5 DNGR-1 controls endocytic handling of dead cell-associated antigens

Mechanistically, the ability of DNGR-1 to promote cross-presentation of dead cell-associated antigens is dependent on its interaction with Syk kinase, as Syk-deficient animals phenocopied DNGR-1-deficient ones (Sancho et al., 2009). The exact molecular mechanism of how DNGR-1 mediates cross-presentation remains elusive. However, DNGR-1 was shown to regulate intracellular trafficking of internalized material. In particular, DNGR-1 ligation led to targeting of dead cell-associated antigens to a non-degradative recycling endosomal compartment characterised by presence of Rab5 and Rab11 endosomal markers, while in DNGR-1-deficient cells the endocytic cargo was targeted to lysosomal compartment (Zelenay et al., 2012). Consistently, treatment with bafilomycin A1, an inhibitor of lysosomal acidification could restore the cross-presentation potential of DNGR-1 deficient DCs (Iborra et al., 2012), lending further support to the notion that the main function of DNGR-1 is to preserve the integrity of endocytosed dead cell-associated antigens.

Taken together, these observations suggest a model where DNGR-1 affects handling of endocytic cargo through as-of-yet unknown mechanism, resulting in the inhibition of endosomal maturation and/or redirection of dead cell-associated material towards non-degradative endosomal compartments, and consequently increase in the amount of material available for cross-presentation (Fig 1.6).

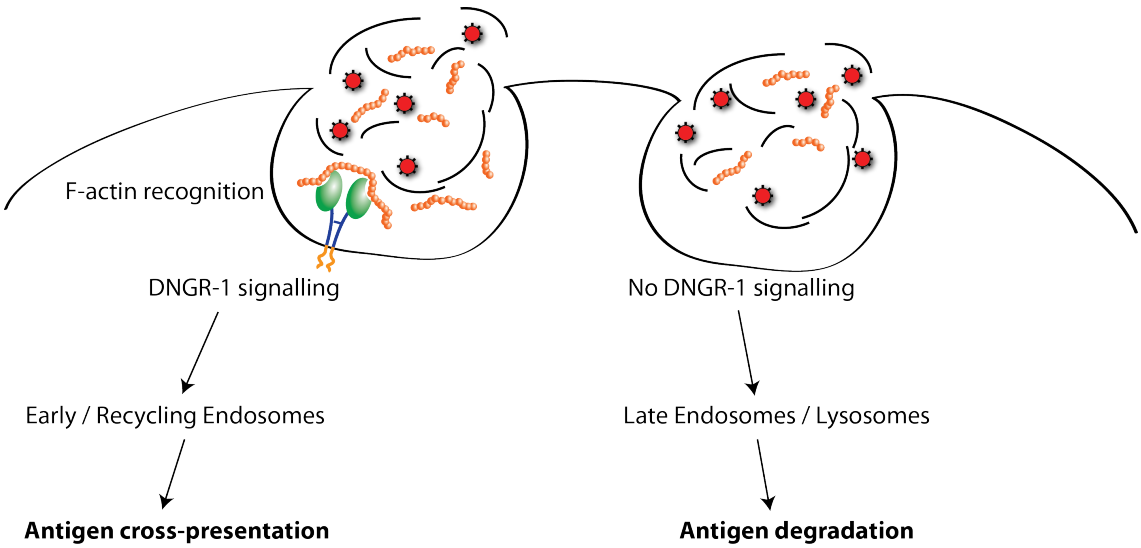

Figure 1.6 DNGR-1 controls endocytic handling of dead cell-associated antigens
Schematic depiction of the current model of DNGR-1 function in DCs, as described in the text.

1.6.6 Identification of DNGR-1 ligand

DNGR-1 was originally found to bind a ubiquitous intracellular molecule revealed in cells that have lost membrane integrity (Sancho et al., 2009). Further analysis showed that the ligand is predominantly cytoplasmic, resistant to nucleases and glycosidases, and susceptible to protease and acid treatment and heat denaturation (Sancho et al., 2009). Subsequently, the identity of the ligand was determined to be the filamentous form of actin (F-actin), while no binding was detected to the monomers of G-actin (Ahrens et al., 2012, Zhang et al., 2012). Actin is evolutionarily highly conserved, and consistent with that fact, human, turkey, trout, *Drosophila* and yeast F-actin could all be recognized by mouse DNGR-1 (Ahrens et al., 2012).

It was also suggested that the minimal requirement for DNGR-1 binding is actin in complex with calponin homology domain-containing actin-binding proteins (ABPs) such as β-spectrin and α-actinin (Zhang et al., 2012). Since F-actin depolymerizes under critical concentration of actin monomers, and this process can be delayed or reversed by presence of ABPs, filaments decorated with such proteins are more stable and possibly also more prone to form bundles, suggesting a plausible

explanation for the apparent increase in binding of DNGR-1 to such filaments (Ahrens et al., 2012).

1.6.7 Cellular distribution of DNGR-1

Among fully differentiated DC subsets in mouse, DNGR-1 expression is restricted to the $CD8\alpha^+$ and $CD103^+$ $CD11b^-$ DCs, as well as, at lower levels, the plasmacytoid DCs (Caminschi et al., 2008, Poulin et al., 2012, Sancho et al., 2008). As such, high expression of DNGR-1 marks the cross-presenting, $XCR\text{-}1^+$ DC subsets both in lymphoid and non-lymphoid tissues (Poulin et al., 2012). In human, none of the DC subsets express CD8α, which historically made it difficult to draw parallels between mouse and human. DNGR-1 expression on such cells, however, remains conserved between the two organisms, and consequently DNGR-1 expression was shown to mark the human equivalent of mouse $CD8\alpha^+$ DCs (Poulin et al., 2012, Poulin et al., 2010).

Notably, in mouse, DNGR-1 is also expressed at low levels on a DC precursor in both spleen and bone marrow (Schraml et al., 2013). Even though DNGR-1 expression is subsequently lost in the $CD11b^+$ DC subset, the history of DNGR-1 expression can be used as a marker for the CDP progeny. Indeed, mice with Cre recombinase inserted into *Clec9a* locus were generated, and when crossed to $Rosa26\text{-}stop^{flox}$ yellow fluorescent protein (YFP) reporter mice, the resulting $Clec9a^{+/cre}$ $Rosa^{+/EYFP}$ animals could be used for lineage tracing and fate-mapping of cells derived from the CDP (Schraml et al., 2013).

1.6.8 Antigen targeting to DNGR-1 promotes immune response

$CD8\alpha^+$ DCs have been shown to potently cross-present exogenous antigens on MHC-I, and activate cytotoxic $CD8^+$ T-cells (den Haan et al., 2000). The expression pattern of DNGR-1 makes it an interesting candidate for antigen delivery to $CD8\alpha^+$-like family of DCs (Sancho et al., 2008). Indeed, antibody targeting of antigens corresponding to tumour-derived peptides to DNGR-1 in the presence of adjuvants led to cytotoxic T-cell-mediated eradication of B16 melanoma lung pseudometastasis (Sancho et al., 2008).

In addition to CTL cross-priming, DCs can also activate $CD4^+$ helper T-cells through antigen presentation on MHC-II, resulting in cellular as well as humoural responses. Hence, targeting of antigens to DNGR-1 does not only lead to MHC-I-mediated cross-presentation to cytotoxic T-cells, but also to MHC-II-mediated presentation to helper T-cells (Caminschi et al., 2008, Caminschi et al., 2012, Joffre et al., 2010).

Multiple anti-DNGR-1 antibodies have been raised by different groups and utilised for antigen targeting to the receptor. Interestingly, different results were obtained with different antibodies, regarding the requirement (Joffre et al., 2010, Sancho et al., 2008), or not (Caminschi et al., 2008, Caminschi et al., 2012) for adjuvant co-administration. In particular, targeting antigens to DNGR-1 with antibody clone 7H11 required adjuvants to induce immunity. In their absence the induction of tolerance and generation of $FoxP3^+$ regulatory T-cells was observed, while using different types of adjuvants resulted in different modality of T-helper cell responses – Poly I:C inducing T_H1 response and curdlan inducing T_H17 response (Joffre et al., 2010). In contrast, antibody clone 10B4 was capable of inducing humoural responses towards antigen fused to it in an adjuvant-independent manner (Caminschi et al., 2008, Caminschi et al., 2012). In an attempt to reconcile these apparently conflicting data, a recent study (Li et al., 2015) compared side by side multiple anti-DNGR-1 antibodies, confirming the previously observed phenomena: treatment with 10B4 antibody resulted in efficient humoural response against the rat antibody in the absence of adjuvants, while 7H11 treatment resulted in efficient response only in the presence of adjuvants. The authors note that most properties of the two antibodies are comparable, however, the rat IgG2a heavy chain appears in general more immunogenic than IgG1κ (but not λ), suggesting that the difference between different DNGR-1 antibodies may be due to their different isotypes: 10B4 - IgG2a and 7H11 - IgG1 (Li et al., 2015).

Targeting antigens to endocytic receptors expressed on DCs has shown promise in experimental as well as clinical settings (Steinman and Banchereau, 2007), and phase I and II clinical trials of vaccination are currently under way with antigen-coupled antibodies against DEC205, an uptake receptor expressed by DCs (Trumpfheller et al., 2012).

Targeting DNGR-1 with antibodies in the murine model of vaccination resulted in potent induction of both cytotoxic (Sancho et al., 2008) and humoural (Caminschi et

al., 2008, Caminschi et al., 2012, Joffre et al., 2010) responses, suggesting possible usefulness of DNGR-1 for targeting of vaccines to DCs. Importantly, induction of humoral responses was also observed in non-human primate model with *Macaca nemestrina* monkeys even in the absence of adjuvants (Li et al., 2015). Important caveat, however, is that the antibody used in the macaque was the same rat IgG2a that elicited humoral responses in mouse without the need for adjuvants. Given that the potency of this antibody was likely at least in part due to its isotype (Li et al., 2015), it remains to be seen if DNGR-1 targeting would hold as much promise with humanised antibodies, which would need to be used should anti-DNGR-1 antibodies ever be used in human medicine (Caminschi and Shortman, 2012).

1.7 Summary and objectives

DNGR-1 is a C-type lectin receptor expressed by dendritic cells, involved in the cross-presentation of dead cell-associated antigens. While much is already known about its function and biology, certain critical questions still remain unanswered both at the level of its biochemical and structural properties, and at the level of its function *in vivo*.

Consequently, in the following sections, I will attempt to provide answers to several of these questions, focusing on the biochemical and structural properties of the protein and its interaction with its ligand, F-actin, where possible drawing conclusions relevant for the biological function of the receptor, as well as highlighting some novel, previously unappreciated questions.

Chapter 2. Materials & Methods

2.1 Reagents

2.1.1 Buffers

G-actin buffer: 5 mM Tris-HCl, pH 8.0 + 0.2 mM $CaCl_2$

F-actin buffer (10x): 100 mM Tris-HCl, pH 7.5 + 500 mM KCl + 20 mM $MgCl_2$ + 10 mM ATP

Blocking buffer for Western blots and dot blots: 5% (w/v) milk in PBS + 0.05% (v/v) Tween-20

Interaction buffer for biolayer interferometry: F-buffer + 0.1% (w/v) BSA + 0.02% (v/v) Tween-20

Quenching buffer for biolayer interferometry: F-buffer + 0.1% (w/v) BSA + 0.02% (v/v) Tween-20 + 10 µg/ml biocytin

FACS buffer: 5 mM EDTA + 1% (v/v) FCS + 0.0125% (w/v) NaN_3 in PBS

CPRG 10x: 30 mM chlorophenol red-β-D-galactopyranoside (CPRG) in Z-buffer

Z-buffer: 0.6 M $Na_2HPO_4{\cdot}7H_2O$ + 0.4 M $NaH_2PO_4{\cdot}H_2O$ + 0.1 M KCl + 0.01 M $MgSO_4{\cdot}7H_2O$ + 0.5 M β-mercaptoethanol

CPRG lysis buffer: 1 x CPRG + 0.1% NP-40 + 10 mM $MgCl_2$ in PBS

PBS-based cell lysis buffer: 1% SDS in PBS

Bis Tris-based cell lysis buffer: 1% SDS in 10 mM Bis Tris pH 5.5

MES-based cell lysis buffer: 1% SDS in 10 mM MES pH 6.1

6x Laemmli buffer: 12% SDS + 50% Glycerol + 60 mM Tris-HCl pH 6.8 + 0.6 mg/ml bromophenol blue

8 M Urea loading buffer: 8 M Urea + 2% SDS + 250 mM Tris-HCl pH 6.2 + 0.001% bromophenol blue

Buffers used for generating the 3D graph in Figure 3.3C: BisTris pH 6.5; PIPES pH 6.8; BES pH 7.1; MOPS pH 7.2; HEPES pH 7.5; Tricine pH 8.05, all 15 mM with addition of 0 – 250 mM NaCl

2.1.2 Proteins

G-actin was bought lyophilised (Cytoskeleton), reconstituted in sterile water at the final concentration 10 mg/ml and stored at -80°C. Before use, the G-actin aliquots were diluted into G-actin buffer to final concentration 1 mg/ml and incubated for at least 30 minutes on ice.
To polymerise G-actin into F-actin, 10x F-actin buffer was added to reconstituted G-actin (1 mg/ml), and the mixture was incubated for 1 hour at room temperature.
Human platelet actin, biotinylated rabbit muscle actin, rabbit skeletal muscle α-actinin, and human recombinant plasma gelsolin were purchased from Cytoskeleton.
DNGR-1 ECD proteins were generated by transient transfection of 293F cells.

2.1.3 DNA

Vector coding for *long* DNGR-1 ECD in CMV-9 backbone was prepared previously in the lab (Ahrens et al., 2012).
Vectors coding for DNGR-1 or in pMSCV and pFB vectors were prepared previously in the lab (Sancho et al., 2009, Zelenay et al., 2012).
DNA coding for human DNGR-1 isoform in pCDNA3.1 vector backbone was purchased from GenScript.

2.1.4 Antibodies

HRP-conjugated mouse anti-FLAG, clone M2 (Sigma Aldrich)
HRP-conjugated rabbit anti-β-actin, clone 13E5 (Cell Signalling)
HRP-conjugated rabbit anti-rat IgG (H+L), polyclonal (Jackson ImmunoResearch)
purified rat anti-DNGR-1, clone 397 (Sancho et al., 2008)
purified rat anti-DNGR-1, clone 7H11 (Sancho et al., 2008)
PE-conjugated rat anti-DNGR-1, clone 1F6 (Sancho et al., 2008)
Cy3-conjugated mouse anti-FLAG, clone M2 (Sigma Aldrich)
M2-anti-FLAG affinity gel (Sigma Aldrich)
anti-HA-Agarose, clone HA-7 (Sigma Aldrich)

2.1.5 Enzymes

Calf intestinal phosphatase (New England Biolabs)
Phusion High-Fidelity DNA polymerase (Thermo)
PNGase F (New England Biolabs)
Sortase A (kind gift from J. Huotari)
T4 DNA ligase (New England Biolabs)

2.1.6 Kits

HiSpeed Plasmid Maxi Kit (Qiagen)
QIAprep Spin Miniprep Kit (Qiagen)
QIAquick Gel Extraction Kit (Qiagen)
QIAquick PCR Purification Kit (Qiagen)
QuikChange Lightning and Quick Change II XL Side-Directed Mutagenesis Kits (Agilent Technologies)

2.2 Cloning

2.2.1 Targeted mutagenesis of DNGR-1 constructs

All mutations in all constructs were introduced using the QuikChange Lightning or QuikChange II XL kits with primer sequences shown in Table 2. All constructs were verified by sequencing.

mutation	direction of primer	primer sequence (5'–3')
K57 – L66 deletion	fw	CAAGGATGACGATGACAAGCTTGCGGCCGCGGAGCAGCAGGAAAGACTCATCCAACAGGAC
	rev	GTCCTGTTGGATGAGTCTTTCCTGCTGCTCCGCGGCCGCAAGCTTGTCATCGTCATCCTTG
L64 – I73 deletion	fw	CGGCCGCGAAGTTCTTCCAGGTATCCTCTCAACAGGACACAGCATTGGTGAACCTTACAC
	rev	GTGTAAGGTTCACCAATGCTGTGTCCTGTTGAGAGGATACCTGGAAGAACTTCGCGGCCG

L72 – L82 deletion	fw	CCTCTCTTGTCTTGGAGCAGCAGGAAAGAACACAGTGGCAGAGGAAA TACACACTGGAATACTGCC
	rev	GGCAGTATTCCAGTGTGTATTTCCTCTGCCACTGTGTTCTTTCCTGCT GCTCCAAGACAAGAGAGG
L72 – L82 all Ala	fw	GGTATCCTCTCTTGTCTTGGAGCAGCAGGAAAGAGCCGCCGCCGCC GCCGCCGCCGCCGCCGCCGCCACACAGTGGCAGAGGAAATACACA CTGGAATACTGCCAAGCC
	rev	GGCTTGGCAGTATTCCAGTGTGTATTTCCTCTGCCACTGTGTGGCGG CGGCGGCGGCGGCGGCGGCGGCGGCTCTTTCCTGCTGCTCCA AGACAAGAGAGGATACC
N81 – T90 deletion	fw	GGAAAGACTCATCCAACAGGACACAGCATTGGTGCTGGAATACTGCC AAGCCTTACTGCAGAGATCTCTCC
	rev	GGAGAGATCTCTGCAGTAAGGCTTGGCAGTATTCCAGCACCAATGCT GTGTCCTGTTGGATGAGTCTTTCC
N81–T90 all Ala	fw	GCAGGAAAGACTCATCCAACAGGACACAGCATTGGTGGCCGCCGCC GCCGCCGCCGCCGCCGCCGCCCTGGAATACTGCCAAGCCTTACTGC AGAG
	rev	CTCTGCAGTAAGGCTTGGCAGTATTCCAGGGCGGCGGCGGCGGCG GCGGCGGCGGCGGCCACCAATGCTGTGTCCTGTTGGATGAGTCTTT CCTGC
R87 – A96 deletion	fw	GACACAGCATTGGTGAACCTTACACAGTGGCAGTTACTGCAGAGATC TCTCCATTCAGGCAC
	rev	GTGCCTGAATGGAGAGATCTCTGCAGTAACTGCCACTGTGTAAGGTT CACCAATGCTGTGTC
R87 – A96 deletion + Cys	fw	GACACAGCATTGGTGAACCTTACACAGTGGCAGTGCTTACTGCAGAG ATCTCTCCATTCAGGCAC
	rev	GTGCCTGAATGGAGAGATCTCTGCAGTAAGCACTGCCACTGTGTAAG GTTCACCAATGCTGTGTC
R87 – A96 all Ala + Cys	fw	GACACAGCATTGGTGAACCTTACACAGTGGCAGGCCGCCGCCGCCG CCGCCGCCTGCGCCGCCTTACTGCAGAGATCTCTCCATTCAGGCAC
	rev	GTGCCTGAATGGAGAGATCTCTGCAGTAAGGCGGCGCAGGCGGCG GCGGCGGCGGCGGCCTGCCACTGTGTAAGGTTCACCAATGCTGTGT C
Q95 – S104 deletion	fw	CAGTGGCAGAGGAAATACACACTGGAATACTGCGGCACAGATGCTTC TACTGGACCAG
	rev	CTGGTCCAGTAGAAGCATCTGTGCCGCAGTATTCCAGTGTGTATTTC CTCTGCCACTG
Q95 – S104 all Ala	fw	GTGAACCTTACACAGTGGCAGAGGAAATACACACTGGAATACTGCGC CGCCGCCGCCGCCGCCGCCGCCGCCGGCACAGATGCTTCTAC TGGACCAGTTCTTCTGAC
	rev	GTCAGAAGAACTGGTCCAGTAGAAGCATCTGTGCCGGCGGCGGCGG CGGCGGCGGCGGCGGCGGCGCAGTATTCCAGTGTGTATTTCCTCTG CCACTGTGTAAGGTTCAC
C94S	fw	GGAAATACACGCTGGAATACAGCCAAGCCTTACTGCAGAGATC
	rev	GATCTCTGCAGTAAGGCTTGGCTGTATTCCAGCGTGTATTTCC

H139A	fw	GACTGCAGCCCTTGTCCAGCCAACTGGATTCAGAATGG
	rev	CCATTCTGAATCCAGTTGGCTGGACAAGGGCTGCAGTC
H139N	fw	GACTGCAGCCCTTGTCCAAACAACTGGATTCAGAATGG
	rev	CCATTCTGAATCCAGTTGTTTGGACAAGGGCTGCAGTC
N140A	fw	GCAGCCCTTGTCCACACGCCTGGATTCAGAATGGAAAAAG
	rev	CTTTTTCCATTCTGAATCCAGGCGTGTGGACAAGGGCTGC
W141A	fw	GCAGCCCTTGTCCACACAACGCCATTCAGAATGGAAAAAGTTG
	rev	CAACTTTTTCCATTCTGAATGGCGTTGTGTGGACAAGGGCTGC
Y150A	fw	GATTCAGAATGGAAAAAGTTGTTACGCCGTCTTTGAACGCTGGGAAA TGTGG
	rev	CCACATTTCCCAGCGTTCAAAGACGGCGTAACAACTTTTTCCATTCTG AATC
E153A	fw	GGAAAAAGTTGTTACTATGTCTTTGCCCGCTGGGAAATGTGGAACAT CAG
	rev	CTGATGTTCCACATTTCCCAGCGGGCAAAGACATAGTAACAACTTTTT CC
W155A	fw	GTTGTTACTATGTCTTTGAACGCGCCGAAATGTGGAACATCAGTAAGA AG
	rev	CTTCTTACTGATGTTCCACATTTCGGCGCGTTCAAAGACATAGTAACA AC
K167A	fw	CATCAGTAAGAAGAGCTGTTTAGCCGAGGGCGCTAGTCTCTTTC
	rev	GAAAGAGACTAGCGCCCTCGGCTAAACAGCTCTTCTTACTGATG
E168A	fw	CATCAGTAAGAAGAGCTGTTTAAAAGCCGGCGCTAGTCTCTTTCAAAT AGAC
	rev	GTCTATTTGAAAGAGACTAGCGCCGGCTTTTAAACAGCTCTTCTTACT GATG
G188R	fw	GAAGAAATGGAGTTCATCAGCAGTATAAGGAAACTCAAAGGAGGAAA TAAATATTGGG
	rev	CCCAATATTTATTTCCTCCTTTGAGTTTCCTTATACTGCTGATGAACTC CATTTCTTC
K189A	fw	GGAGTTCATCAGCAGTATAGGGGCCCTCAAAGGAGGAAATAAATATT GGG
	rev	CCCAATATTTATTTCCTCCTTTGAGGGCCCCTATACTGCTGATGAACT CC
K191A	fw	CATCAGCAGTATAGGGAAACTCGCCGGAGGAAATAAATATTGGGTG
	rev	CACCCAATATTTATTTCCTCCGGCGAGTTTCCCTATACTGCTGATG
K189A K191A	fw	GGAGTTCATCAGCAGTATAGGGGCCCTCGCCGGAGGAAATAAATATT GGG
	rev	CCCAATATTTATTTCCTCCGGCGAGGGCCCCTATACTGCTGATGAAC TCC

K195D	fw	GGGAAACTCAAAGGAGGAAATGACTATTGGGTGGGAGTGTTTC
	rev	GAAACACTCCCACCCAATAGTCATTTCCTCCTTTGAGTTTCCC
E225A	fw	GACTTGTTGCCAGCAGCGAGACAGCGATCAGCCGGCC
	rev	GGCCGGCTGATCGCTGTCTCGCTGCTGGCAACAAGTC
R226A	fw	GACTTGTTGCCAGCAGAAGCGCAGCGATCAGCCGGCC
	rev	GGCCGGCTGATCGCTGCGCTTCTGCTGGCAACAAGTC
Q227A R228A	fw	GACTTGTTGCCAGCAGAAAGAGCCGCCTCAGCCGGCCAGATCTGTGG
	rev	CCACAGATCTGGCCGGCTGAGGCGGCTCTTTCTGCTGGCAACAAGTC
S229A	fw	GTTGCCAGCAGAAAGACAGCGAGCCGCCGGCCAGATCTGTGGATACC
	rev	GGTATCCACAGATCTGGCCGGCGGCTCGCTGTCTTTCTGCTGGCAAC
Q232A	fw	GCAGAAAGACAGCGATCAGCCGGCGCCATCTGTGGATACCTCAAAGATTC
	rev	GAATCTTTGAGGTATCCACAGATGGCGCCGGCTGATCGCTGTCTTTCTGC
K238A	fw	GGCCAGATCTGTGGATACCTCGCCGATTCTACTCTCATCTCAG
	rev	CTGAGATGAGAGTAGAATCGGCGAGGTATCCACAGATCTGGCC
D248A	fw	GATTCTACTCTCATCTCAGATAAGTGCGCCAGCTGGAAATATTTTATCTGTGAG
	rev	CTCACAGATAAAATATTTCCAGCTGGCGCACTTATCTGAGATGAGAGTAGAATC
W250A	fw	CATCTCAGATAAGTGCGATAGCGCCAAATATTTTATCTGTGAGAAGAAGGC
	rev	GCCTTCTTCTCACAGATAAAATATTTGGCGCTATCGCACTTATCTGAGATG
K251A	fw	CTCAGATAAGTGCGATAGCTGGGCCTATTTTATCTGTGAGAAGAAGG
	rev	CCTTCTTCTCACAGATAAAATAGGCCCAGCTATCGCACTTATCTGAG
ΔLoop	fw	CTCTCTGACTTGTTGCCAGCAGCCGCCGCCGCCGCCGCCGCCATCTGTGGATACCTCAAAGATTC
	rev	GAATCTTTGAGGTATCCACAGATGGCGGCGGCGGCGGCGGCGGCGGCTGCTGGCAACAAGTCAGAGAG

Table 2 Sequences of primers used for DNGR-1 mutagenesis

2.2.2 Expression vectors for *short* mouse and human DNGR-1 and Dectin 1 ECD protein production

Desired amplicons corresponding to the extracellular domains of *short* mouse and human DNGR-1 isoforms and mouse Dectin 1 were obtained using polymerase chain reaction (PCR) with Phusion High-Fidelity DNA polymerase, primers shown in Table 3 and template DNA in different vector backbones prepared previously by D. Sancho (unpublished), S. Zelenay (Zelenay et al., 2012) or purchased from GenScript respectively. PCR products were purified and digested with appropriate restriction endonucleases alongside empty CMV-9 vector backbone. Vector backbone was dephosphorylated by calf intestinal phosphatase treatment and both the digested amplicons and vector backbone were gel-purified by agarose gel electrophoresis. Purified backbone and amplicons were mixed and ligated with T4 DNA ligase. All constructs were verified by sequencing.

2.2.3 Generation of C9C7 chimeric receptors

A “megaprimer” spanning the entire length of the neck region of *long* mouse DNGR-1 isoform with short sequences complementary to the regions upstream and downstream of the Dectin-1 neck region was generated using PCR with Phusion High-Fidelity DNA polymerase, primers shown in Table 3, and DNA template containing the sequence of entire DNGR-1. “Megaprimer” was agarose gel-purified and used in a modified site-directed mutagenesis reaction using QuikChange II XL site-directed mutagenesis kit as per manufacturer’s instructions. The constructs were verified by sequencing.

2.2.4 Generation of CMV-9 vector for expression of HA-tagged proteins

CMV-9 vector backbone contains sequence coding for 3xFLAG tag upstream of the sequence coding for the protein of interest. To replace the 3xFLAG-coding sequence with one coding for HA, QuikChange II XL mutagenesis kit and primers shown in Table 3 were used. The resulting construct was verified by sequencing.

2.2.5 Generation of sortagged DNGR-1 constucts

Sortag together with His tag were introduced at the C-terminus of DNGR-1 in CMV-9 vector using QuikChange II XL mutagenesis kit and primers shown in Table 3. The resulting constructs were verified by sequencing.

construct	direction of primer	primer sequence (5'–3')
short mouse DNGR-1 ECD	fw	AAAAAACTCGAGGCCGCCGCCGCCATGCATGCGGAAGAAATATATACCTCTCTTCAGTGGG
	rev	AAAAAAAAGCTTCAGATGCAGGATCCAAATGCTTTCTTCTCACAG
human DNGR-1 ECD	fw	AATTGCGGCCGCGAAGTTGTTGCAGGTGTCCACCATTGCGATGC
	rev	AATCTAGATCAGACAGAGGATCTCAACGCATACTTCTCACAG
Dectin1 ECD	fw	AAAAAACTCGAGCCGCCATGAAATATCACTCTCATATAGAGAATCTGGATGAAGATGGATATACTC
	rev	TTTTTTGCGGCCGCTCACAGTTCCTTCTCACAGATACTGTATGAAGAAGTATTGCAG
"megaprimer" for C9C7 generation	fw	GCTGGGTGCCCTAGCATTTTGGAAGTTCTTCCAGGTATCCTCTCTTG
	rev	CCATGCATGATCCAATTAGGAAGGCATGTTTCCTTGCTGTCCAGGGTCTG
HA –tagged DNGR-1	fw	GCTCTTGTTGGAGCTGCAGTTGCTTACCCTTACGATGTGCCCGATTACGCCGCGGCCGCGAAGTTCTTCCAG
	rev	CTGGAAGAACTTCGCGGCCGCGGCGTAATCGGGCACATCGTAAGGGTAAGCAACTGCAGCTCCAACAAGAGC
C-terminally sortagged DNGR-1	fw	GCATCCTACCGGAAACAGGGCATCATCACCATCACCACTGATCTAGAGGATCCCGGG
	rev	CCCGGGATCCTCTAGATCAGTGGTGATGGTGATGATGCCCTGTTTCCGGTAGGATGC

Table 3 Sequences of primers used for generation of indicated constructs

2.3 Cells

Phoenix, B3Z-Syk (Sancho et al., 2009) and GP2-293 cells were grown in RPMI1640 medium supplemented with glutamine, penicillin, streptomycin, 2-mercaptoethanol and 10% heat-inactivated foetal calf serum (FCS) at 37°C and 5% CO_2.

MuTuDC1940 (Fuertes Marraco et al., 2012) cells were grown in IMDM medium supplemented with 2-mercaptoethanol and 10% heat-inactivated foetal calf serum (FCS) at 37°C and 5% CO_2.
293F cells were grown in FreeStyle 293 Expression Medium at 37°C, 8% CO_2 and constant shaking on an orbital shaker at 120 rpm.
For Flt3 ligand DC cultures, bone marrow was flushed out of femurs and tibiae of mice of desired genotype, washed and seeded in a 6-well plate at 2 x 10^6 cells per well. The cells were cultured for 9 days in complete RPMI1640 medium additionally supplemented with 150 ng/ml recombinant Flt3 ligand.

2.3.1 Transient transfections of 293F cells

293F cells grown in 30 ml of medium in T-75 flasks were adjusted to density of 1 x 10^6 per ml and transfected with a mixture of 60 µl 293fectin and 30 µg of DNA coding for the desired protein in CMV-9 backbone in 2 ml of Opti-MEM medium.

2.3.2 Retroviral transductions

70% confluent GP2-293 packaging cells in 10 cm dish were transfected with a mixture of 18 µl GeneJuice, 6 µg of VSV-G envelope protein-coding plasmid and 6 µg of plasmid coding for the desired protein in pMSCV or pFB backbone in 600 µl of Opti-MEM medium. On days 1, 2 and 3 post-transfection, the pseudotyped virus-containing culture medium was replaced with fresh one, filtered through 0.44 µm filter, supplemented with 8 µg/ml polybrene and immediately applied onto Phoenix cells grown in a 6-well plate format. The plate was centrifuged for 90 minutes at 2500 x g at room temperature and left in the incubator for further 90 minutes. After the incubation, the medium was exchanged for fresh complete RPMI1640 medium. On the third day, the Phoenix cells were re-plated into a 10 cm dish and expanded.
For transduction of B3Z-Syk, MuTuDC1940 and Flt3L DCs, ecotropic virus-containing supernatant from Phoenix cells was used, and in case of Flt3L DCs protamine sulphate was used instead of polybrene.

2.4 Protein production and purification

2.4.1 DNGR-1 ECD production in 293F cells

All DNGR-1 extracellular domain (ECD) proteins (K57 – I264) were produced by transient transfection of 293F cells as described above. At 72 hours post-transfection, the cells were pelleted by centrifugation and the medium was collected and filtered through 0.22 µm filter to remove any cell debris. Supernatants were then either directly used for protein purification, stored at -80°C or used for experiments and stored for short times at 4°C.

2.4.2 Protein purification

Following protein production, the proteins were purified by combination of affinity and size exclusion chromatography. M2-anti-FLAG gel (Sigma) was stacked into a column according to manufacturer's instructions and the protein supernatant was allowed to pass through by gravity flow. The flow-through was collected and passed through the column one more time. The column was washed with 15 column volumes of PBS and the protein was eluted by 5 column volumes of PBS with 200 µg/ml of 3xFLAG peptide. Eluate was concentrated in centrifugation concentrators (Merck Millipore) to approximately 500 µl and purified using size exclusion chromatography on Superdex S200 column (GE Healthcare). Fractions corresponding to DNGR-1 peak were pooled and concentrated using centrifugation concentrators to approximately 1 mg/ml. Aliquots of concentrated DNGR-1 ECD were stored at -80°C and thawed directly before each experiment.

2.4.3 Heterodimeric DNGR-1 ECD generation and purification

293F cells were transfected with a mixture of constructs coding for the desired dimer parts (HA-W155A W250A ECD + FLAG-WT ECD or HA-WT ECD + FLAG-WT ECD) at 2:1 ratio of HA:FLAG, and the supernatant was harvested 3 days later, filtered through 0.22 µm filter and allowed to pass through anti-HA agarose (Sigma) column by gravity flow. The column was washed with 15 column volumes of TBS buffer supplemented with 10 mM $CaCl_2$, and the protein was

eluted with HA peptide (200 µg/ml, 5 column volumes) in TBS + $CaCl_2$. The eluate (3ml) was used in sortagging reaction with 5 µM evolved sortase A and 5 µM AF647 peptide at room temperature for 1 hour. After the reaction, the mixture was allowed to pass through the anti-FLAG (Sigma) column by gravity flow, the column was washed with 5 column volumes of TBS, followed by 10 column volumes of PBS, and the protein was eluted with 5 column volumes of 3xFLAG peptide (200 µg/ml) in PBS.

2.5 Protein-based assays

2.5.1 Densitometry of DNGR-1 proteins in culture supernatants

Equal amounts of cell culture supernatants after DNGR-1 ECD production in 293F cells were analysed by SDS-PAGE and Western blot with HRP-conjugated anti-FLAG antibody used for detection. The signal of DNGR-1 bands was quantified using ImageJ software, and relative concentration of DNGR-1 proteins in the supernatants was determined as the ratio between signal of DNGR-1 mutant and WT.

2.5.2 Dotblot for DNGR-1 mutants

F-actin stabilised by 5 µM phalloidin was spotted onto a nitrocellulose membrane in twofold dilution starting at 40 µg/ml, 100 µl per spot. The membrane was blocked in 5% milk in PBS + 0.05% Tween-20 overnight. Following day, the membrane was incubated with supernatants containing relevant proteins at equal concentration. Membrane was washed 5 times in PBS + 0.05% Tween-20, and incubated with HRP-conjugated anti-FLAG antibody in 5% milk in PBS + 0.05% Tween-20, washed 5 times in PBS + 0.05% Tween-20, and DNGR-1 binding was revealed using SuperSignal West Pico Chemiluminescent substrate. Signal in blots was quantified using ImageJ software and made relative to signal of WT.

2.5.3 Dotblot for DNGR-1 interaction with F-actin under different pH

F-actin stabilised by 5 μM phalloidin was spotted onto a nitrocellulose membrane in twofold dilution starting at 40 μg/ml, 100 μl per spot. The membrane was blocked in 5% milk in PBS + 0.05% Tween-20 overnight. Following day, the membrane strips were transferred into 3 ml of either PBS or MES pH 6.1 buffers and 3 μg of purified DNGR-1 ECD or 500 μl of protein supernatant was added for 1 hour. The membrane was washed 5 times in PBS + 0.05% Tween-20 or MES + 0.05% Tween-20, for half of the membrane strips, the buffers were swapped for the last wash, and the membrane was incubated for another hour with HRP-conjugated anti-FLAG antibody in PBS + 0.05% Tween-20 or MES + 0.05% Tween-20, washed 5 times in the corresponding buffer, and DNGR-1 binding was revealed using SuperSignal West Pico Chemiluminescent substrate.

2.5.4 Pelleting assay

2 μg of F-actin in 10 μl of F-buffer was mixed with decreasing amounts of DNGR-1 ECD (WT or indicated mutant) in 30 μl of PBS, starting at 5 μg and decreasing in twofold dilution. As a control, 5 μg of DNGR-1 ECD was mixed with F-buffer only. Mixture was left for 1 hour at room temperature and pelleted at 120 000 x g for 90 minutes. Both pellet and supernatant were analysed by SDS-PAGE and Western blot with HRP-anti-FLAG antibody.

2.5.5 Biolayer interferometry with DNGR-1 in solution

All biolayer interferometry (BLI) experiments were carried out using Octet RED96 System (ForteBio). Streptavidin (SA) biosensors (ForteBio) were pre-wetted in water for 20 minutes and equilibrated in F-buffer for 30 s. Biotinylated and non-biotinylated G-actin were mixed in 1:4 ratio, diluted to final concentration of 1 μM in 200 ml of F-buffer, and allowed to polymerize directly on the SA biosensors. Free binding sites on SA were blocked in the quenching buffer. Baseline was determined in the interaction buffer and association with DNGR-1 WT or mutants at different concentrations (2.5 μM, 1 μM, 0.4 μM, 0.167 μM and 0.064 μM) was

monitored for 300 s. Dissociation was monitored for 900 s. Data analysis was performed in Data Analysis 4.1 software (ForteBio).

2.5.6 Biolayer interferometry with DNGR-1 on the sensor

23 μM actin was polymerised in the presence of 0.23μM gelsolin to reduce the size of the resulting filaments, as large filaments caused artefacts in BLI signal. Anti-FLAG (FLG) biosensors (ForteBio) were pre-wetted in water for 20 minutes and equilibrated in PBS for 60 s. DNGR-1 ECD was diluted to 0.15 μM and allowed to bind to the sensor for 180 s. Baseline was established in the interaction buffer containing 5 μM phalloidin, and association with 1 μM short actin filaments was observed for 600 s in the interaction buffer. Dissociation was monitored for 900 s in the interaction buffer with 5 μM phalloidin to prevent depolymerisation of the filaments bound to DNGR-1. Data analysis was performed in Data Analysis 4.1 software (ForteBio).

2.5.7 Multi-angle light scattering

Purified DNGR-1 ECD was concentrated to 4 mg/ml and immediately before the analysis, 200 μg of the protein was mixed 1:1 with PBS or 10 mM MES pH 6.1. Size exclusion chromatography was performed on Superdex S75 column, and MALS data were acquired on Dawn Heleos instrument (Wyatt).

2.5.8 Far-UV circular dichroism

Long mouse DNGR-1 ECD was concentrated to 7 mg/ml and immediately before analysis diluted into PBS or 10 mM MES pH 6.1 to final concentration 170 μg/ml. Human ECD was concentrated to 1.4 mg/ml and immediately before analysis diluted into PBS or 10 mM MES pH 6.1 to final concentration 140 μg/ml. 20 CD spectra per sample per condition were acquired in the region between 196 nm and 260 nm and averaged to obtain final spectra.

2.5.9 Near-UV circular dichroism

Long mouse DNGR-1 ECD was concentrated to 5 mg/ml and immediately before analysis diluted tenfold into PBS or 10 mM MES pH 6.1. 20 CD spectra per sample per condition were acquired in the region between 255 nm and 450 nm and averaged to obtain final spectra.

2.6 Cellular assays

2.6.1 Dead cell staining

HeLa cells were UV-irradiated (UVC 240 mJ/cm^2) and left to undergo secondary necrosis. Next day, the cells were washed in FACS buffer and stained with WT or mutant DNGR-1 ECD supernatants at equal concentration. The cells were washed in FACS buffer and binding of DNGR-1 was revealed using Cy3-anti FLAG antibody. Data were acquired on LSR Fortessa flow cytometer (BD Biosciences). To discriminate cells that had lost their membrane integrity, DAPI was added to each sample immediately before analysis. Data were analysed using FlowJo 9.6.2 software (Treestar), and to quantify the binding, binding index was calculated as the mean fluorescence intensity of DNGR-1$^+$ cells multiplied by their frequency in the DAPI$^+$ population and normalized to WT.

2.6.2 Internalization assay

Phoenix cells expressing full length WT or mutant DNGR-1 proteins were treated with 1 μM F-actin, F-buffer only, 5 μg/ml anti-DNGR-1 antibody (clone 7H11) or isotype control antibody and incubated at 37°C for 1 hour. Following the incubation, the cells were washed in ice-cold PBS + 5 mM EDTA, stained with LIVE/DEAD Fixable Dead Cell Stain (Life Technologies) and fixed in 2% formaldehyde. Fixed cells were washed in FACS buffer and stained with PE-conjugated anti-DNGR-1 antibody (clone 1F6). Data were acquired on LSR Fortessa flow cytometer (BD Biosciences) and analysed using FlowJo 9.6.2 software (Treestar). The extent of internalization was determined by comparing the median fluorescence intensity (MFI) of F-actin treated samples with F-buffer treated samples, and anti-DNGR-1

treated samples with isotype control treated samples. For mutant DNGR-1 proteins, the data were normalized to the maximal internalization induced by antibody treatment by using formula (MFI [F-buffer] – MFI [F-actin]) / (MFI [isotype control] – MFI [anti-DNGR-1]) and plotted relative to the internalization of WT.
To confirm that 7H11 antibody binding does not interfere with 1F6 antibody binding, we treated cells on ice with 7H11 before fixation and analysis as described above.

2.6.3 B3Z-Syk reporter assay

B3Z-Syk cells had been prepared and used in the lab previously (Ahrens et al., 2012, Sancho et al., 2009). To compare their response to dead cells, B3Z-Syk cells expressing full length WT or mutant DNGR-1 proteins were plated at 1 x 10^5 per well of a flat-bottom 96-well plate in 100 µl of AIM-V medium, and previously UV-irradiated HeLa cells were added at indicated ratios in further 100 µl of medium. For plate-bound antibody stimulation, the wells were pre-coated with 100 µl of 10 µg/ml 7H11 in PBS. As a control, medium alone was added. The cells were incubated for 16–18 hours at 37°C and 5% CO_2, washed in PBS and lysed in CPRG-containing lysis buffer. LacZ activity was determined by measuring O.D. 595 (using O.D. 655 as a reference) at multiple time points. To account for different levels of expression of various DNGR-1 mutants, the response to dead-cell stimulation was made relative to the response induced by the plate-bound antibody and compared to that of the WT.

2.6.4 *In vitro* cross-presentation assay

The assay was performed by Salvador Iborra and David Sancho (Centro Nacional de Investigaciones Cardiovasculares, Madrid, Spain) as described before (Iborra et al., 2012). RAW264.7 cells were infected with rVACV-OVA for 4 hours, UV-irradiated (UVC 240 mJ/cm^2) or left un-irradiated, and cultured for further 16 hours. WT or DNGR-1 KO Flt3L DCs transduced with desired constructs were generated as described above. On day 9 of culture, the cells were harvested, mixed with the rVACV-OVA infected and irradiated or non-irradiated RAW264.7 cells for 2 hours before OVA-specific $CD8^+$ T-cells were added. After further

6 hours of incubation, brefeldin A (Sigma-Aldrich, 5 μg/ml) being added for the last 4 hours, the cells were fixed in 4% formaldehyde, permeabilised with 0.1% saponin, and stained with APC–anti–IFN-γ. Data were acquired on LSR Fortessa flow cytometer (BD Biosciences) and analysed using FlowJo 9.6.2 software (Treestar).

2.7 Microscopy

2.7.1 Electron cryomicroscopy

All electron cryomicroscopy experiments were carried out by Takashi Fujii and Keiichi Namba (Riken Quantitative Biology Center, Osaka, Japan). Human platelet actin was polymerized in a 30 μl solution of 25 mM HEPES buffer (pH 7.5), 100 mM KCl, 1 mM $MgCl_2$, and 1 mM ATP. F-actin and DNGR-1 were mixed in final concentrations of 1.8 μM and 7.6 μM, respectively. A 2.4 μl aliquot was applied onto a holey carbon molybdenum EM grid (R0.6/ 1.0, Quantifoil), blotted and plunge-frozen into liquid ethane by Vitrobot (FEI). The grid was observed at temperatures of ~ 80 K using a JEOL JEM3200FSC electron cryomicroscope equipped with an U-type energy filter and a field emission electron gun operated at 200 kV. Zero energy-loss images, with a slit setting to remove electrons of an energy-loss larger than 10 eV, were recorded on a 4k x 4k 15 μm/pixel slow-scan CCD camera (TemCamF415MP, TVIPS) at a magnification of 109,489 x (1.37 Å/pixel), a defocus range of 1.0–2.0 μm and an electron dose of ~20 electrons/$Å^2$. Helical image analysis and 3D image reconstruction was carried out as previously described (Fujii et al.) by using the iterative helical real-space refine method (Egelman, 2000). The resolution of the reconstructed 3D image was determined by the Fourier shell correlation (FSC) method, in which the filament images were randomly divided into two sets, image analysis was carried out independently for the two sets of data to produce two 3D images, and the FSC was calculated from these two 3D images.

2.7.2 TIRF microscopy of single actin filaments

In vitro biotinylated spectrin was allowed to adhere to a coverslip, washed, and G-actin mixed with F-buffer and 5 μM AF488 Phalloidin immediately beforehand was applied and allowed to polymerise for 5 minutes. Phalloiding-labelled short actin filaments were then decorated with AF-647-labelled DNGR-1 proteins and observed under a TIRF microscope.

2.8 Statistical analysis

For the statistical analysis of the quantification of dot blot, dead-cell staining assay and internalization assay, one-way ANOVA with Dunnett's multiple comparisons test was performed in GraphPad Prism version 6.0 for Mac OS X (GraphPad Software).
For the steady state analysis of biolayer interferometry data, non-linear regression (curve fit, one site – specific binding) was performed using GraphPad Prism version 6.0 for Mac OS X (GraphPad Software).

Chapter 3. The neck region of DNGR-1 acts as a pH and ionic strength specific sensor

3.1 Introduction

DNGR-1 is a member of the C-type lectin superfamily and this is reflected by its overall domain organization (Huysamen et al., 2008, Sancho et al., 2008). The extracellular portion of DNGR-1 comprises a single CTLD and a neck region of isoform-specific length (Huysamen et al., 2008, Sancho et al., 2008). Both human and one of the murine isoforms have been shown to be dimeric, a property which is predicted to be attributable to a disulphide bond within the neck region (Huysamen et al., 2008, Sancho et al., 2008).

Historically, the neck regions of both C-type lectins and other receptors used to be considered a mere “scaffold” on which the ligand binding domains rest and which connect them to the membrane and the intracellular signalling motifs. As such, the contribution of the neck regions to the properties and functions of receptors were rarely assessed and in structural studies the neck regions tended to be ignored altogether. This notion, however, is quickly becoming an out-dated one, as neck regions of multiple receptors have now been shown to regulate their various functional properties. Among the C-type lectins, the neck of Ly49 receptors was shown to regulate their binding to MHC-I molecules (Back et al., 2009) while the neck of DC-SIGN serves as a pH-sensor controlling oligomerization of the receptor (Tabarani et al., 2009).

Consequently, when we set out to assess the properties of DNGR-1, we decided to use the entire extracellular domain including the neck region, rather than the ligand-binding domain alone.

3.2 Results

3.2.1 The cysteine in the neck region is responsible for covalent dimerization of both *long* and *short* mDNGR-1

In order to assess the properties of DNGR-1, we expressed the entire extracellular domain (ECD) of both *long* and *short* mDNGR-1 isoforms in 293F cells as

described previously (Ahrens et al., 2012). Consistently with previous reports (Ahrens et al., 2012, Sancho et al., 2009, Sancho et al., 2008), *long* mDNGR-1 ECD expressed as a disulphide-bonded homodimer, which could under normal conditions be reduced to its constitutive monomers using reducing agents such as dithiothreitol (DTT) or β-mercaptoethanol (β-ME) (Fig 3.1A). Contrary to a previous report describing expression of the *short* isoform as a monomer (Huysamen et al., 2008), we observed the ECD protein as a disulphide-bonded dimer (Fig 3.1A), consistent with the presence of the putative dimerization cysteine at position 94 in both isoforms. Supporting the idea that the cysteine in the neck region is responsible for covalent dimerization of DNGR-1, mutating it to serine (C94S) resulted in a mutant protein with electrophoretic mobility corresponding to that of a monomer under both reducing and non-reducing conditions (Fig 3.1B). The mutation, however, had a strong adverse effect on the expression efficiency (data not shown).

All mouse DNGR-1 isoforms contain two putative N-glycosylation sites (Gavel and von Heijne, 1990) – one in the neck region and one in the CTLD itself (Fig 3.1C). While the *long* DNGR-1 isoform has been shown to be glycosylated (Sancho et al., 2008), the short isoform has been reported to be non-glycosylated (Huysamen et al., 2008). In an attempt to reconcile these contradictory observations, we subjected both *long* and *short* DNGR-1 ECD isoforms expressed in 293F cells to deglycosylation treatment using PNGase F, followed by analysis by SDS-PAGE and Western blot (Fig 3.1D). Interestingly, we observed a clear shift in the electrophoretic mobility of both proteins after the deglycosylation treatment, suggesting that both are decorated with N-linked glycans (Fig 3.1D), consistent with the conservation of the glycosylation sites.

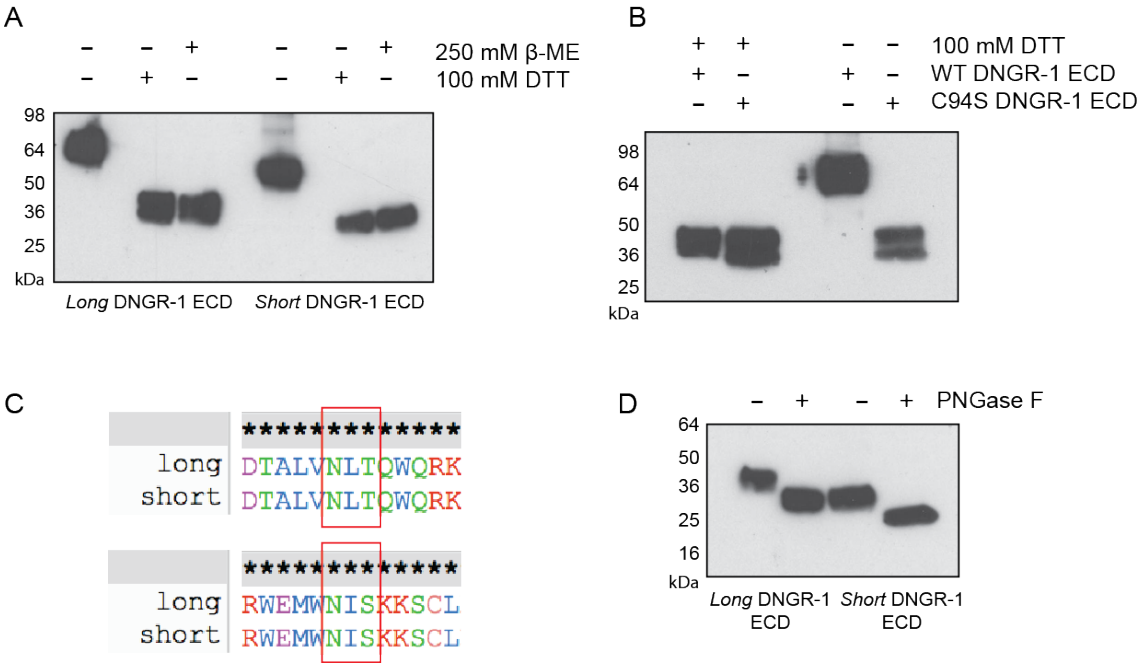

Figure 3.1 *Long* and *short* mouse DNGR-1 isoforms are expressed as glycosylated, disulphide-bonded dimers

A, Supernatants after protein production of *long* and *short* DNGR-1 ECD were prepared for SDS-PAGE and Western Blot analysis under reducing (100 mM DTT or 250 mM β-mercaptoethanol) or non-reducing conditions. **B**, Supernatant after protein production of C94S mutant was 200x concentrated and analysed by SDS-PAGE and Western blot under reducing and non-reducing conditions alongside control WT supernatant. **C,** Alignment of the regions of *long* and *short* DNGR-1 isoforms containing the putative N-glycosylation sites (highlighted by the red rectangle). **D**, Supernatants after protein production of long and short DNGR-1 ECD were denatured by treatment with DTT at 100°C and treated with PNGase-F overnight, or mock-treated without the addition of the enzyme. After the treatment all samples were analysed by SDS-PAGE and Western Blot. HRP-conjugated anti-FLAG antibody was used for detection of all proteins. Numbers on the side of blots indicate positions of MW markers.

3.2.2 DNGR-1 can form reduction insensitive dimers

Surprisingly, we noticed that under certain conditions, the dimers of DNGR-1 ECD could become resistant to DTT-mediated reduction and maintained their dimeric status even in the presence of the reducing agent.

We speculated that ligand binding might cause the reduction insensitivity of DNGR-1 dimers. To test this hypothesis, we mixed a constant amount of purified DNGR-1 ECD with increasing amounts of *in vitro* polymerised F-actin, or F-actin buffer only as a control. Presence of F-actin, however, had no effect on the sensitivity of

DNGR-1 ECD to reducing agents (Fig 3.2A). Diluting DNGR-1 ECD into buffers of lower pH and ionic strength proved to be effective in inducing the reduction insensitive state though (Fig 3.2B). We tested buffers of different ionic strengths and pH (the range of pH 6.5 – 8.0 and ionic strength 15 – 250 mM), while keeping the buffering capacity of all buffers constant. After analysis by SDS-PAGE with 100 mM DTT, we observed a clear trend towards higher abundance of reduction insensitive dimers as the pH and ionic strength decreased (Fig 3.2C). Interestingly, the conditions under which the reduction insensitive dimers were abundant correspond to the conditions found in the endocytic pathway, while the conditions where no reduction insensitive dimers were observed correlate with those in the extracellular milieu (Scott and Gruenberg, 2011).

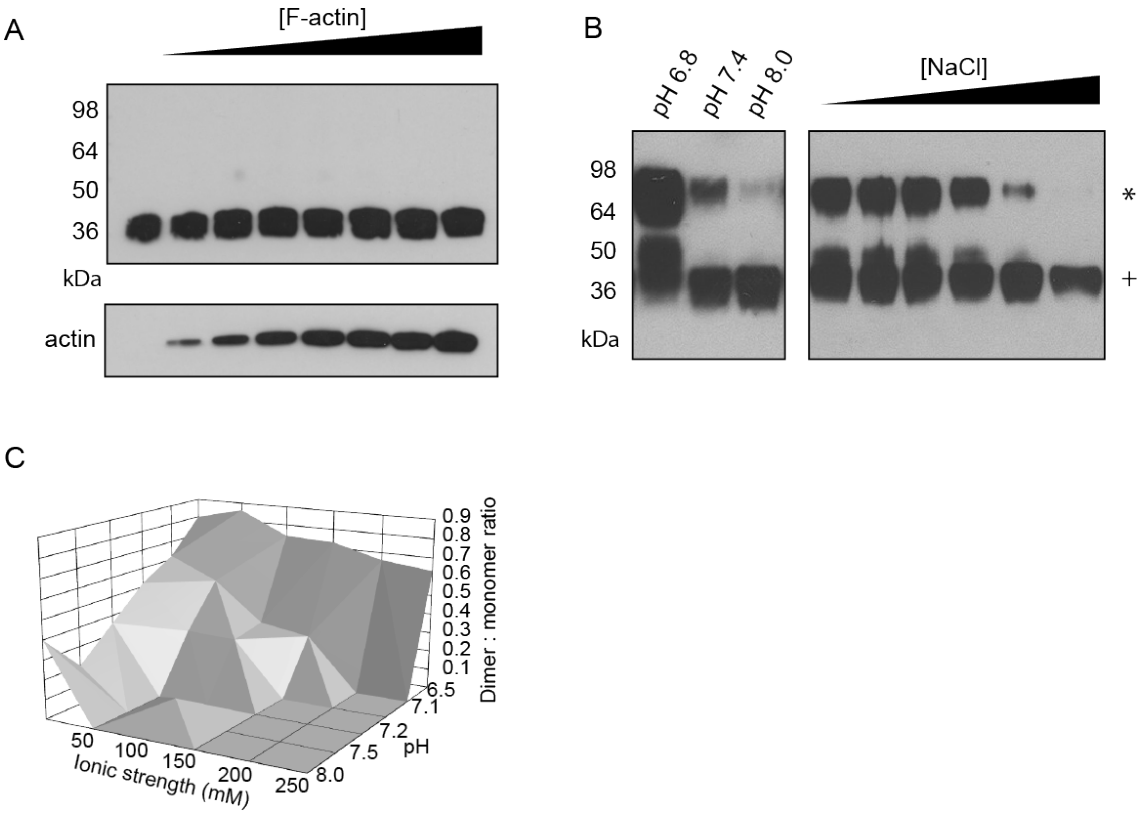

Figure 3.2 Reduction insensitive dimers of DNGR-1 ECD can be induced by low pH and ionic strength

A, 0.25 µg of DNGR-1 ECD was mixed with increasing amount of *in vitro* polymerised F-actin (0.15 – 10 µM), and reduction sensitivity of DNGR-1 was assessed by reducing SDS-PAGE and Western blot. Numbers on the side of blots indicate positions of MW markers. **B,** 0.25 µg of DNGR-1 ECD was diluted into 10 mM Tris buffer of indicated pH (left panel) or into 10 mM Tris pH 7.4 buffer supplemented with increasing amounts of NaCl (1 – 250 mM), and reduction

sensitivity of DNGR-1 was assessed by reducing SDS-PAGE and Western blot. Numbers on the side of blots indicate positions of MW markers. Reduction-resistant dimers are indicated with an * and reduction-sensitive protein with a +. **C,** 0.25 µg of DNGR-1 was diluted into thirty-six different buffers of different pH and ionic strength, and its reduction sensitivity was assessed by reducing SDS-PAGE and Western blot. The strength of bands corresponding to dimer and monomer was determined densitometrically, and their ratio was plotted as function of ionic strength and pH. HRP-conjugated anti-FLAG antibody was used for detection of all proteins.

3.2.3 Conformational change in the neck region is responsible for the formation of reduction insensitive dimers

Since the neck region is responsible for dimerization of DNGR-1, we hypothesized that a conformational change in this portion of the protein could be responsible for the buffer-dependent reduction insensitivity of DNGR-1 ECD. Conceivably, the effect could be mediated either by means of sterical protection of the disulphide bond from the reducing agents, or by conformational rearrangement that makes the disulphide bond dispensable for maintaining the dimeric status of the protein. In either case, a change in the structural elements of the protein would need to be involved. To test this hypothesis, we subjected the reduction insensitive form of DNGR-1 ECD to mildly denaturing (Leammli buffer) or strongly denaturing (8 M urea) conditions before applying DTT. As predicted, strongly denaturing conditions abolished the ability of DNGR-1 ECD to resist reduction, while under weakly denaturing conditions reduction insensitive dimers could be observed. As expected, in the absence of reduction agents, the protein maintained its dimeric status regardless of the denaturing conditions (Fig 3.3A). To the same end, we gradually increased the stringency of the heat denaturation step by increasing the time of boiling in Laemmli buffer. When analysed by Western blot, DNGR-1 ECD appeared exclusively as a monomer after 5 minutes of boiling under neutral conditions, while the protein kept under mildly acidic conditions (MES pH 6.1) was not completely reduced by 15 minutes of treatment (Fig 3.3B).

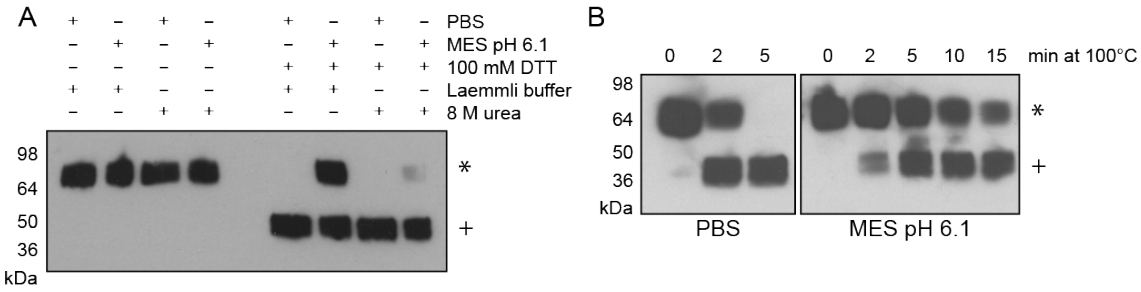

Figure 3.3 Conformational change in DNGR-1 is responsible for the formation of reduction-resistant dimers

A, 0.25 µg of DNGR-1 ECD was diluted into PBS or 10 mM MES pH 6.1 buffer, and its reduction sensitivity was tested under mildly (Laemmli buffer) or strongly denaturing (8 M urea) conditions by reducing SDS-PAGE and Western blot. **B,** 0.25 µg of DNGR-1 ECD was diluted into PBS or 10 mM MES pH 6.1 buffer, and its reduction sensitivity after different length of heat-denaturation in Laemmli buffer was tested by reducing SDS-PAGE and Western blot. HRP-conjugated anti-FLAG antibody was used for detection of all proteins. Numbers on the side of blots indicate positions of MW markers. Reduction-resistant dimers are indicated with an * and reduction-sensitive protein with a +.

3.2.4 The conformational change of DNGR-1 is reversible

To evaluate reversibility of the conformational change, we subjected DNGR-1 ECD to mildly acidic treatment (MES pH 6.1) to induce the reduction insensitivity, or kept it in PBS as a control. Half of the MES-treated sample and the PBS sample were then dialyzed against PBS and together with the un-dialyzed MES sample analysed using reducing SDS-PAGE and Western blot. As expected, we observed increase in reduction insensitivity in the protein kept under mildly acidic condition. However, the protein that had been MES-treated and dialysed back into PBS afterwards showed no increase in reduction insensitivity (Fig 3.4). This suggests that the conformational change is not just non-specific aggregation of the protein but rather a controlled, reversible process.

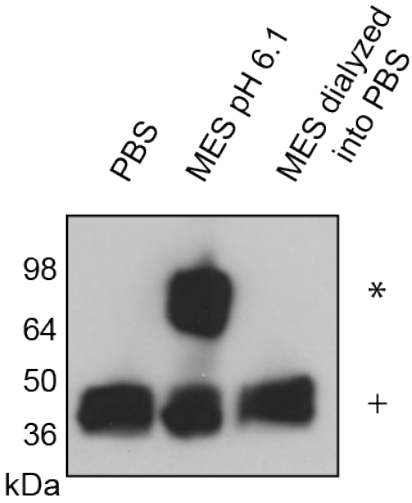

Figure 3.4 The conformational change in DNGR-1 is reversible

1 µg of DNGR-1 ECD was transferred into MES pH 6.1 and 0.5 µg into PBS. Half of the MES sample and the whole PBS sample were dialyzed against 2 l of PBS overnight at 4°C. After dialysis, all the samples were prepared for SDS-PAGE and Western blot. HRP-conjugated anti-FLAG antibody was used for detection of all proteins. Numbers on the side of the blot indicate positions of MW markers. Reduction-resistant dimers are indicated with an * and reduction-sensitive protein with a +.

3.2.5 The neck region is sufficient for the conformational change

To test whether the neck region is involved in and sufficient for the formation of reduction insensitive dimers, we generated a chimeric ECD where the neck region of DNGR-1 was fused to the CTLD of another C-type lectin, Dectin-1 (C9C7 chimera; Fig 3.5A). As expected, unlike the Dectin-1 ECD control, the chimeric ECD expressed as a disulphide-bonded homodimer (Fig 3.5B), consistent with our data showing that the neck region mediates dimerization of DNGR-1. Notably, under conditions, which induced reduction insensitive state in DNGR-1 ECD, the C9C7 chimera was also refractory to DTT-mediated reduction (Fig 3.5C). We conclude that the neck region of DNGR-1 can serve as a sensor of pH and ionic strength responding to some conditions by undergoing a reversible conformational switch.

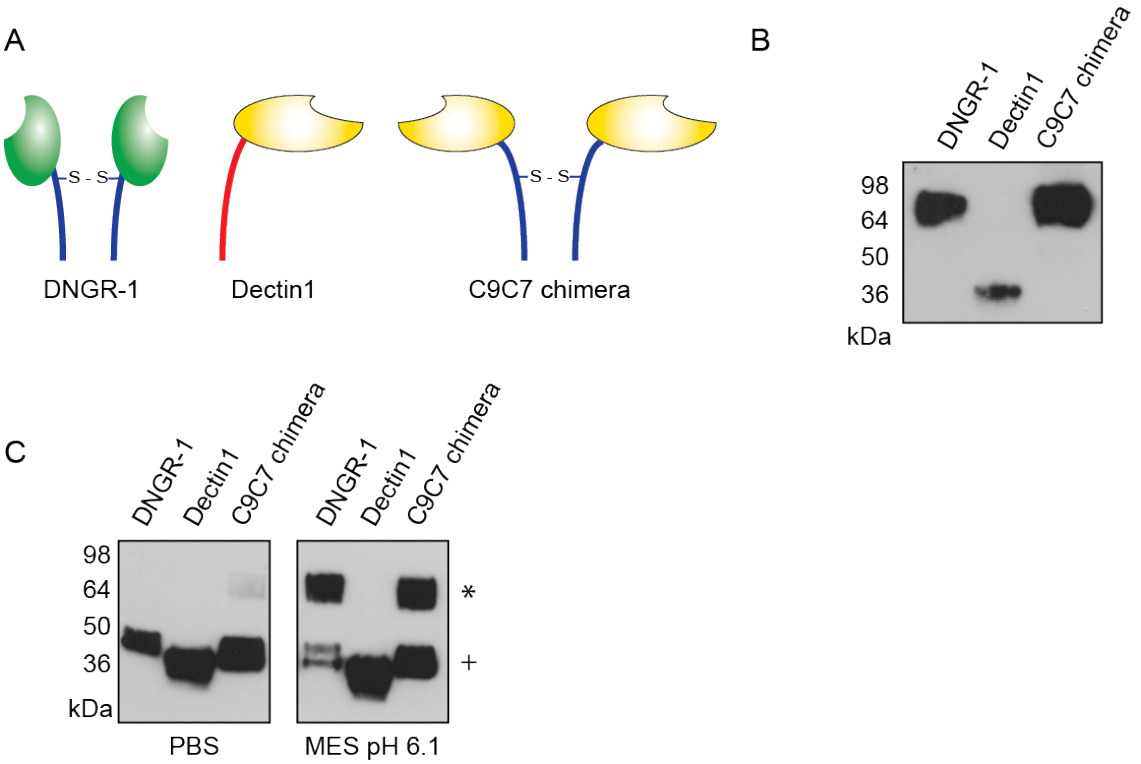

Figure 3.5 DNGR-1 neck region is sufficient and necessary for the formation of reduction-resistant ECD dimers

A, Schematic depiction of DNGR-1, Dectin-1 and the C9C7 chimeric receptor **B,** protein production supernatants containing ECD of DNGR-1, Dectin-1 and C9C7 chimera were prepared for SDS-PAGE and Western blot under non-reducing conditions. **C,** Supernatants after protein production of indicated proteins were diluted into PBS or pH 6.1 MES buffer and analysed using SDS-PAGE and Western blot under reducing conditions. HRP-conjugated anti-FLAG antibody was used for detection of all proteins. Numbers on the side of blots indicate positions of MW markers. Reduction-resistant dimers are indicated with an * and reduction sensitive protein with a +.

3.2.6 Ability to undergo pH and ionic strength-induced conformational change is conserved between mouse and human DNGR-1 isoforms

To confirm that the ability to undergo conformational change is not an isoform-specific property, we made recombinant proteins corresponding to the ECD of human and both *long* and *short* mouse DNGR-1 isoforms, and tested their reduction sensitivity in different buffers. All of the proteins were expressed as disulphide-bonded homodimers, and when subjected to weakly acidic conditions (pH 6.1) showed increased resistance to DTT-mediated reduction (Fig 3.6). This

suggests that the ability to undergo the conformational change is an evolutionarily conserved property of DNGR-1.

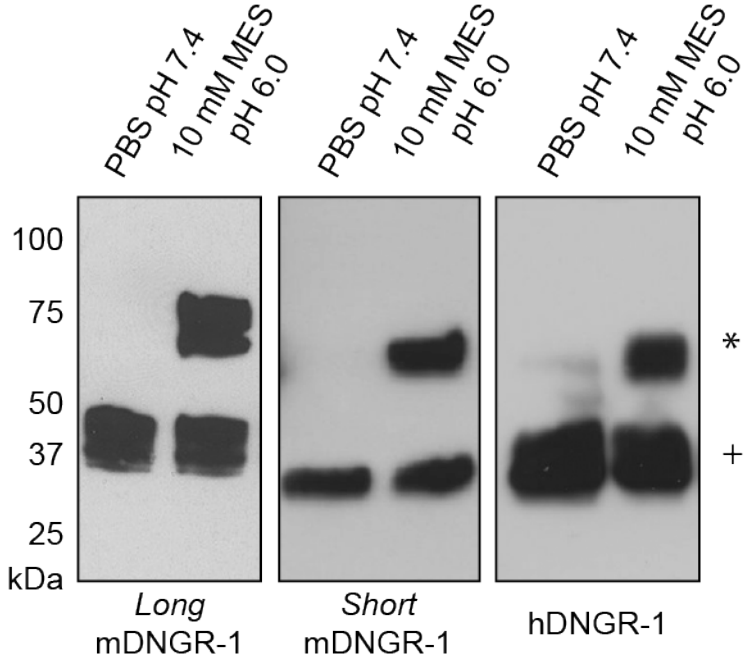

Figure 3.6 Formation of reduction-resistant dimers is conserved between various DNGR-1 isoforms

Supernatants after protein production in 293F cells were harvested and diluted into indicated buffers at a 2:3 ratio and analysed using reducing SDS-PAGE and Western blot. HRP-conjugated anti-FLAG antibody was used for detection of all proteins. Numbers on the side of blots indicate positions of MW markers. Reduction-resistant dimers are indicated with a * and reduction-sensitive protein with a +.

3.2.7 Membrane-bound DNGR-1 can undergo the conformational change

DNGR-1 proteins in which we observed the conformational change were all expressed as soluble ECDs, lacking the transmembrane and intracellular domains. To assess whether the phenomenon could be observed in the context of the full-length protein, we lysed DNGR-1-expressing transfected cells under neutral or mildly acidic conditions and tested the reduction sensitivity of DNGR-1 contained in the lysates. While SDS-lysis under neutral conditions resulted in complete reducibility of DNGR-1 dimers, SDS-lysis under mildly acidic conditions induced reduction insensitive state in the full-length receptor (Fig 3.7, left panel). Similar results were also obtained using MuTu DC1940 CD8α^{+}-like DC line (Fuertes

Marraco et al., 2012) that expresses DNGR-1 from its endogenous locus (Fig 3.7, right panel).

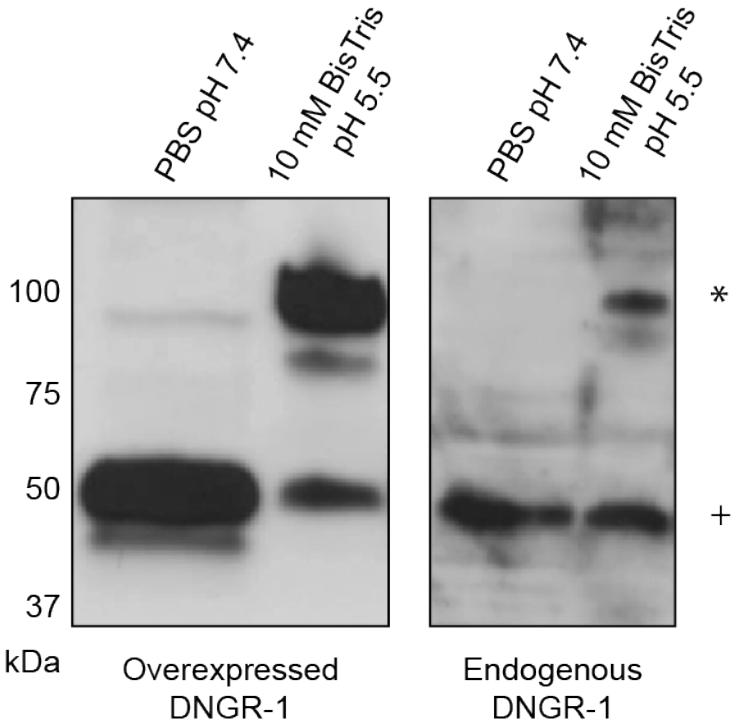

Figure 3.7 Membrane-bound DNGR-1 can undergo the conformational change

Cells retrovirally transduced to overexpress mouse DNGR-1 (*long* isoform; left panel) or cells endogenously expressing DNGR-1 (right panel) were lysed in 1% SDS in PBS or 10 mM BisTris pH 5.5 buffer and prepared for reducing SDS-PAGE and Western blot. Monoclonal anti-DNGR-1 antibody (397) in combination with HRP-coupled anti-rat monoclonal antibody was used for detection. Numbers on the side of blots indicate positions of MW markers. Reduction-resistant dimers are indicated with a * and reduction-sensitive protein with a +.

3.2.8 The conformational change happens at the level of tertiary structure

In order to characterize the conformational change further, we made use of circular dichroism (CD). Far-UV CD spectra of proteins are representative of their secondary structure content, and such analysis can reveal the relative contribution of elements of secondary structure to the overall structural composition of the protein. In contrast, near-UV CD spectra are specific for particular residues (Phe, Tyr, Trp) and disulphide bonds, and are reflective of the residues' environment and dipole orientation, and the torsion angle of the disulphide bonds (Martin and Schilstra, 2008). First, we utilized far-UV CD to determine if the conformational

change we observed happens at the level of secondary structure. We acquired spectra of both *long* mouse and human DNGR-1 ECDs under neutral (PBS) and mildly acidic (MES pH 6.1) conditions, and we observed almost perfect overlap between the two conditions (Fig 3.8A). Detailed analysis revealed for both mouse and human ECDs only a very minor increase in the content of alpha helical structure, corresponding to approximately four residues (Table 4).

		alpha helix	beta sheet	beta turn	random
mDNGR-1 ECD	PBS	16.1 %	22.5 %	17.1 %	44.3%
	MES	17.8 %	21.8 %	17.0 %	43.5%
hDNGR-1 ECD	PBS	22.3 %	21.3%	19.5 %	37.2%
	MES	24.2 %	20.7 %	20.8 %	34.2 %

Table 4 Relative contributions of the elements of secondary structure to mouse and human DNGR-1 ECD under different conditions

Interestingly, the different amount of disordered structure observed in mouse and human isoform (44% vs. 37% in PBS; Table 4) corresponds to approximately twenty six residues. The human and mouse isoforms differ by the presence of an extra exon coding for a stretch of twenty-six residues in the neck region of mouse DNGR-1. Thus, our data suggest that the amino acids in the extra exon of mouse *long* DNGR-1 isoform form an unstructured loop, and that the conformational change we observed does not happen at the level of secondary structure.

With no large change in the ECD secondary structure, we speculated that mutual repositioning of the two neck regions within the dimer might be at the root of the observed reduction resistance. To test this hypothesis, we acquired near-UV CD spectra of *long* mouse DNGR-1 ECD under neutral (PBS) and mildly acidic (MES pH 6.1) conditions (Fig 3.8B). The spectra showed clear differences, with a broad band between 270 nm and 350 nm indicating a change in the torsion angle of a disulphide bond, and narrow bands in the area around 280 nm and 290 nm indicating a change in the environment of at least one tryptophan residue. Taken together, near-UV and far-UV CD thus suggest that a change in the tertiary structure, but not secondary structure happens when DNGR-1 undergoes transition to the reduction insensitive form. These data are consistent with a model where

repositioning of the neck regions within the dimer results in protection of the disulphide bond, explaining the phenomenon of reduction resistance of DNGR-1 under certain conditions. To make a clear distinction of the two conformational states, we propose to call the reduction sensitive form “Type-1 dimer” and the reduction insensitive form “Type-2 dimer” (Fig 3.8C).

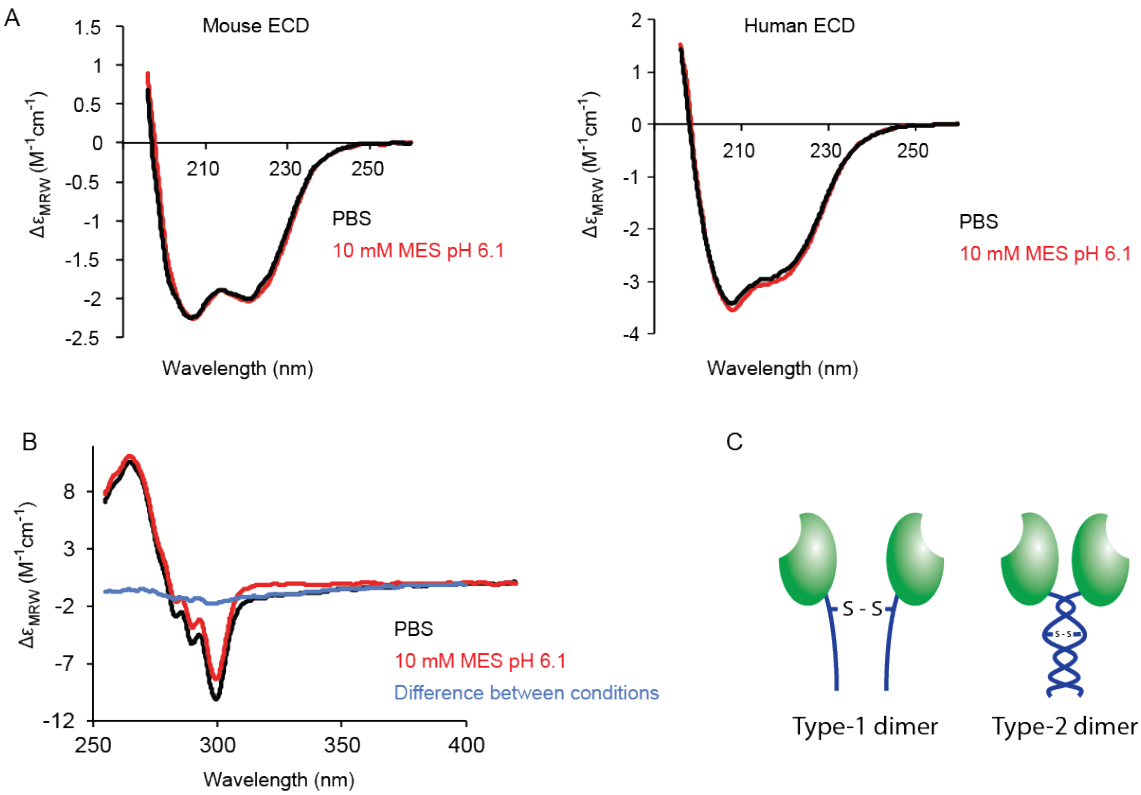

Figure 3.8 A change in the tertiary structure is responsible for the formation of reduction-resistant dimers

A, Mouse and human DNGR-1 ECD were diluted to the final concentration of 150 µg/ml in PBS or 10 mM MES pH6.1 buffer and 20 far-UV spectra were acquired for each condition (red and black lines depict the composite curve for each condition) **B,** Mouse DNGR-1 ECD was diluted to the final concentration of 500 µg/ml in PBS or 10 mM MES pH 6.1 buffer and 20 near-UV spectra were acquired for each condition (red and black lines depict the composite curve for each condition and the blue line shows the difference between the two). **C,** Schematic representation of the suggested conformational states of DNGR-1.

3.2.9 Mutations in the neck region affect Type-2 dimer formation and dimerization of DNGR-1

We observed Type-2 dimer formation in both mouse and human DNGR-1, suggesting that the part of the neck region involved in the process is conserved between the two proteins. Hence, in order to assess which parts of the neck play a role in Type-2 dimer formation, we genetically removed overlapping blocks of ten or eleven amino acids from the conserved part of the neck (K57 – L66 (Δ1), L64 – I73 (Δ2), L72 – L82 (Δ3), N81 – T90 (Δ4), R87 – A96 (Δ5) and Q95 – S104 (Δ6) (Fig 3.9A)), expressed the resulting constructs as ECDs, and tested their ability to form Type-2 dimers (Fig 3.9B). The mutants devoid of the first two blocks (Δ1 and Δ2) expressed to a comparable extent to the WT and showed no phenotype with respect to Type-1 or Type-2 dimers formation. The expression of Δ3 mutant was significantly reduced in comparison to the WT, even though it also exhibited no obvious phenotype. Δ6 mutant failed to express completely (Fig 3.9B). On the other hand, Δ4 mutant expressed as efficiently as the WT, but showed enhanced Type-2 dimer formation even under neutral conditions (Fig 3.9B). Δ5 mutant lacks the dimerization cysteine (C94), and consequently behaves as a monomer when analysed in both reducing and non-reducing conditions using SDS-PAGE (Fig 3.9B). Unlike the C94S mutant, however, the Δ5 mutant expressed as efficiently as the WT (Fig 3.9B). Reintroduction of a cysteine residue alone into Δ5 mutant (Δ5+C) resulted in a drastic decrease of expression (Fig 3.9C), which could be rescued by mutating all the residues in block 5 except for the cysteine to alanines (Δ5A+C). Furthermore, Δ5A+C protein was dimeric with an increased propensity for Type-2 dimer formation (Fig 3.9C), presumably due to partial overlap of blocks 4 and 5 (Fig 3.9A).

To confirm that the effects we saw with the “block mutants” were a specific result of the loss of the different regions and not just a non-specific consequence of parts of the neck region getting “out of sync” due to part of the helices missing, we substituted all the residues within blocks 3, 4 and 6 with strings of alanines of appropriate lengths and expressed the proteins as soluble ECDs. Importantly, replacing all the residues in block 4 (Δ4A) resulted in a protein mimicking the behaviour of the Δ4 mutant (Fig 3.9D), suggesting a specific involvement of some of the residues present in this region. Interestingly, and unlike the Δ3 and Δ6

mutants, the mutants with residues in blocks 3 and 6 replaced with alanines (Δ3A and Δ6A) got expressed, even though in the case of Δ6A to lower extent than the WT. Notably, while Δ3A mutant showed no phenotype, Δ6A mutant failed to form Type-2 dimers under conditions which were effective in inducing their formation in the WT protein (Fig 3.9D).

We noticed a putative N-glycosylation site (NxT sequence) (Gavel and von Heijne, 1990) at the boundary of blocks 3 and 4, which is disrupted in both Δ3 and Δ4 mutants (Fig 3.9A). Consistent with this site being glycosylated in mouse DNGR-1, both Δ3A and Δ4A mutants showed higher electrophoretic mobility than WT or Δ6A mutant (Fig 3.9D). As Δ3A and Δ4A mutants do not exhibit the same phenotype, however, the glycosylation appears not to be involved in Type-2 dimer formation.

Taken together, our data are consistent with a model where residues in the block 4 serve as spring “pushing” the neck regions apart, preventing Type-2 dimer formation under normal conditions, while residues in the block 6 appear to be directly responsible for Type-2 dimer formation. Residues in the block 5 appear to serve as mere “filling,” allowing for covalent dimerization through the disulphide bond, and their exact identity seems largely irrelevant, consistent with their limited conservation between mouse and human DNGR-1 (Fig 3.9A).

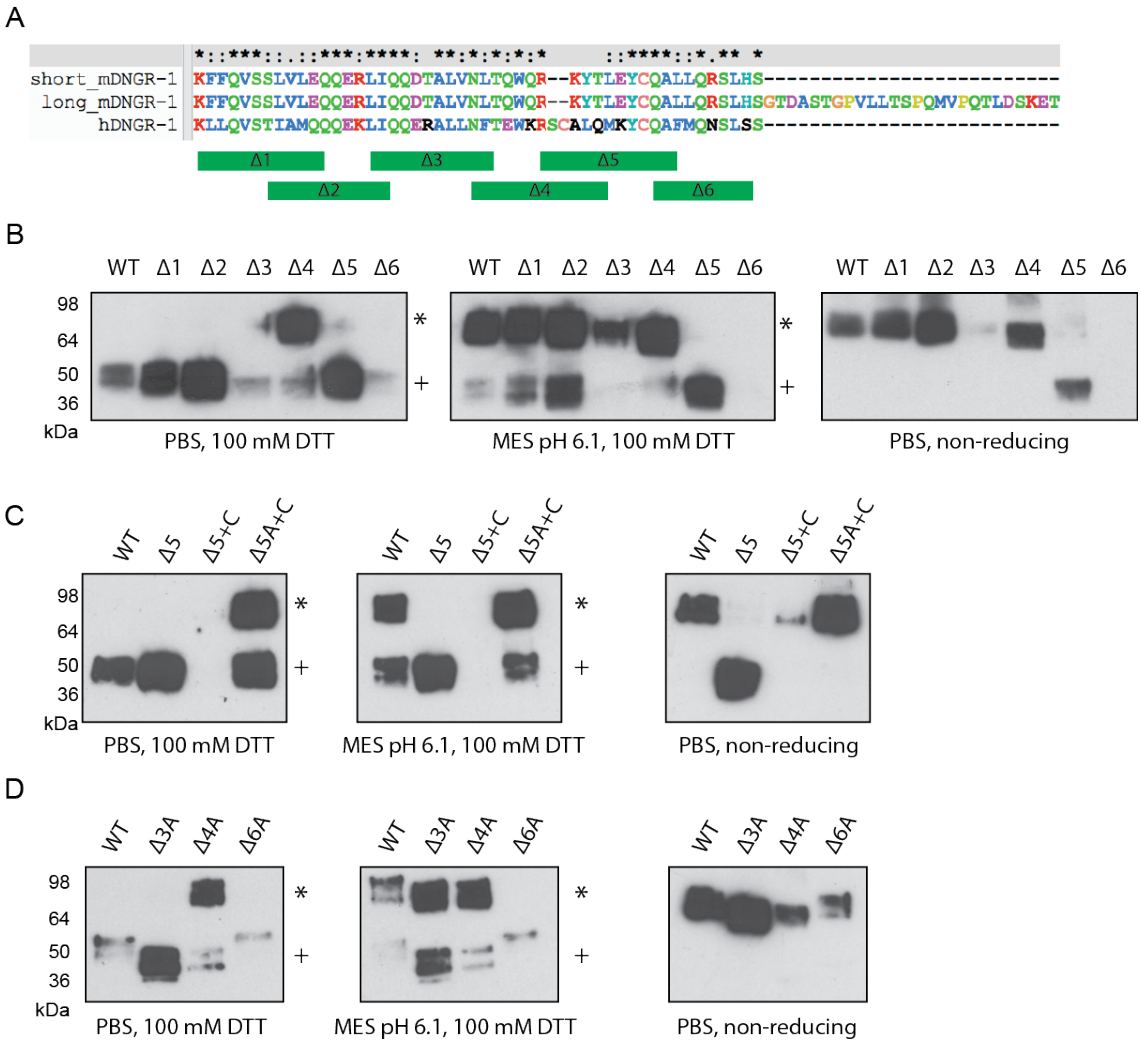

Figure 3.9 Distinct parts of the neck region contribute to regulation of Type-2 dimer formation

A, Sequences of the neck region of human and *long* and *short* isoform of mouse DNGR-1 aligned in Clustal X software. Parts of the neck corresponding to the block deletions are depicted as green bars. **B,C** and **D,** Supernatants after production of indicated ECD proteins (mouse, *long* isoform) were diluted into indicated buffers in 1:2 ratio and analysed by SDS-PAGE and Western blot under reducing or non-reducing conditions. HRP-conjugated anti-FLAG antibody was used for detection of all proteins. Numbers on the side of blots indicate positions of MW markers. Reduction-resistant dimers are indicated with an * and reduction-sensitive protein with a +.

3.2.10 The conformational change does not grossly affect oligomerization status of DNGR-1

The neck region of another C-type lectin, DC-SIGN has previously been reported to serve as a pH-sensor regulating oligomerization of the receptor (Tabarani et al.,

2009). To test whether the neck region of DNGR-1 could serve a similar purpose, we tested the oligomerization status of DNGR-1 ECD under different conditions using multi-angle light scattering (MALS). While we observed no gross changes in the oligomerization status, we saw subtle changes in the apparent molecular weight ranging between 60 – 90kDa in different buffers (data not shown). The reasons for this heterogeneity are currently unclear and focus of an on-going investigation, however, our data suggest that the oligomerization status of DNGR-1 is not grossly affected by the formation of Type-2 dimers.

3.2.11 Type-2 dimer formation does not affect the ability of DNGR-1 to bind F-actin

A pH-induced conformational change in another C-type lectin, DEC205, has recently been shown to allow the protein to recognise a ligand in apoptotic and necrotic cells (Cao et al., 2015). Consequently, we set out to determine if the conformational change in DNGR-1 affects its ability to bind F-actin. To this end we utilised the dot blot assay (Ahrens et al., 2012) (Fig 3.10) where decreasing amounts of *in vitro* polymerised actin were spotted onto a membrane, and the membrane was blocked and incubated with DNGR-1 WT, Δ4 or Δ6A mutant ECDs in PBS or MES pH 6.1 buffers. Binding of ECD was then revealed using anti-FLAG antibody. To account for possible artefacts caused by different ability of the anti-FLAG antibody to bind under different conditions, two pieces of membrane were incubated with each DNGR-1 protein under each condition, and one of them was then switched to the second buffer condition for antibody detection step, while the other was kept in the same buffer. Using this setup, we could not observe any differences in the binding ability of WT, Δ4 or Δ6A DNGR-1 ECDs in any of the buffers (Fig 3.11), suggesting that the conformational change is not involved in the regulation of DNGR-1 ligand-binding.

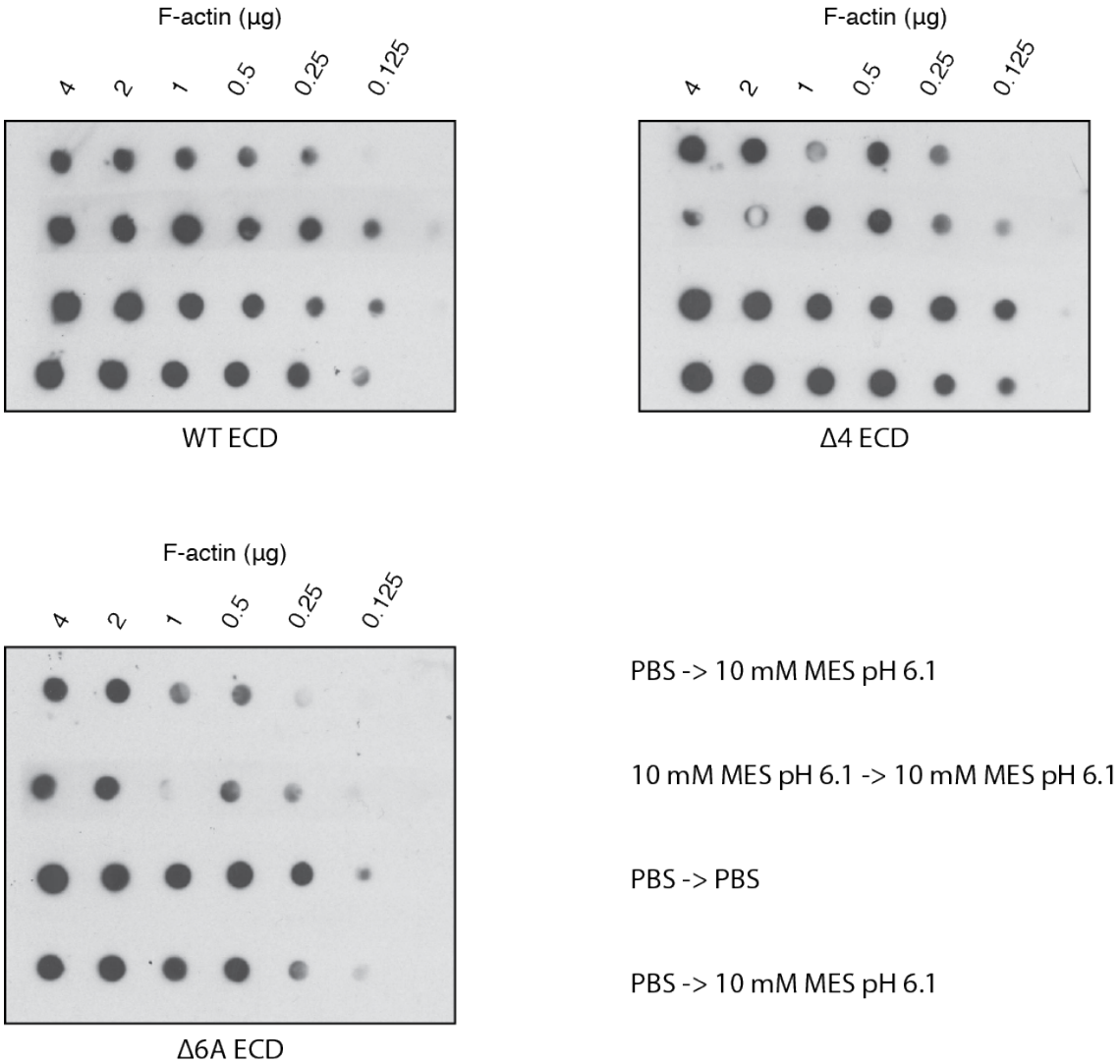

Figure 3.10 The conformational change does not affect binding of DNGR-1 to F-actin

Decreasing amounts of F-actin were spotted onto a nitrocellulose membrane and binding of indicated DNGR-1 ECD proteins (mouse, *long* isoform) was tested under conditions shown in the lower right corner, first column. HRP-conjugated anti-FLAG antibody was used for detection in conditions shown in the lower right corner, second column.

3.2.12 The phenotypes observed in "block mutant" ECDs are maintained when expressed as transmembrane proteins.

To test the functional capability of the Δ4 and Δ6A DNGR-1 mutants in cells, we re-made them as transmembrane proteins and retrovirally introduced them into Phoenix cells. First, to confirm that the phenotypes we observed for the soluble

ECD “block mutant” proteins are also valid for transmembrane proteins, we lysed the Phoenix cells in 1% SDS in either 10 mM MES pH 6.1 or PBS buffers and prepared the samples for reducing SDS-PAGE and Western blot analysis. As expected, WT protein appeared exclusively as Type-1 dimer in the PBS sample, while lysis in the MES buffer induced Type-2 dimer formation (Fig 3.11). On the other hand, the Δ4 mutant appeared in the form of Type-2 dimers in both buffers, while the Δ6A mutant exhibited no Type-2 dimer formation in either (Fig 3.11). In the case of the Type-2 dimer samples, (WT in MES buffer and Δ4 mutant in both conditions), we observed multiple bands, seemingly corresponding to reduction-insensitive higher oligomers (Fig 3.11). We never observed similar phenomenon for the soluble protein, and given that under normal conditions DNGR-1 dimerization is mediated by the single cysteine residue in the neck region, it is unclear how the higher oligomers arise.

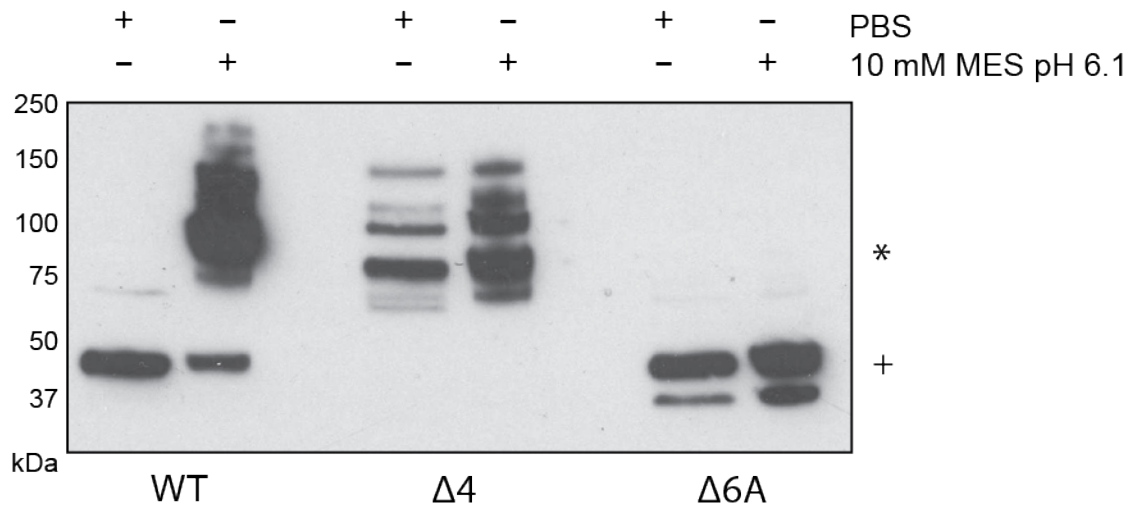

Figure 3.11 Type-2 dimer formation in transmembrane "block" mutants

Cells expressing indicated proteins (mouse, *long* isoform) were lysed in 1% SDS in PBS or 10 mM MES pH 6.1 buffer and the lysates were analysed by reducing SDS-PAGE and Western blot. Signal was revealed using anti-DNGR-1 (397) followed by HRP-conjugated anti-rat antibodies. Numbers on the side of the blot indicate positions of MW markers. Reduction-resistant dimers are indicated with a * and reduction-sensitive protein with a +.

3.2.13 DNGR-1 internalization in response to stimuli

When cross-linked by antibody or F-actin, DNGR-1 expressed both endogenously in dendritic cells and heterologously in unrelated cells gets internalized (Huysamen

et al., 2008, Sancho et al., 2008), which can be read out by flow cytometry as a decrease in surface staining (Fig 3.12). This effect is not caused by blocking of the epitope recognised by the detection antibody, as treatment on ice results in only minimal decrease in signal (Fig 3.13).

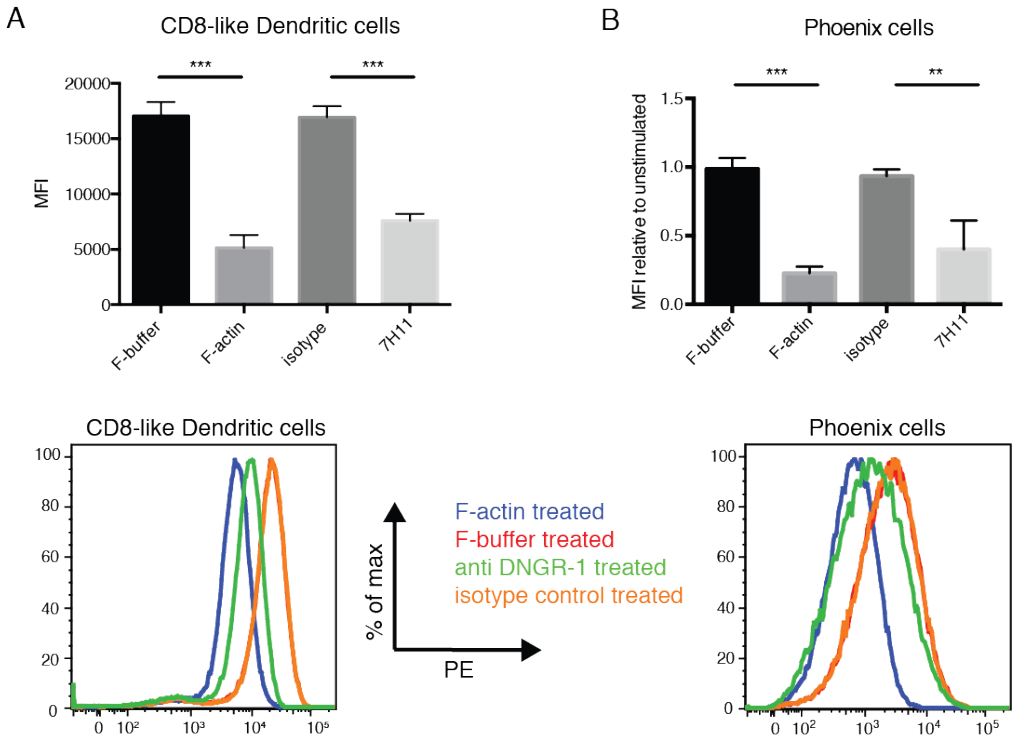

Figure 3.12 Crosslinking of DNGR-1 induces its internalization

A, Dendritic cells generated by culture of mouse bone marrow in the presence of Flt3 ligand were treated for 45 minutes as shown, fixed in formaldehyde, stained for DNGR-1, CD172a (SIRPα) and B220, and analysed by flow cytometry. The $CD8\alpha^{+}$-like dendritic cells were identified as $CD172a^{-}$, $B220^{-}$ and their surface staining of DNGR-1 was assessed. One representative of three biological replicates (lower panel) and quantitation of the three (upper panel) are shown. The bars represent mean ± s.d., *P < 0.05, **P < 0.01, ***P < 0.001; One-way ANOVA with Tukey's multiple comparison test. **B,** Full-length DNGR-1 was retrovirally introduced into Phoenix cells. The cells were treated for 45 minutes as shown, fixed in formaldehyde, and stained for DNGR-1. The intensity of DNGR-1 staining was assessed by flow cytometry. One representative of three experimental replicates (lower panel) and quantitation of the three (upper panel) are shown. The bars represent mean ± s.d., *P < 0.05, **P < 0.01, ***P < 0.001; One-way ANOVA with Tukey's multiple comparison test.

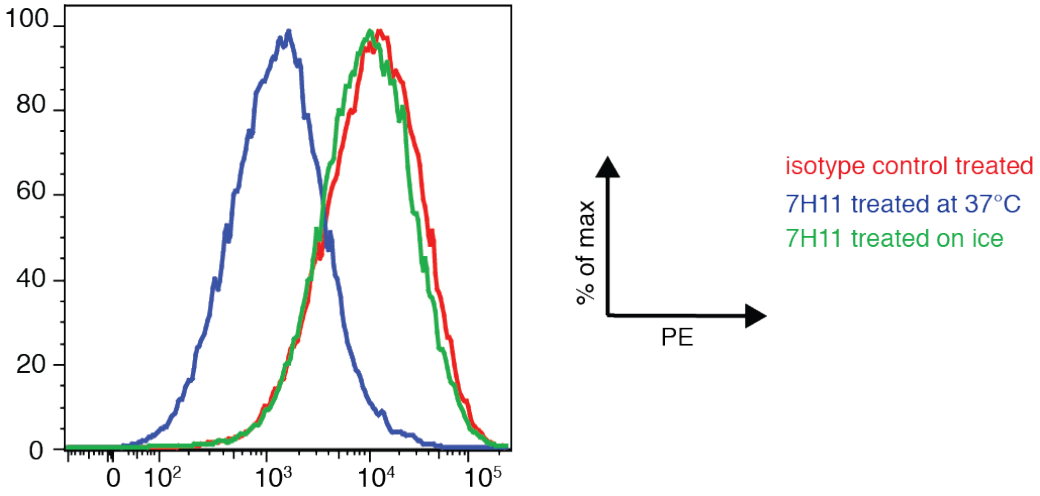

Figure 3.13 DNGR-1 cross-linking on ice does not result in decreased staining

Phoenix cells stably expressing DNGR-1 were treated with anti-DNGR-1 antibody (clone 7H11) and incubated at 37°C or on ice for 30 minutes, fixed in formaldehyde, surface-stained for DNGR-1 (clone 1F6) and analysed by flow cytometry.

3.2.14 The ability of Δ4 and Δ6A DNGR-1 mutants to undergo ligand-dependent endocytosis is unaffected

To assess the ability of Δ4 and Δ6A mutants to be internalised upon stimulation, we treated Phoenix cells expressing transmembrane WT, Δ4 or Δ6A DNGR-1 with F-actin, anti-DNGR-1 antibody (7H11), F-buffer or isotype-matched control antibody for 1 hour at 37°C. Following the incubation, the cells were fixed and stained for surface DNGR-1 with anti-DNGR-1 antibody (1F6). As expected, WT protein got internalised upon both F-actin and antibody treatment, while control treatments induced no detectable receptor internalization. Both mutants mimicked the behaviour of the WT and internalised to comparable extent (Fig 3.14), suggesting that the neck region is not involved in the regulation of the internalization process.

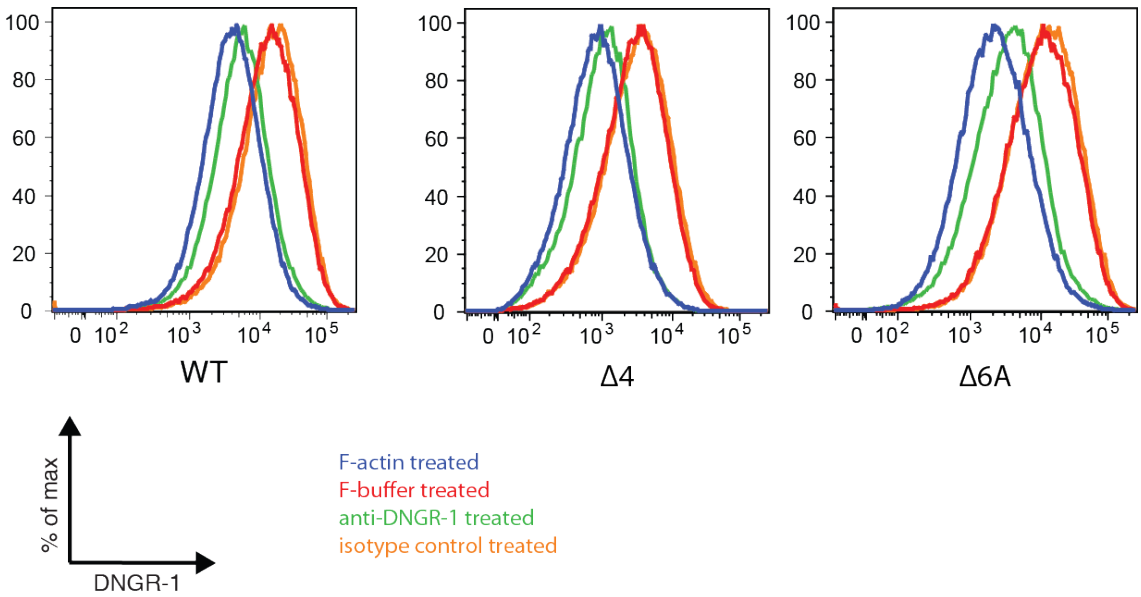

Figure 3.14 Type-2 dimer formation does not affect the ability of DNGR-1 to internalize

Phoenix cells expressing indicated mutant or WT DNGR-1 proteins were treated with F-actin, F-buffer, anti-DNGR-1 antibody or isotype-matched antibody of irrelevant specificity for 60 minutes, fixed in formaldehyde, surface-stained for DNGR-1 and analysed by flow cytometry. One representative of two experiments is shown.

3.3 Discussion

Multiple isoforms of mouse DNGR-1 have been described previously. Surprisingly, disparate results regarding glycosylation and dimerization of the proteins have been reported. While human and one of the mouse isoforms were shown to be dimeric and glycosylated (Huysamen et al., 2008, Sancho et al., 2008), another mouse isoform was reported to be monomeric and non-glycosylated (Huysamen et al., 2008). In contrast, our data show that proteins corresponding to the ECD of both of the mouse isoforms both behave as disulphide-bonded, glycosylated dimers. This observation is in line with the fact that both the dimerization cysteine and the glycosylation sites are conserved between the two isoforms. It is possible that proper glycosylation of certain DNGR-1 isoforms may be required for their dimerization and that DNGR-1 expressed in NIH3T3 cells (Huysamen et al., 2008) is not glycosylated, in the same manner as DNGR-1 expressed in 293F cells (this study).

Interestingly, we show that DNGR-1 can undergo a conformational change in a manner independent of ligand binding, but induced by changes in pH and ionic strength. The conformational change affects the neck region, and appears to happen predominantly at the level of tertiary structure, suggesting a rearrangement of the α-helices that likely form the majority of the neck. pH-induced conformational changes have been described for multiple proteins, and mechanistically, they often are mediated by protonation of one or more histidine residues (Dai et al., 2014, Kalani et al., 2013, Krukenberg et al., 2009, Cao et al., 2015). This is due to the pKa of the His side chain, which falls in physiologically relevant pH-range, allowing formation of a His^+ cation, and consequently repulsion between His^+ and other positively charged residues (Harrison et al., 2013). The neck region of DNGR-1, however, does not contain any conserved histidine residues (Fig 3.9A), suggesting that a different mechanism needs to be at play. Notably, in addition to histidine, negatively charged residues have also been implicated in pH-induced conformational changes (Yeo et al., 2014). Depending on their environment, these residues can have heightened pKa, also allowing protonation in a physiologically relevant pH-range. Contrary to the protonation of histidine residues, protonation of glutamic or aspartic acid does not result in the introduction of a repulsive force but rather in its relief due to the Glu^- or Asp^- switching to their uncharged states (Harrison et al., 2013). The regions of the DNGR-1 neck which appear to be involved in the conformational change based on our experiments with “block mutants,” however, do not contain any conserved negatively charged residues either (Fig 3.9A). On the other hand, the regions we putatively identified contain multiple hydrophobic residues and residues potentially capable of forming hydrogen bonds and salt bridges. While neither of these interactions can provide destabilizing forces quite like repulsion, in sufficient quantity these forces can contribute to and perhaps even be sufficient for pH-sensitive conformational rearrangements (Harrison et al., 2013). Importantly, involvement of salt bridges could help explain the effects of ionic strength (Hendsch and Tidor, 1994) that we observed, while involvement of hydrogen bonds could explain the effects of pH (Wood, 1974). Finally, both pH and ionic strength can affect hydrophobicity of amino acids and by extension the strength of hydrophobic interactions (Gulyaeva et al., 2003). If the model outlined above is correct and multiple amino acids contribute to the overall effect while no one single one is essential, then singly

mutating any residue within the neck region should result in no observable phenotype. Arguing in favour of such model, despite an extensive mutagenesis effort (data not shown), we have so far been unable to identify a single residue within the neck, mutation of which would significantly affect Type-2 dimer formation. pH-induced conformational changes have been shown to regulate function of other C-type lectin receptors. Namely, the neck region of DC-SIGN has been shown to serve as a pH and ionic strength-specific sensor regulating oligomerization status of the receptor, allowing release of bound ligands into endosomes (Tabarani et al., 2009). Similarly, pH-induced conformational change in DEC205 has been shown to correlate with the receptor binding to as-of-yet unidentified ligand in apoptotic and necrotic cells (Cao et al., 2015). The conformational change in DNGR-1, however, does not markedly affect either of these properties. Notably, the conformational change happens between the conditions that DNGR-1 would encounter on cell surface and within the endosomal pathway (Scott and Gruenberg, 2011), suggesting that it might allow DNGR-1 to regulate its function based on its subcellular localization.

It has been previously suggested that the hemITAM motifs of dimeric C-type lectin receptors could function as a single ITAM motif, allowing recruitment of the two SH2 domains of the Syk kinase (Sancho and Reis e Sousa, 2012, Hughes et al., 2010). Reported flexibility between the two SH2 domains as well as the ability of Syk to bind to ITAM motifs with linkers between the two phosphorylated tyrosines differing in length by as much as 50% (Kumaran et al., 2003) argues in favour of such model. It is still easily conceivable though that certain positioning of the two hemITAMs might not be permissive for Syk binding, while others could be more favourable. Changes in the secondary structure of the extracellular portion of single-pass transmembrane proteins are generally unable to transmit across plasma membrane to the intracellular portions involved in signalling. This, however, does not apply to dimeric receptors, where changes in the tertiary structure and/or relative positioning of the monomers within the dimer have the potential to translate into repositioning of the intracellular domains, and vice versa, as extensively described for example for integrins (Shimaoka et al., 2002). Furthermore, at least for some receptors, there appear to be not only “on” and “off” positions, but the relative positioning of the extracellular domains can result in different modalities of signalling (Moraga et al., 2015, Rowlinson et al., 2008). This is similar to the

concept of “biased signalling” where one G-protein coupled receptor (GPCR) can activate different pathways depending on the bound ligand (Drake et al., 2008). It is thus tempting to speculate that the conformational change in the neck of DNGR-1 could transmit to the intracellular portion, and affect positioning of the two hemITAM signalling motifs, in turn controlling the ability of DNGR-1 to signal based on its cellular localization. Of course other possibilities unrelated to signalling, including for example unmasking of a protease cleavage site or docking site for another protein cannot be ruled out at present. Obviously, the first experiment to do in order to assess the relevance of the conformational change for biology of DNGR-1 is the cross-presentation assay with DNGR-1 KO DCs transduced with Δ4 and Δ6A mutant proteins. Unfortunately, due to technical reasons we have so far been unable to conduct such experiment, but the work is on-going.

Chapter 4. Biophysical and Structural Characterization of DNGR-1 : F-actin interaction

4.1 Introduction

DNGR-1 has recently been reported to specifically recognize F-actin (Ahrens et al., 2012, Zhang et al., 2012). While other members of the C-type lectin family have also been shown to bind protein ligands (Sancho and Reis e Sousa, 2012), the specificity for F-actin appears to be unique to DNGR-1. This suggests that the only way to gain insight into the interaction is by directly determining its biophysical characteristics, and solving the three-dimensional (3D) structure of DNGR-1 in complex with F-actin.

X-ray crystallography has been an extremely successful method for determining 3D structure of proteins ranging in size from several amino acids to complexes as large as ribosome. In fact, the large majority of the approximately 100 000 protein structures currently deposited in the Protein Data Bank have been determined using this powerful technique (Wlodawer et al., 2013). The critical condition for using X-ray crystallography, however, is very high degree of purity and homogeneity of the analysed sample. Given the inherent heterogeneity of F-actin, any attempt at using this technique to determine the structure of F-actin in complex with DNGR-1 would consequently be bound to fail.

Hence, the technique of choice to accomplish such a goal is electron microscopy. Electron microscopy has been successfully used for imaging actin filaments, and with the advent of electron cryomicroscopy with helical image analysis, the resolution of F-actin structures has been increased to 6.6 Å, allowing resolution of all the elements of secondary structure, in turn making modelling of the structure at atomic resolution possible (Fujii et al., 2010).

Consequently, in order to obtain structure of DNGR-1 in complex with F-actin we established collaboration with Takashi Fujii and Keichii Namba (Riken Quantitative Biology Center, Osaka, Japan). They used DNGR-1 ECD prepared in our laboratory to make preparations of DNGR-1:F-actin complexes that were then subjected to electron cryomicroscopy and helical image analysis to derive the structure of F-actin decorated with DNGR-1. As these results form the foundation of

my ensuing work, they have been included here in the first few figures and acknowledged in figure legends. The validation of the structure was subsequently carried out by me and constitutes the remainder of the chapter.

4.2 Results

4.2.1 Electron cryomicroscopy reveals uncommon mode of binding of DNGR-1 to F-actin

In order to obtain the structure of DNGR-1 in complex with F-actin, we expressed and purified the extracellular domain (ECD) of mDNGR-1 as described previously (Ahrens et al., 2012). The protein was used to decorate *in vitro* polymerised human platelet actin filaments and the complexes were subjected to electron cryomicroscopy (Cryo-EM) (Fig 4.1) and helical image analysis. The image was reconstructed at 7.7 Å resolution as determined by the Fourier shell correlation (FSC) method at FSC = 0.143.

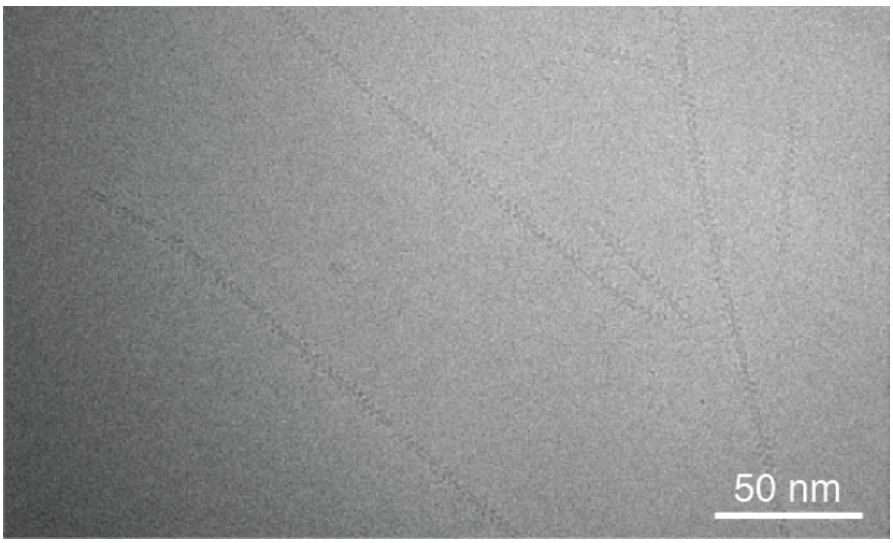

Figure 4.1 DNGR-1 decorated actin filaments

In vitro polymerized actin filaments were decorated with DNGR-1 ECD and subjected to electron cryomicroscopy. Image courtesy of T. Fujii and K. Namba.

An electron density corresponding to DNGR-1 CTLD was observed binding into the groove between two actin protofilaments, making contacts with three actin subunits – two across the filament as well as two along one of the protofilaments (Fig 4.2A and B). Specificity for such composite site clearly explains the selective binding of

DNGR-1 exclusively to F-actin, with no detectable binding to monomeric G-actin. We could not observe any electron density corresponding to the neck region of DNGR-1, consistent with its flexibility, which will discussed in more detail in the following chapter (Fig 4.2A).

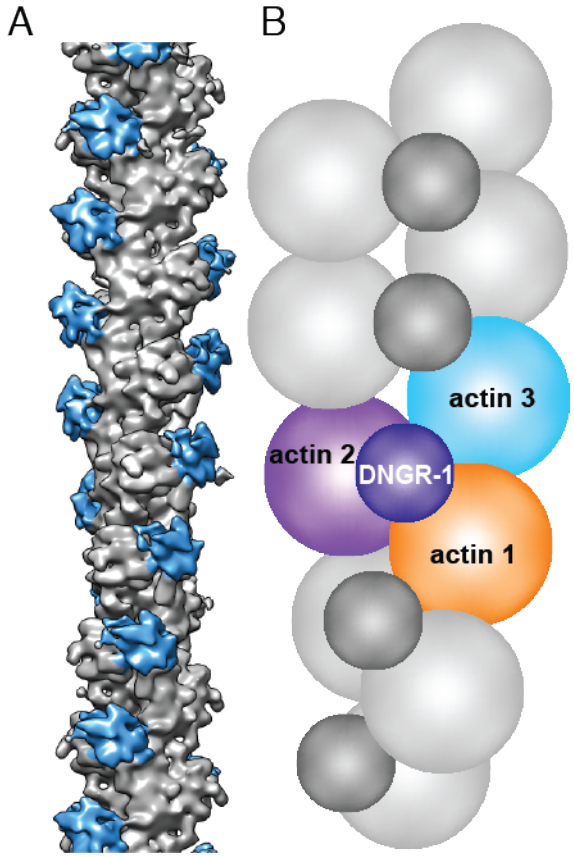

Figure 4.2 Helical image analysis of cryoelectron micrographs of DNGR-1 decorated actin filaments

A, Helical image analysis of DNGR-1 decorated actin filaments showed electron density corresponding to DNGR-1 CTLD (in blue) bound in the groove between two actin protofilaments, making contact with three actin subunits in all. No density corresponding to the DNGR-1 neck region could be observed. **B,** Schematic depiction of the interacting molecules as shown in panel **A**. Images courtesy of T. Fujii and K. Namba.

Previously published structures of hDNGR-1 CTLD (PDB ID 3VPP) (Zhang et al., 2012) and F-actin (PDB ID 3MFP) (Fujii et al., 2010) could be fitted into the observed electron densities and FlexEM program (Topf et al., 2008) was used to build an atomic model of the complex (Fig 4.3).

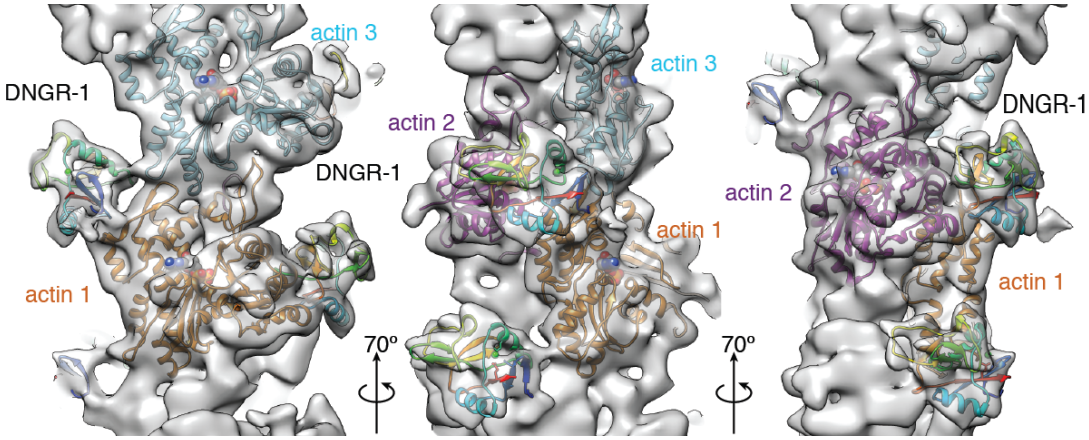

Figure 4.3 Structure of DNGR-1 F-actin complex

View of DNGR-1 and F-actin structures fitted into the electron density map. DNGR-1 is in rainbow colouring, G-actin subunits are coloured in orange, magenta and cyan, and their positioning corresponds to that in Fig 4.2 B. Images courtesy of T. Fujii and K. Namba.

4.2.2 Electron cryomicroscopy identifies a loop absent in the crystal structure of DNGR-1 CTLD

The structure of hDNGR-1 (Zhang et al., 2012) that was used to fit into the observed electron density map lacks five amino acids (R203 – A207), which presumably form a flexible loop. Unfilled electron density corresponding to this loop was observed in the electron density map of DNGR-1, suggesting that binding to F-actin results in folding and stabilization of the loop. To complete the model of DNGR-1 bound to F-actin (Fig 4.3) the missing residues (R226 – A230 in mDNGR-1) were modelled into the unfilled electron density (Fig 4.4).

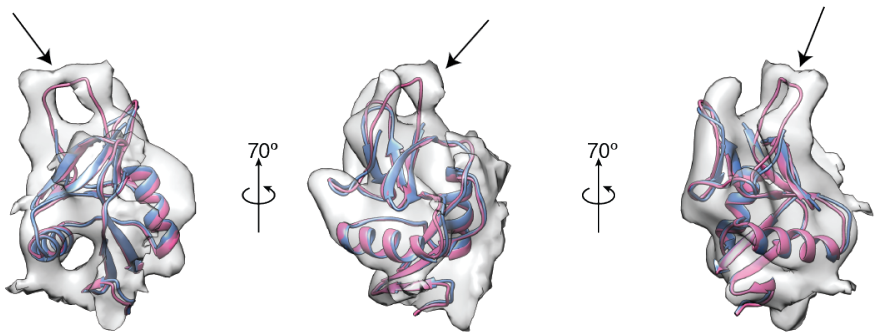

Figure 4.4 Flexible loop in DNGR-1 is stabilised by binding to F-actin

Overlay of the published crystal structure of hDNGR-1 (blue) and model of mDNGR-1 (magenta) including the flexible loop (indicated with the arrow) fitted into the electron density map. Images courtesy of T. Fujii and K. Namba

4.2.3 Identification of the residues involved in the interaction of DNGR-1 with F-actin

While the resolution of the Cryo-EM electron density map was sufficient for unambiguous fitting of both DNGR-1 and F-actin structures, the side-chains of amino acids were not resolved. Consequently, only surfaces putatively involved in the interaction with the three actin subunits could be identified. Importantly, the surface putatively involved in the interaction with actin subunit 2 includes W155 and W250, residues corresponding to W131 and W227 in hDNGR-1, which were previously suggested to play a role in the interaction (Zhang et al., 2012). In all, sixteen residues, thirteen of which are conserved between mouse and human were identified in the putative interaction surfaces (Table 5).

human DNGR-1	mouse DNGR-1	residue conserved	interacting actin subunit
N115	H139	no	1
N116	N140	yes	1
W117	W141	yes	1
Y126	Y150	yes	1
E129	E153	yes	1
W131	W155	yes	2
K143	K167	yes	1
E144	E168	yes	1
R165	G188	no	3
K166	K189	yes	3
K168	K191	yes	3
D172	K195	no	2
K215	K238	yes	2
D225	D248	yes	2
W227	W250	yes	2
K228	K251	yes	2

Table 5 Residues putatively involved in the interaction between DNGR-1 and F-actin

In order to address the contribution of the surfaces and residues putatively implicated in the interaction, we carried out mutational analysis of DNGR-1 ECD. We mutated each of the residues present in the identified surfaces as well as the residues forming the flexible loop, and expressed the mutants recombinantly as soluble FLAG-tagged proteins in 293F cells. All of the ECD mutants got expressed and secreted into the medium, albeit with different efficiency (Fig 4.5). We used densitometric analysis of Western blots to equilibrate the concentrations between the mutants and used the resulting supernatants at equal protein concentrations in a dot blot assay (Ahrens et al., 2012) (Fig 4.6) to assess their binding ability to F-actin. Decreasing amounts of *in vitro* polymerised actin were spotted onto a membrane, and the membrane was blocked and incubated with DNGR-1 ECD mutant supernatants and Dectin-1 ECD supernatant as a negative control. Binding of DNGR-1 was then revealed using anti-FLAG antibody. Consistently with the previous report (Zhang et al., 2012), W155A W250A double mutant failed to bind to F-actin. Mutating W250 alone also resulted in a complete loss of binding, while mutating W155 resulted in a significant decrease in binding. Both of these residues are involved in the interaction with actin subunit 2. Of the other residues putatively involved in the interaction with the same subunit, mutating K251 also resulted in a significant decrease in binding, while K238A mutant exhibited only mild phenotype. None of the other mutants (K195A, D248A) showed any decrease in binding to F-actin (Fig 4.6A). Collectively, these data suggest that W250, W155, K251 and to a smaller extent K238 are involved in the interaction of DNGR-1 with actin subunit 2.

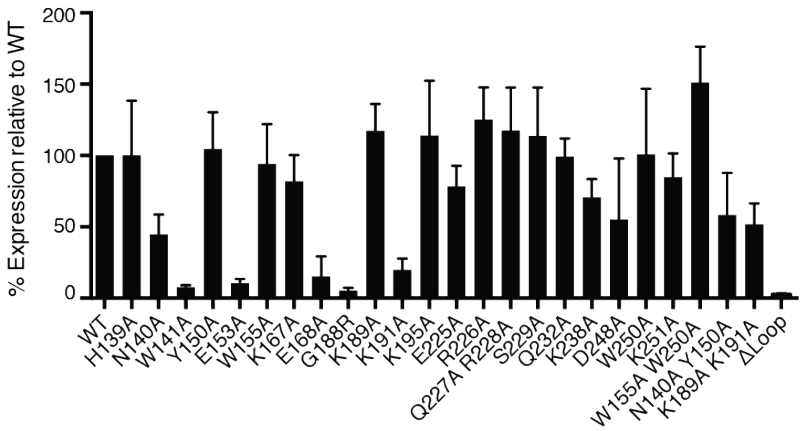

Figure 4.5 Expression efficiency of DNGR-1 mutants

Expression efficiency of all DNGR-1 mutants in 293F cells relative to WT protein. Data pooled from 5 different experiments. Bars represent mean ± s.d.

Of the residues putatively involved in the interaction with actin subunit 1, W141A mutant showed no binding and E153A mutant showed a significant decrease in binding. Of the other residues putatively involved in the interaction with the same actin subunit, mutating N140 and Y150 singly or doubly resulted in only minimal phenotype. No phenotype was observed when the other residues (H139, K167 and E168) were mutated (Fig 4.6A). Taken together, these data suggest that W141 and E153, and to a smaller extent N140 and Y150 residues are involved in the interaction with actin subunit 1. Both W141A and E153A mutants expressed poorly, suggesting the residues may play a role in the folding of the protein. Importantly though, both of the mutants were recognised by two different anti-DNGR-1 antibodies (clone 7H11 and 1F6), suggesting the proteins were not grossly misfolded. Furthermore, W141 is oriented inwards in the crystal structure of hDNGR-1 CTLD, however, it is not part of the hydrophobic core of the protein, and is located on the hydrophilic side of the three-stranded β-sheet formed by the N- and C-terminal chains. Together with a density observed in the Cryo-EM data, this suggests that W141 may be able to flip out to interact with a hydrophobic patch on actin.

Of the residues putatively involved in the interaction with actin subunit 3, only two are conserved between mouse and human (K189 and K191), and mutating them singly or doubly led to no detectable decrease in F-actin binding. The last residue (G188) was replaced with arginine in human DNGR-1. Substituting the glycine with arginine (G188R) in the context of mDNGR-1 led to a dramatic decrease in expression efficiency (Fig 4.5), however, the resulting protein appeared to bind to F-actin with increased efficiency (Fig 4.6A), suggesting a possible role for this residue.

Interestingly, mutating the residues of the flexible loop, or replacing the whole loop with a string of 8 alanines (ΔLoop), resulted in no detectable decrease in binding (Fig 4.6B) despite the fact that the ΔLoop mutant showed drastic decrease in expression efficiency. (Fig 4.5)

Collectively, these data suggest that only a handful of residues are crucial for the interaction of DNGR-1 with F-actin, and the interaction involves mostly actin subunits 1 and 2, while interaction with subunit 3 and the flexible loop appear to be dispensable for binding.

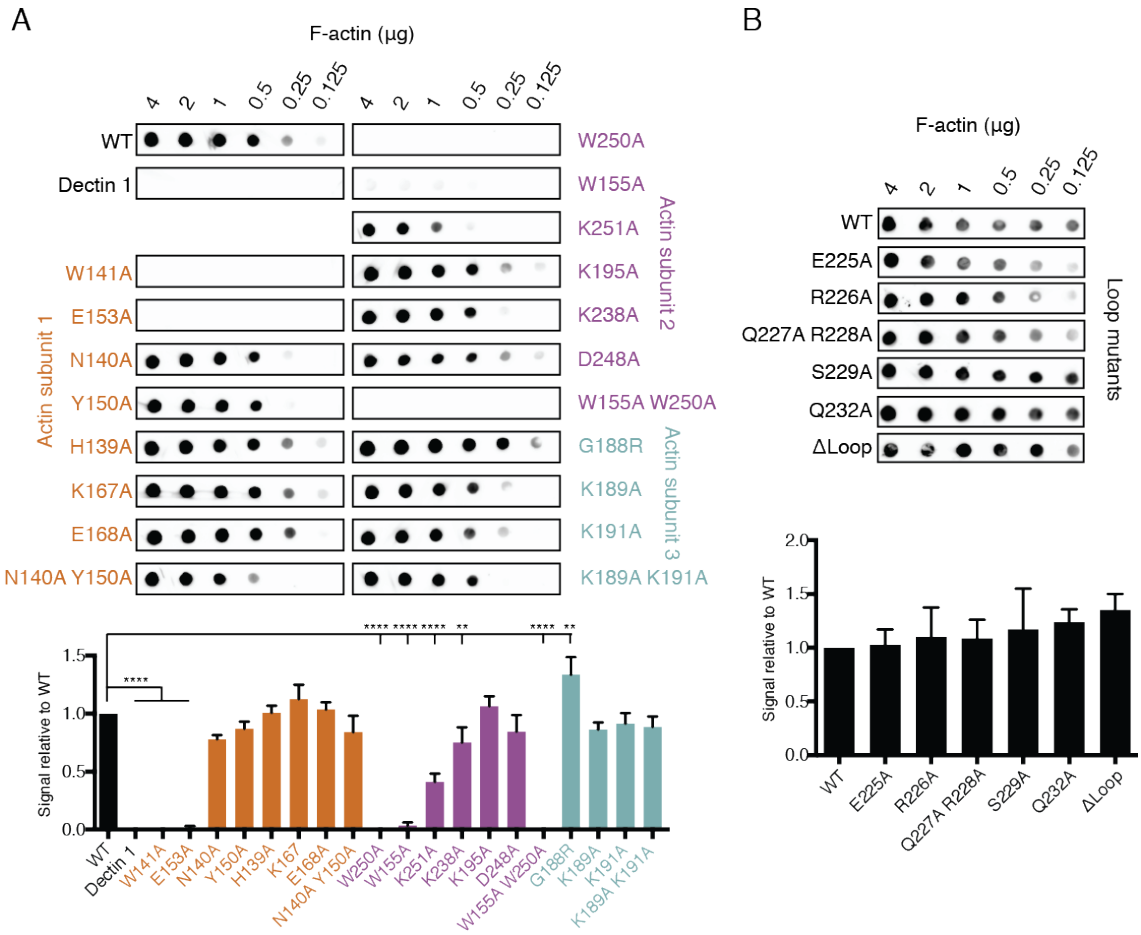

Figure 4.6 Identification of residues involved in the interaction of DNGR-1 with F-actin

Decreasing amounts of F-actin were spotted onto a nitrocellulose membrane and binding of indicated DNGR-1 mutants at equal concentration was tested. One representative experiment of three (upper panels) and quantitation relative to WT of three experiments (lower panels) are shown. Colour of the font and bars reflects the G-actin subunit that the residue is involved in interaction with, colours for the subunits are the same as in Figure 4.3. Bars represent mean ± s.d. *P < 0.05, **P < 0.01, ***P < 0.001, ****P < 0.0001; One-way ANOVA with Dunnett's multiple comparisons test.

4.2.4 Binding of DNGR-1 to actin in dead cells is mediated by the same residues as to purified actin *in vitro*.

In order to confirm that the observations we made using, *in vitro* polymerised F-actin are valid also for F-actin contained in dead cells, we utilised a flow cytometry (FACS) based assay. HeLa cells were UV-irradiated and left overnight to undergo secondary necrosis. Same protein supernatants as in the dot blot assay

were then used to stain the cell corpses. Using this assay, we observed a pattern of binding identical to that observed in the dot blot assay (Fig 4.7 A and B, compare with 4.6 A and B). The only difference was a seemingly lower binding of the G188R and ΔLoop mutant. This result could be an artefact caused by an overestimate of the abundance of low-expressing mutants in the densitometric analysis. While such overestimate does not pose problems for dot-blot analysis, because limited amount of ligand spotted on the membrane allows for saturation of binding, hence masking minor differences in concentration of different DNGR-1 mutants, reaching saturation may not be feasible for the much larger amount of actin present in dead cells, causing very low-expressing mutants to show apparently lower binding.

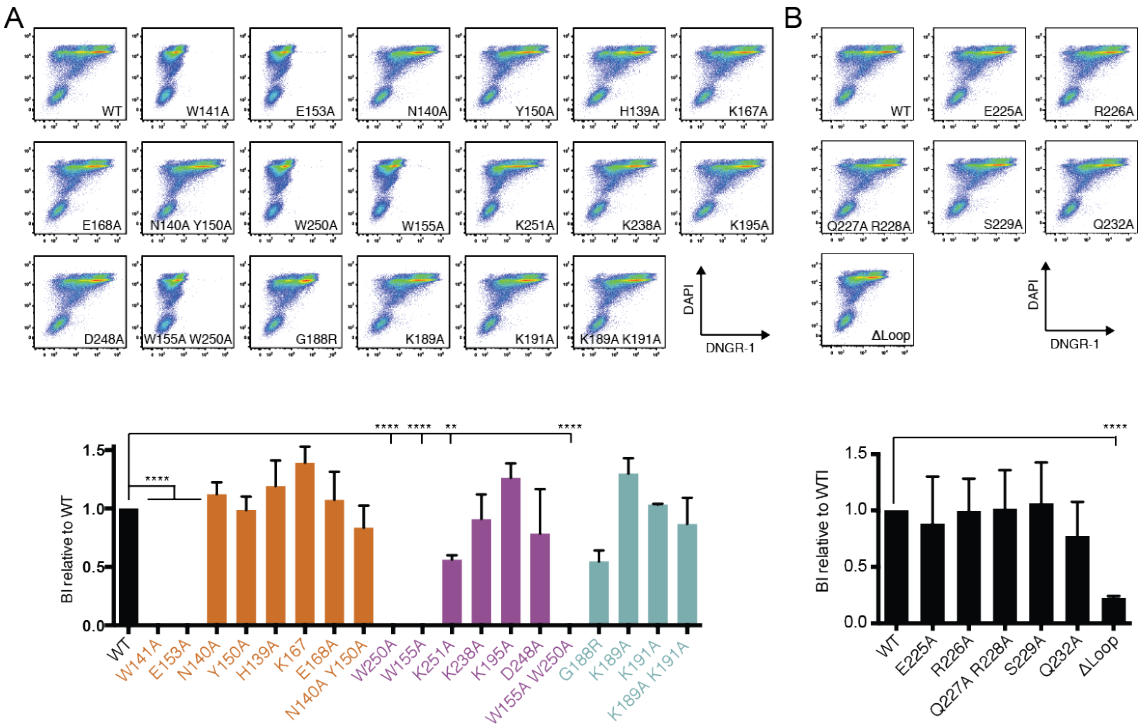

Figure 4.7 Binding of DNGR-1 mutants to secondary necrotic HeLa cells

HeLa cells were UV-irradiated and left to undergo secondary necrosis overnight. Following the incubation, the cell corpses were stained with WT and mutant DNGR-1 containing supernatants. Binding was assessed by flow cytometry with DAPI used to discriminate dead cells. One representative experiment of three is shown (upper panels). Binding index was calculated for each mutant and made relative to that of WT. Colour of the font and bars reflects the G-actin subunit that the residue is involved in interaction with, colours for the subunits are the same as in Figure 4.3. Results from three experiments were pooled and the bars represent mean ± s.d. P < 0.05, **P < 0.01, ***P < 0.001, ****P < 0.0001; One-way ANOVA with Dunnett's multiple comparisons test.

4.2.5 Pelleting assay confirms DNGR-1 mutant phenotypes

Of the DNGR-1 mutants shown above, we selected those that expressed efficiently and showed different degree of F-actin binding – namely W155A W250A mutant as a non-binder, K251A mutant as a binder with significantly decreased affinity, and N140A Y150A as a binder with only minimal phenotype – and tested them in F-actin pelleting assay (Ahrens et al., 2012). Decreasing amount of DNGR-1 proteins was incubated with constant amount of F-actin. Following the incubation, F-actin was pelleted, and both the pellet and supernatant were analysed by SDS-PAGE and Western blot for presence of DNGR-1. As expected, WT protein was largely found in the pellet. On the other hand, and consistently with the results of the dot blot assay, we observed no accumulation of the W155A W250A mutant in the pelleted material. Similarly, majority of the K251A mutant was also retained in the supernatant, confirming significant decrease of affinity of this mutant. On the contrary, N140A Y150A mutant was found predominantly in the pellet, consistent with its largely unchanged affinity for F-actin (Fig 4.8).

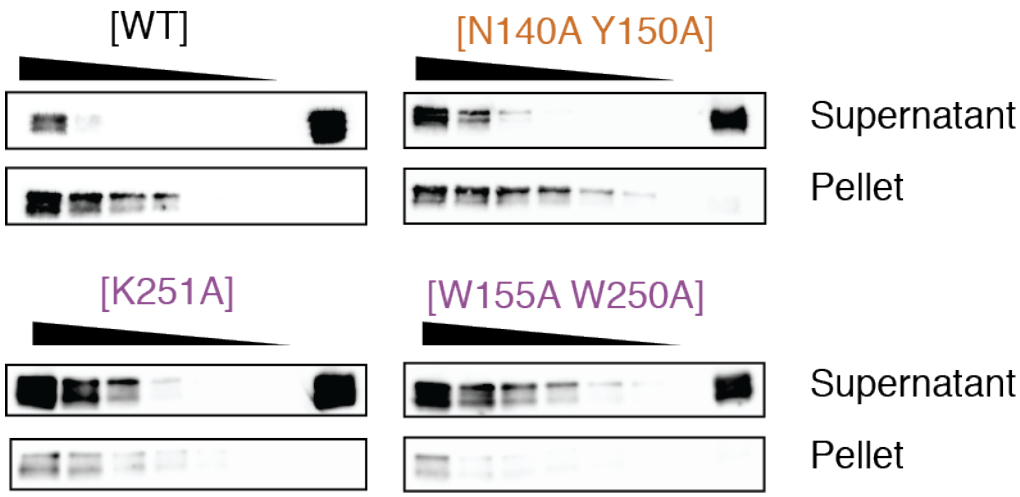

Figure 4.8 Selected DNGR-1 mutants in pelleting assay

Constant amount of F-actin was incubated with decreasing amount of indicated DNGR-1 proteins (decreasing protein concentration indicated by the wedge). The mixtures were ultracentrifuged and both pellet and supernatant were analysed using SDS-PAGE and Western blot. Data are representative of four experiments for WT and two experiments for each mutant. Colour of the font reflects the G-actin subunit that the residue is involved in interaction with, colours for the subunits are the same as in Figure 4.3.

4.2.6 Biolayer interferometry for F-actin binding proteins

In order to obtain real-time binding data for DNGR-1 and F-actin interaction, we developed a method based on biolayer interferometry (BLI) (Abdiche et al., 2008). We mixed biotinylated and non-biotinylated actin (1:4) and allowed it to polymerise directly on a streptavidin-coated biosensor. F-actin polymerised in this way showed exceptional stability over prolonged periods of time (Fig 4.9), making it a suitable platform for testing binding of actin-binding proteins.

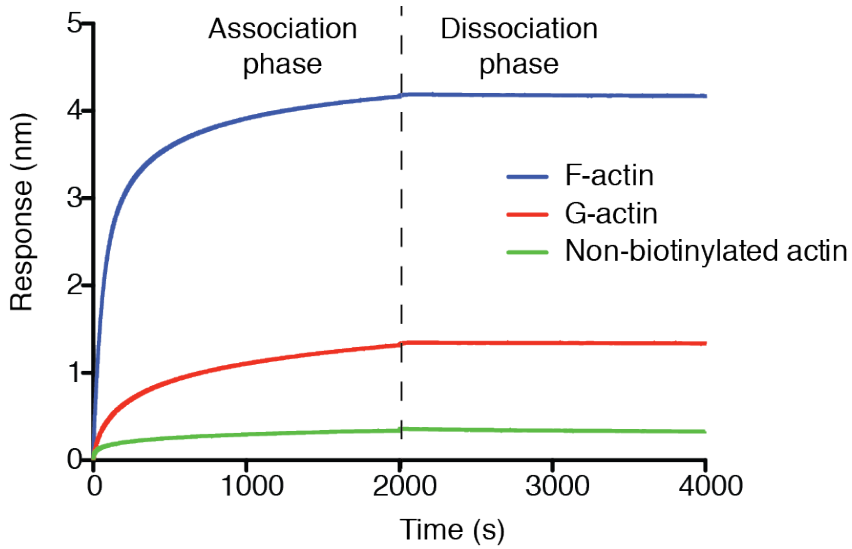

Figure 4.9 F-actin polymerised on BLI biosensor is stable over prolonged periods of time

Biotinylated and non-biotinylated actin preparations were mixed at 1:4 ratio, transferred into F-buffer, and allowed to polymerise directly on a streptavidin-coated biosensor (blue line). Same amount of biotinylated actin as present in the mixture was left in G-buffer and allowed to bind to the sensor (red line). Non-biotinylated actin at concentration equal to the final concentration of actin in the mixture was transferred into F-buffer, and allowed to polymerise in the presence of a streptavidin-coated biosensor (green line). After 2000 seconds of polymerisation, the sensors were moved to wells containing appropriate buffers, and dissociation phase was monitored for further 2000 seconds.

To validate the assay, we first tested binding of α-actinin, a known actin-binding protein to the F-actin bound to the sensor. We observed specific binding of α-actinin in concentration dependent manner (Fig 4.10A). Steady state analysis of the binding curves from two experiments revealed K_d = 0.15 ± 0.04 μM (Fig 4.10B).

This result is in good agreement with results obtained using different methods and published previously (Wachsstock et al., 1993).

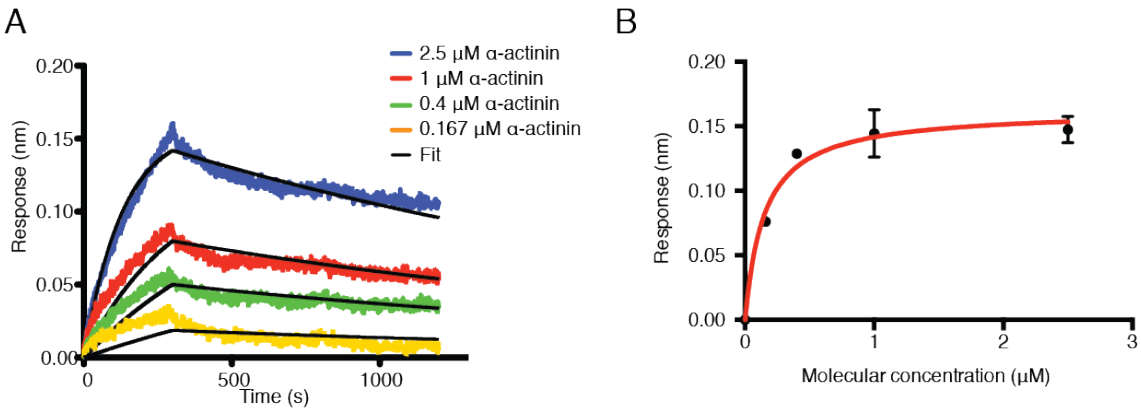

Figure 4.10 Validation of biolayer interferometry setup for F-actin binding proteins

A, Mixture of biotinylated and non-biotinylated actin was allowed to polymerise directly on a streptavidin-coated sensor and binding of α-actinin at the indicated concentrations was tested. Black lines denote mathematically fitted curves. One representative experiment of two is shown. **B,** Steady state analysis of α-actinin binding. Data are pooled from two independent experiments and represent mean ± s.d.

4.2.7 DNGR-1 interaction with F-actin shows rapid kinetics but only modest affinity

In order to explore binding of DNGR-1 to F-actin in more detail, we utilised the BLI setup that we developed and tested for α-actinin. In case of DNGR-1, we also observed a specific binding in concentration-dependent manner, however, dynamic analysis showed rapid kinetics of both association and dissociation ($1.5\times10^{6} \pm 4.2\times10^{5}$ $M^{-1}s^{-1}$ and $8.48\times10^{-1} \pm 9.6\times10^{-2}$ s^{-1} respectively) (Fig 4.11A), and suggested a K_d in low micromolar range. Steady state analysis of the binding curves from seven independent experiments then showed K_d = 1.6 ± 0.3 µM (Fig 4.11B), well within the range predicted previously by pelleting assay (Ahrens et al., 2012).

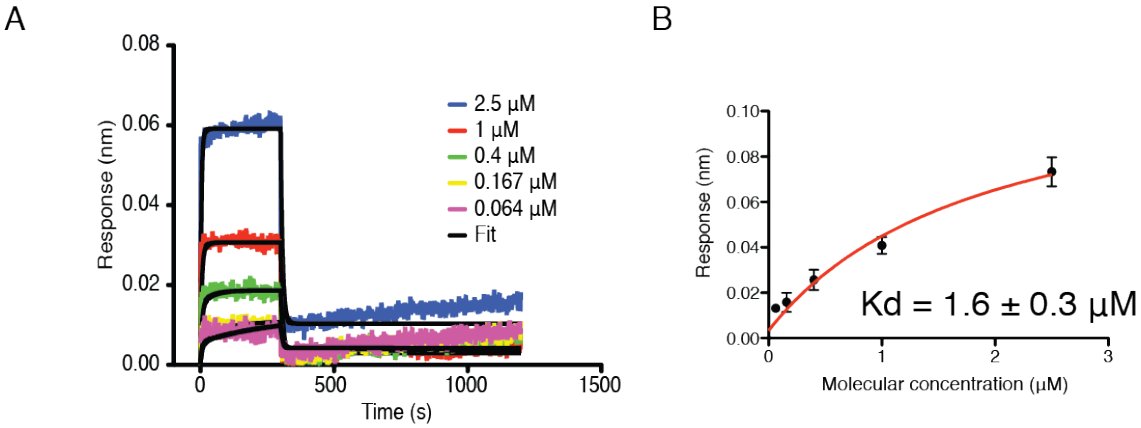

Figure 4.11 DNGR-1 binds F-actin with rapid kinetics but only modest affinity

A, Mixture of biotinylated and non-biotinylated actin was allowed to polymerise directly on a streptavidin-coated sensor, and binding of DNGR-1 at the indicated concentrations was tested. Black lines denote mathematically fitted curves. One representative experiment of seven is shown. **B,** Steady state analysis of DNGR-1 binding. Data are pooled from seven independent experiments and represent mean ± s.d.

4.2.8 Biolayer interferometry confirms DNGR-1 mutant phenotypes

To confirm the phenotypes of DNGR-1 mutants we observed in dot blot and pelleting assay, we tested the previously selected mutants in the biolayer interferometry setup. Consistently with what we observed using the other techniques, W155A W250A mutant showed no binding in our BLI setup, suggesting K_d > 100 µM (Fig 4.12A). For the K251A mutant we observed only weak signs of binding at the highest concentration used, suggesting K_d > 50 µM (Fig 4.12B). Finally, for the N140A Y150A mutant we observed only minimal decrease in affinity for F-actin (K_d = 2.7 ± 1.1 µM; Fig 4.12C). Thus, the results of all the biochemical assays are concordant and confirm the relative contribution of DNGR-1 residues to F-actin binding suggested by the dot blot screen of alanine mutants.

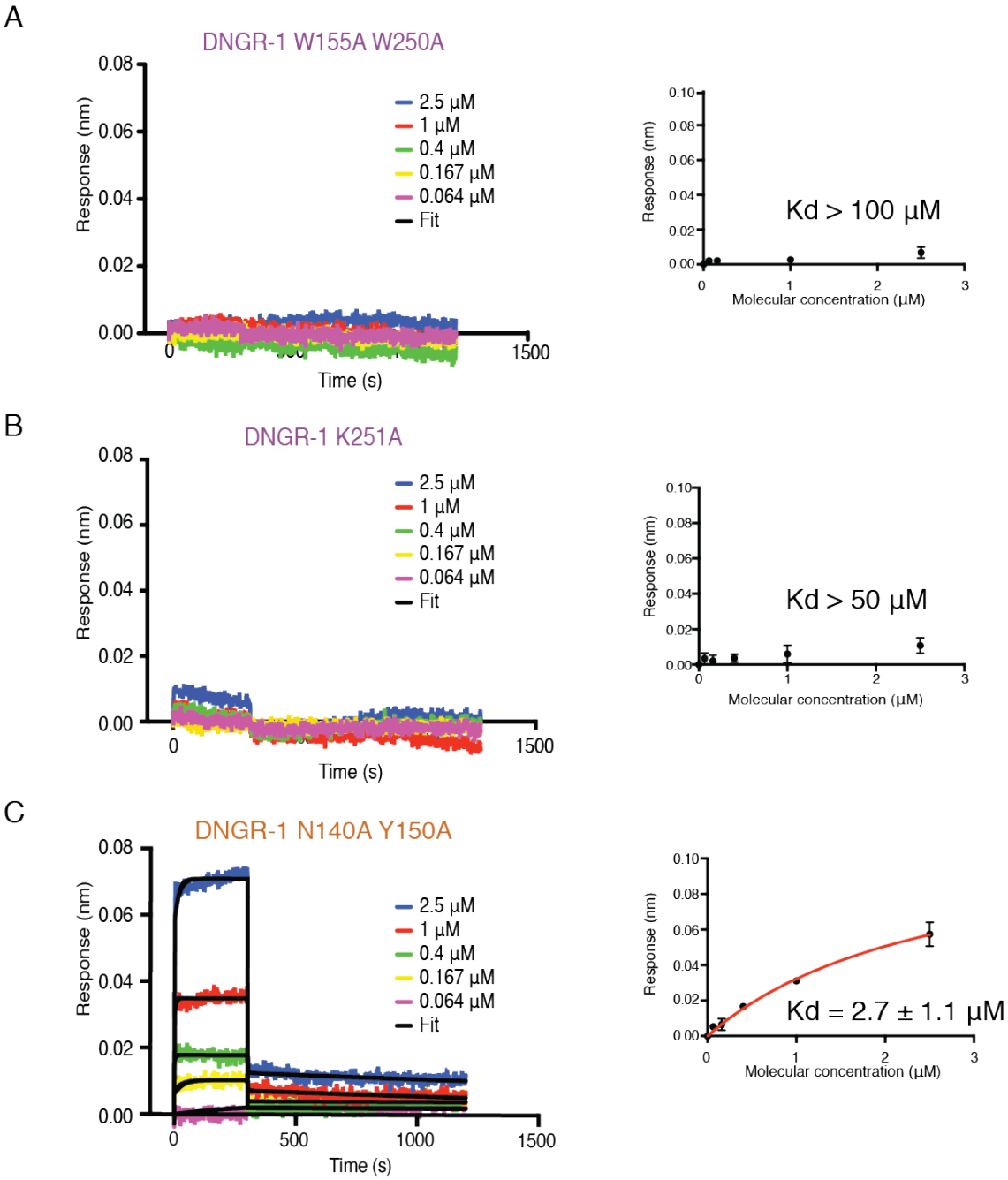

Figure 4.12 DNGR-1 mutants in biolayer interferometry

Mixture of biotinylated and non-biotinylated actin was allowed to polymerise directly on a streptavidin-coated biosensor and binding of **(A)** W155A W250A, **(B)** K251, and **(C)** N140A Y150A DNGR-1 mutants at the indicated concentrations was tested (left panels). One representative experiment of three for N140A Y150A or two for the other mutants is shown. Black lines denote mathematically fitted curves. Steady state analysis (right panels) was performed on pooled data from all experiments and the data points represent mean ± s.d. Numbers represent best-fit curve values ± standard error.

4.2.9 The dimeric status of DNGR-1 is essential for its efficient binding to F-actin

DNGR-1 is constitutively expressed as a disulphide-bonded homodimer. This suggests that the affinity we determined for the DNGR-1 : F-actin interaction has a component of cooperativity, where binding of one part of the dimer potentiates binding of the other half. To assess to what extent is the dimeric status of DNGR-1 important for efficient F-actin binding, we compared the binding of dimeric ECD protein with that of monomeric CTLD in the BLI assay. While the dimeric DNGR-1 ECD showed clear binding to F-actin (Fig 4.13A and 4.11), in the case of the monomeric CTLD we saw no observable binding at the same concentrations, indicating K_d > 100 μM (Fig 4.13B). Taken together these results show that the dimeric status of DNGR-1 is essential for efficient recognition of F-actin and dramatically increases the strength of binding.

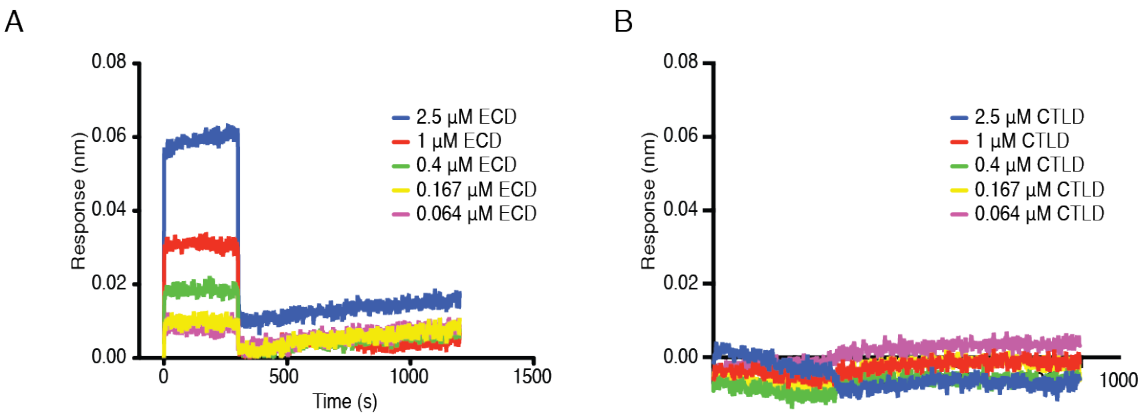

Figure 4.13 Dimeric status of DNGR-1 enhances its ligand binding ability

Mixture of biotinylated and non-biotinylated actin was allowed to polymerise directly on a streptavidin-coated biosensor, and binding of **A,** DNGR-1 ECD and **B,** CTLD at indicated concentrations was tested. One representative of seven experiments is shown for ECD and one representative of two experiments is shown for CTLD.

4.2.10 Avidity component of the multivalent DNGR-1 : F-actin interaction dramatically increases the strength of binding *in vitro*

A single actin filament has many DNGR-1 binding sites along its length, making it a polyvalent ligand. The way our BLI experiments were carried out, however, the polyvalency did not come into play, as DNGR-1 molecules were in solution, and

free to diffuse. This allowed DNGR-1 to associate and dissociate at a very fast rate, as shown in Fig 4.11, but it does not reflect the physiological reality of the interaction. Under physiological settings DNGR-1 is anchored into the cell membrane, restricting the interaction to only two dimensions. Thus, when an actin filament binds to DNGR-1 on the cell surface, it gets in close proximity of other DNGR-1 molecules, increasing the chance of interaction. Furthermore, once the filament is bound to multiple DNGR-1 molecules in the membrane and one of them dissociates, the filament remains bound by the remaining DNGR-1 molecules, and will also remain in close proximity of the dissociated molecule, making the chance of re-association higher, effectively decreasing the off-rate by means of avidity contribution (Fig 4.14).

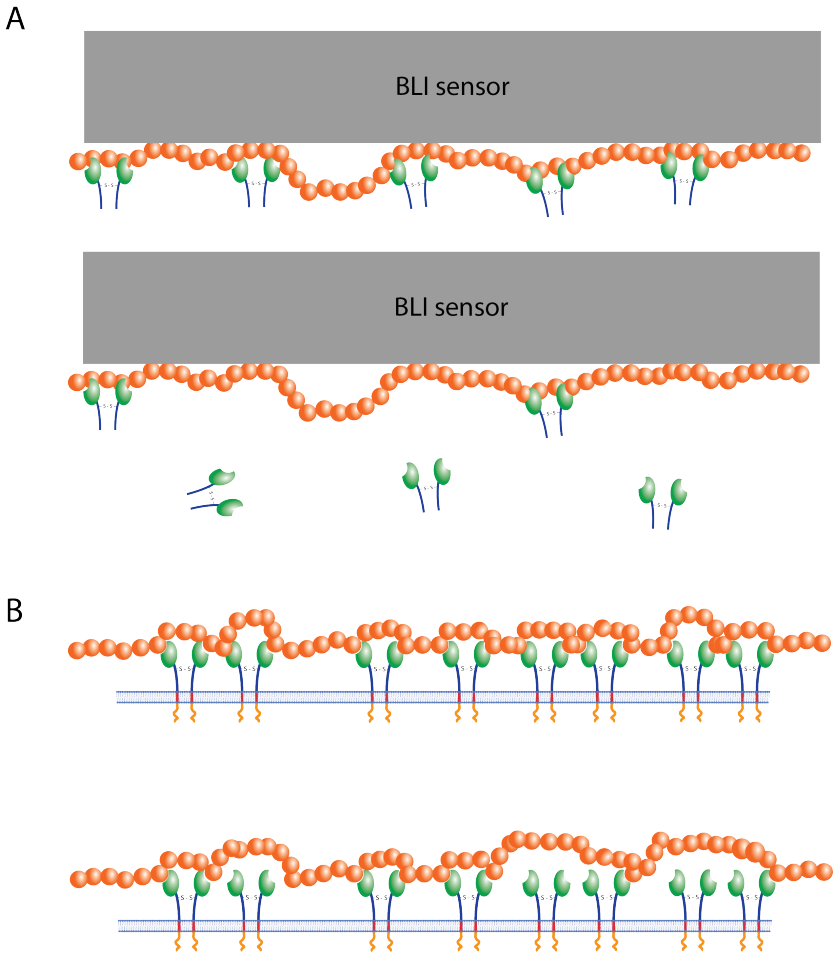

Figure 4.14 Schematic depiction of the involvement of avidity in the interaction between DNGR-1 and F-actin

A, When F-actin is immobilised on a surface (such as the BLI sensor), molecules of DNGR-1 are free to diffuse upon dissociation, and avidity does not come into play. **B,** When in the context of a cell, DNGR-1 is anchored in the membrane, restricting

the interaction to two dimensions and allowing contribution of avidity to the overall strength of binding.

In order to test to what extent avidity plays a role in DNGR-1 : F-actin interaction, we employed an inverted BLI setup. We immobilised DNGR-1 ECD on the surface of anti-FLAG biosensors, and tested binding of actin filaments. The number of concentrations at which binding of F-actin could be tested was severely limited due to the fact that F-actin spontaneously depolymerizes under the critical concentration of 0.6 μM (Pollard, 1986), and filaments at concentrations above 2 μM caused significant artefacts in the BLI signal due to large filament size. In order to get around this limitation, we polymerized actin filaments in the presence of gelsolin (1000 : 1 ratio) to obtain shorter, capped filaments, and we tested binding at 1 μM F-actin. Under these conditions we observed a fast on-rate ($7.6\times10^{3} \pm 1.0\times10^{3}$ $M^{-1}s^{-1}$), but in contrast to what we observed when DNGR-1 was in solution and F-actin on the biosensor, the dissociation exhibited an extremely slow kinetics ($6.4\times10^{-5} \pm 7\times10^{-6}$ s^{-1}) (Fig 4.15). These constants translate into a K_d = 8.7 ± 1.8 nM, suggesting that the avidity can increase the strength of binding by as much as three orders of magnitude. Notably, the extent of avidity contribution is directly dependent on the length of the filaments, and consequently the number we derived here is likely an underestimation, as the filaments were kept deliberately short in our experimental setup.

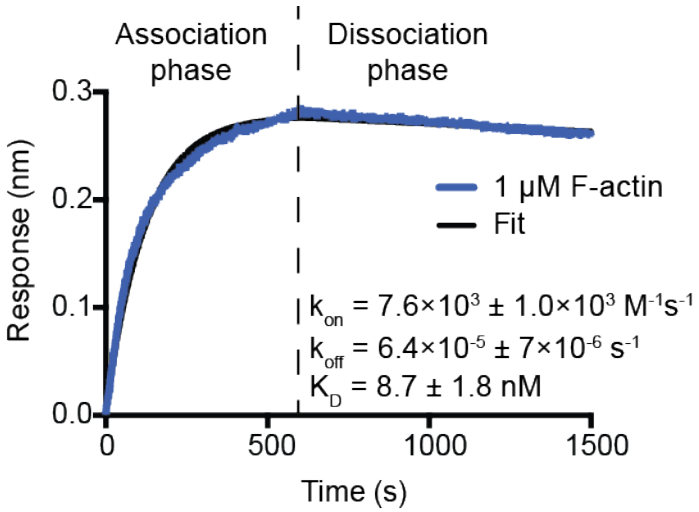

Figure 4.15 Avidity increases strength of DNGR-1 : F-actin interaction

DNGR-1 ECD was bound to anti-FLAG biosensor, and binding of 1 μM F-actin was tested. The curve is representative of six experiments, and the numbers represent the mean ± s.d. of all experiments.

4.2.11 Avidity in DNGR-1 internalization

In vitro experiments suggested that avidity plays an important role in F-actin recognition by DNGR-1. To assess if this is also the case in the context of full-length, transmembrane DNGR-1, we retrovirally introduced WT or W141A, E153A, W155A W250A, W250A, K251A or N140A Y150A mutant DNGR-1 into Phoenix cell line, and tested how the mutants respond to antibody and F-actin cross-linking. As expected (Huysamen et al., 2008, Sancho et al., 2008), when treated with anti-DNGR-1 antibody, all of the mutants got internalised (Fig 4.16 and 4.17), suggesting that they are not grossly misfolded, or otherwise unable to enter the endocytic pathway. On the contrary, when treated with F-actin, the mutants, which showed complete loss of binding in our biochemical assays (W250A, W155A W250A and W141A) also showed complete block of internalization (Fig 4.16 and 4.17). Surprisingly though, the mutants which showed strong defect in binding (K251A, E153A) still got internalised, albeit to smaller extent than the WT (Fig 4.16 and 4.17). Consistently with its largely unaffected affinity for F-actin, N140A Y150A mutant was indistinguishable from WT in its ability to internalise (Fig 4.16 and 4.17).

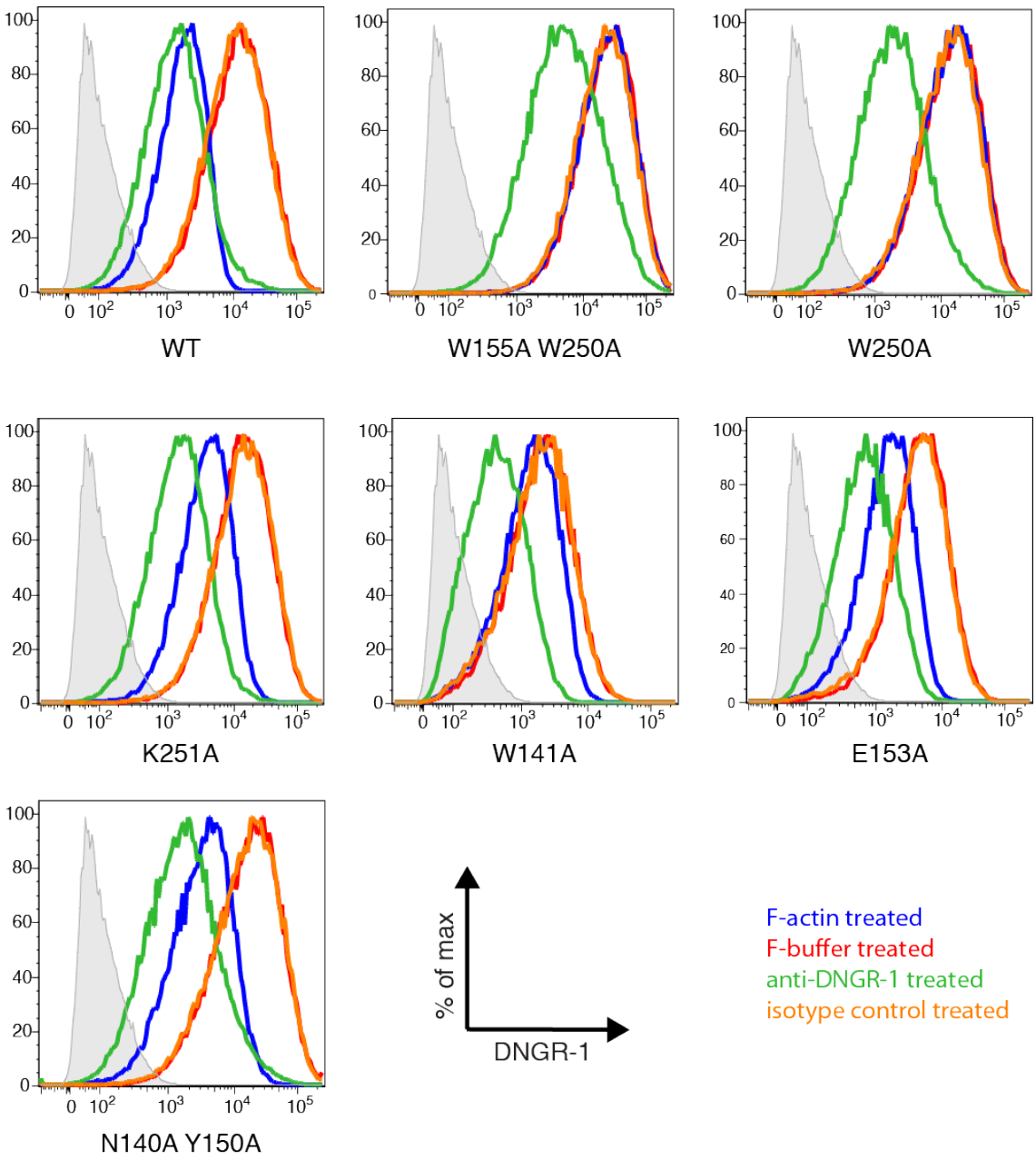

Figure 4.16 All DNGR-1 mutants are capable of being internalized

Phoenix cells expressing indicated mutant or WT DNGR-1 proteins were treated with F-actin, F-buffer, anti-DNGR-1 antibody or isotype-matched antibody of irrelevant specificity for 60 minutes at 37°C, fixed in formaldehyde, surface-stained for DNGR-1 and analysed by flow cytometry. One representative of six experiments is shown.

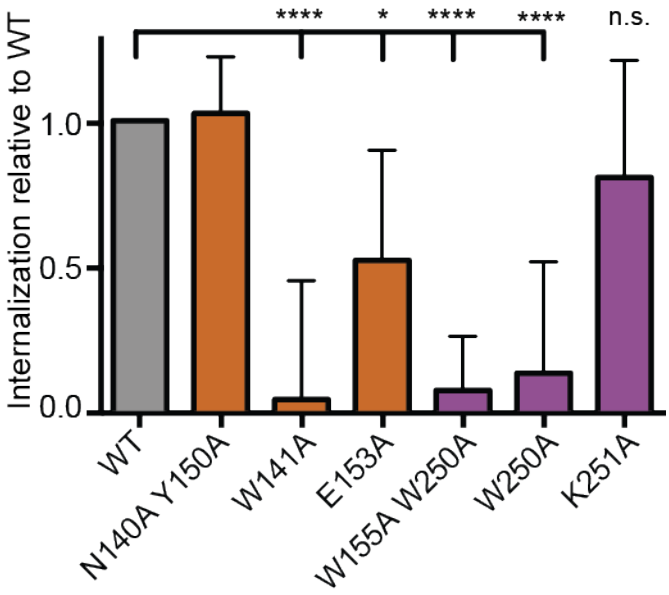

Figure 4.17 Avidity can compensate for a decrease in affinity in DNGR-1 internalization assay

Data from six independent experiments as in Fig 4.16 were normalized to the antibody-induced internalization and made relative to internalization of the WT. The bars depict mean ± s.d. *P < 0.05, **P < 0.01, ***P < 0.001, ****P < 0.0001; One-way ANOVA with Dunnett's multiple comparisons test.

4.2.12 Avidity in DNGR-1 signalling assay

In order to assess whether our observations in the internalization assay are also valid in DNGR-1 signalling assay, we utilized B3Z-Syk reporter cell line, where Syk-mediated NFAT activation results in transcription of β-galactosidase (Sancho et al., 2009). Syk activation can thus be read out using a chromogenic β-galactosidase substrate (CPRG). We stimulated reporter cells expressing WT or W155A W250A, K251A, E153A or N140A Y150A mutants with secondary necrotic cells at different ratios and assessed Syk activation. To account for differential expression of various mutants, we normalised the dead cell-induced response to response induced by plate-bound anti-DNGR-1 antibody. As expected, all the cells responded to antibody stimulation, and WT DNGR-1 allowed the cells to respond to dead cells. Consistently with what we saw in the internalization assay, the W155A W250A mutant showed no response to dead cells, while all the other mutants responded to extent comparable to WT, with only E153A mutant showing a mild decrease in response (Fig 4.18). Taken together, the data from internalization and

B3Z-Syk reporter assays suggest that the avidity component plays a significant role in F-actin recognition by transmembrane DNGR-1, and in both cases can compensate even for a significant decrease in affinity.

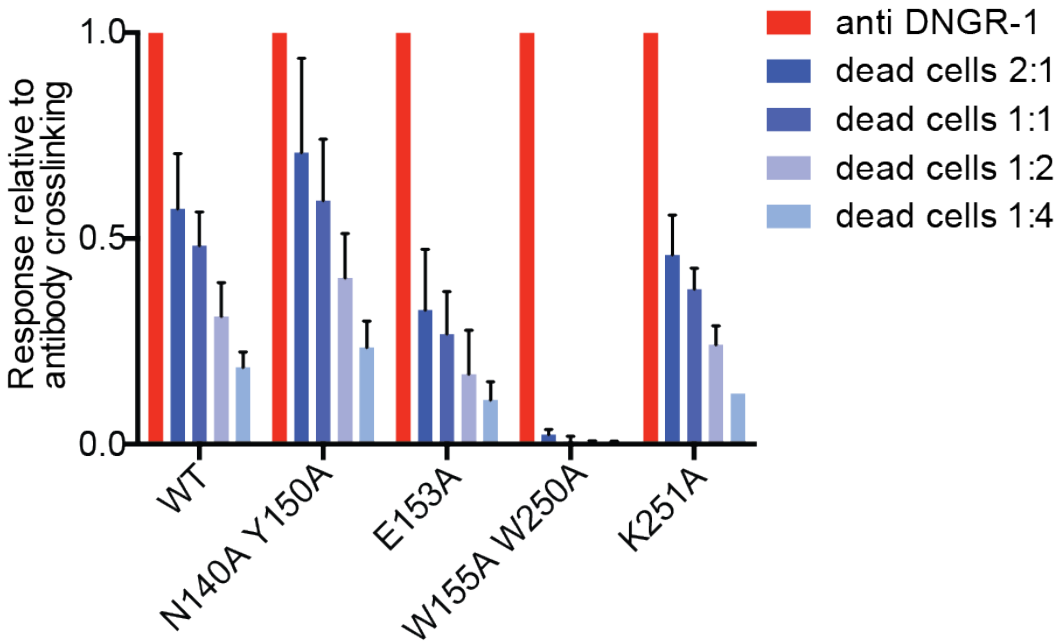

Figure 4.18 DNGR-1 mediated activation of reporter cells in response to dead-cell stimulation

B3Z-Syk reporter cells overexpressing mutant or WT DNGR-1 were incubated overnight with secondary necrotic cells at indicated ratios. Syk-mediated NFAT-activation was read out following the incubation. To account for different surface expression of different mutants, the response was made relative to the response induced by plate-bound anti-DNGR-1 antibody. The bars represent mean ± s.d. of three independent experiments.

4.2.13 DNGR-1-mediated cross-presentation

Cross-presentation of dead cell-associated antigens was previously shown to be DNGR-1 dependent (Iborra et al., 2012, Sancho et al., 2009, Zelenay et al., 2012). In order to confirm a requirement for F-actin recognition in DNGR-1 function, and to assess the effects of decrease in affinity on DNGR-1 mediated cross-presentation, we established collaboration with David Sancho and Salvador Iborra (Centro Nacional de Investigaciones Cardiovasculares, Madrid, Spain). Dendritic cells obtained by culture of bone marrow from DNGR-1 knock out (KO) mice in medium containing Flt3 ligand were transduced with empty retrovirus as a control or retroviruses encoding for WT, W155A W250A and K251A DNGR-1. Transduced

cells were then incubated at different ratios with Vaccinia-OVA-infected RAW264.7 cells, which were or were not UV-irradiated, and the capacity of DCs to present viral antigen to antigen-specific $CD8^+$ T-lymphocytes was assessed by determining the proportion IFN-γ^+ T-cells after the coculture (Iborra et al., 2012). Under conditions where direct antigen presentation was allowed (non-irradiated virus), all DCs presented equally efficiently, confirming no impairment in the process of antigen presentation per se (Fig 4.19, left). Consistently with previously published data, when the virus was UV-irradiated and cross-presentation was the only route of antigen presentation, the DNGR-1 KO cells transduced with the control virus showed a significant impairment in T-cell priming compared to WT cells (Fig 4.19, right) (Iborra et al., 2012). As expected, reintroduction of WT DNGR-1 into KO cells rescued their cross-presentation capability, while the W155A W250A mutant failed to do so (Fig 4.19, right), formally demonstrating that F-actin recognition is essential for DNGR-1 function. Surprisingly, and in contrast with the results obtained with B3Z-Syk reporter cells, the DCs transduced with K251A mutant DNGR-1 showed only an intermediate phenotype (Fig 4.19, right). Whether this result is due to different surface density of DNGR-1, expression levels of Syk, or different extent of cross-linking required for productive signalling in the different cell types is unclear.

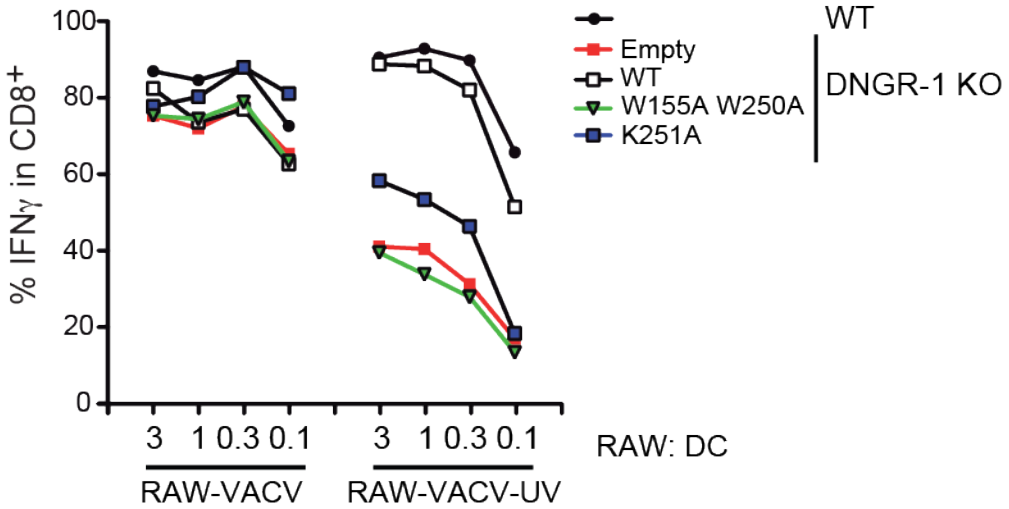

Figure 4.19 F-actin recognition is essential for DNGR-1 mediated cross-presentation of dead cell-associated antigens

Raw264.7 cells were infected with Vaccinia OVA virus and UV-irradiated (RAW-VACV-UV) or left un-irradiated (RAW-VACV) and plated at indicated ratios with dendritic cells and ovalbumin specific T-lymphocytes. Production of IFNγ by T-lymphocytes was read out after 6 hours of stimulation and percentage of IFNγ$^+$

cells within the $CD8^+$ population was determined. One representative of three experiments is shown. Image courtesy of S. Iborra and D. Sancho.

4.3 Discussion

DNGR-1 is the only known transmembrane protein recognizing F-actin in the extracellular environment, and at the same time the only known C-type lectin to bind this polymeric ligand. As such it is of clear interest to understand the mechanism of binding at atomic level. Here we present the structure of actin filament decorated with DNGR-1 at 7.7 Å resolution with a list of residues involved in the interaction validated by mutational analysis. We define a flexible loop missing in the crystal structure of DNGR-1, determine the contribution of avidity to the interaction, and formally demonstrate the requirement of ligand recognition for DNGR-1 function in dendritic cells.

Interestingly, DNGR-1 binds into the groove between two actin protofilaments, making contacts with two actin subunits across the filament and at the same time with two actin subunits along one protofilament. This mode of binding is very uncommon among canonical actin-binding proteins, although it shares some features with that of coronin (Galkin et al., 2008, Ge et al., 2014), Arp2/3 complex (Rouiller et al., 2008) and *Salmonella* SipA protein (Lilic et al., 2003). Binding site of DNGR-1, however, shows only partial overlap with binding sites of any of the above proteins, and is characterized by a surprisingly small interface with only a handful of residues contributing to the interaction. This suggests that DNGR-1 has specifically evolved to bind to F-actin regardless of its decoration with most other actin-binding proteins, even though proteins that affect conformational state of actin are still likely to interfere with DNGR-1 binding. In fact cofilin, an actin binding protein, which changes the helical twist of actin filaments (McGough et al., 1997), has been shown to block DNGR-1 binding to F-actin (Zhang et al., 2012).

In agreement with the small interaction interface, DNGR-1 shows only a modest affinity for F-actin, together with a very rapid kinetics of association and dissociation. This appears counterintuitive for a receptor that recognizes a ligand that is scarce in the extracellular milieu. However, the polymeric state of F-actin suggests that an avidity component is likely to come into play when DNGR-1 is bound in the membrane. Indeed, we demonstrate that when DNGR-1 is bound to a surface, the

strength of binding increases by as much as three orders of magnitude, and the avidity can even compensate for a decrease in affinity, explaining how the evolutionary trade-off between high affinity large binding site, which could be obscured by other actin-binding proteins, and a low-affinity small one, binding to which, however, is unlikely to be hindered by other proteins, can work in favour of the latter.

Finally, DNGR-1 was previously shown to play a role in cross-presentation of dead cell-associated antigens, which was dependent upon its ability to elicit productive signalling through the intracellular hemITAM motif (Sancho et al., 2009). The evidence for direct F-actin involvement in this process, however, has to date been largely indirect. Here we show that DNGR-1 incapable of F-actin recognition does not induce Syk-mediated signalling in reporter cell line when exposed to dead cells, and importantly, we formally demonstrate that the ability to recognize F-actin is essential for the function of DNGR-1 in DCs, as mutant incapable of F-actin binding is also incapable of rescuing the cross-presentation defect in DNGR-1-deficient DCs.

Notably, some of the actin residues present in close proximity to DNGR-1 binding site can undergo posttranslational modifications including phosphorylation, nitration and ubiquitination (Terman and Kashina, 2013). The physiological function of majority of these currently remains enigmatic (Terman and Kashina, 2013), it is, however, tempting to speculate that some of the modifications could serve as a readout of the cellular state and/or modality of cell death, and by means of affecting DNGR-1 binding they could help regulate the immune response to dead cell-associated antigens.

Chapter 5. DNGR-1 can bind with both ligand-binding domains to the same actin filament

5.1 Introduction

Even though our structure of DNGR-1 : F-actin complex allows detailed understanding of the interaction at the level of single ligand-binding domains, the exact spatial organisation of DNGR-1 molecules along the filament remains unknown. It has been suggested previously that DNGR-1 is likely able to bind in *trans*, crosslinking two actin filaments within an F-actin bundle (Ahrens et al., 2012), however, whether binding in *cis* to a single filament with both ligand-binding domains is also possible remains to be established. Consequently, in order to gain insight into the mode of DNGR-1 binding, we decided to set up a system in which we could analyse binding to single actin filaments of a heterodimeric DNGR-1 ECD protein where one half of the dimer is WT and the other half bears the W155A W250A mutation. Such protein, even though dimeric, would behave as a monomer in terms of ligand binding. Consequently, if DNGR-1 can bind in *cis*, the homodimer should exhibit stronger binding to single actin filaments than the heterodimer, owing to the cooperativity between the two ligand-binding domains (Fig 5.1, left). On the other hand, if DNGR-1 can only bind in *trans*, the monomer and dimer should be indistinguishable in binding to single actin filaments, because the cooperativity can not come into play (Fig 5.1, right). Importantly, only binding to single actin filaments can distinguish between the two scenarios, as both ligand-binding domains can come into play in the interaction with bundled actin, as suggested by the difference in affinity we observed between the dimeric ECD and monomeric CTLD (Fig 4.13).

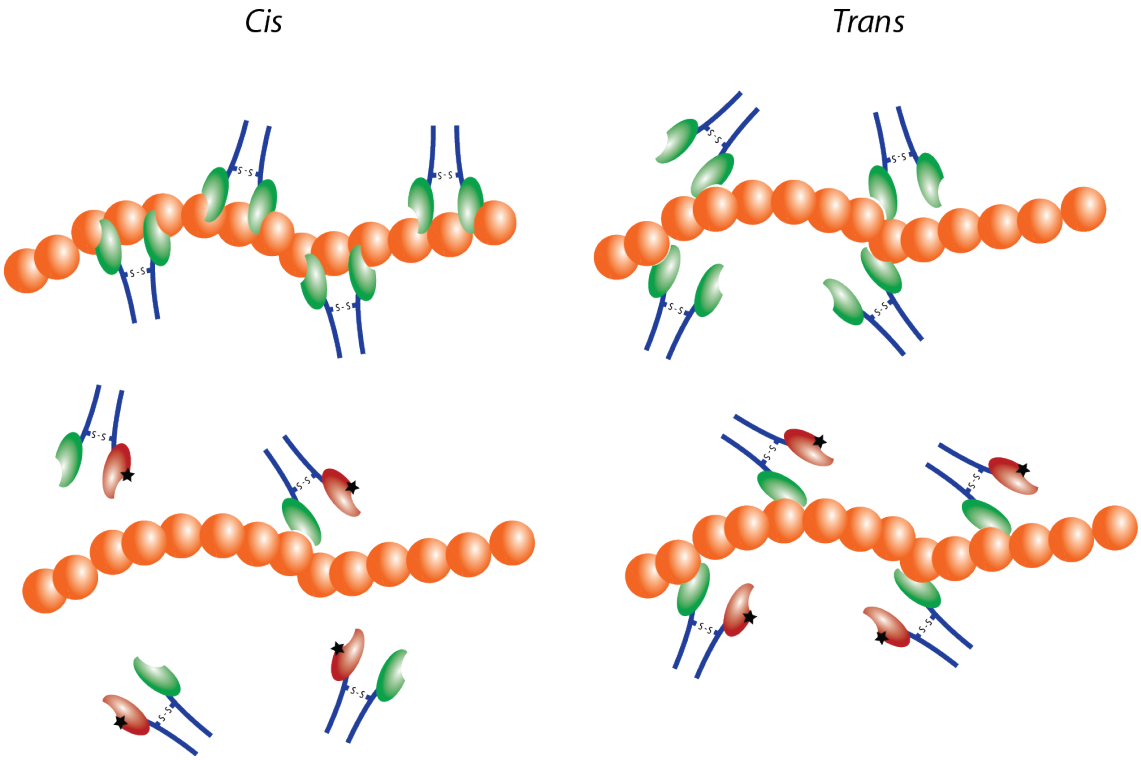

Figure 5.1 Schematic depiction of possible modes of DNGR-1 binding and their impact on the binding of the homo and heterodimeric proteins to single actin filaments

If DNGR-1 can bind with both ligand-binding domains to a single actin filament (*cis*), the heterodimer would show decreased affinity for such filaments compared to the WT (left). If DNGR-1 can bind only in *trans*, crosslinking different filaments, the affinity of WT and heterodimer for single actin filaments would be identical (right).

5.2 Results

5.2.1 Generation of labelled heterodimeric DNGR-1 ECD proteins

In order to generate heterodimeric DNGR-1 ECD, we co-transfected 293F cells with FLAG-tagged W155A W250A DNGR-1 and HA-tagged WT DNGR-1, or, as a control, FLAG-tagged WT and HA-tagged WT DNGR-1. All the proteins additionally possessed a short sequence of amino acids known as a “sortag” fused to their C-terminus, which allows covalent linkage to labelled peptides of specific sequence by means of enzymatic reaction with Sortase A (sortagging) (Popp et al., 2009). The advantage of such labelling, compared to a nonspecific one such as the amine-coupling chemistry, is that exactly one molecule of fluorophore will be

attached to each DNGR-1 monomer. Furthermore, using this setup, the site of labelling is clearly defined and shared among all the molecules, minimising the likelihood of the label being randomly placed in a site where it could interfere with the DNGR-1 binding. Consequently, using sequential affinity purification on M2-anti-FLAG affinity gel and anti-HA-agarose with the sortagging step in between (Fig 5.2), we were able to obtain fluorescently labelled heterodimeric DNGR-1.

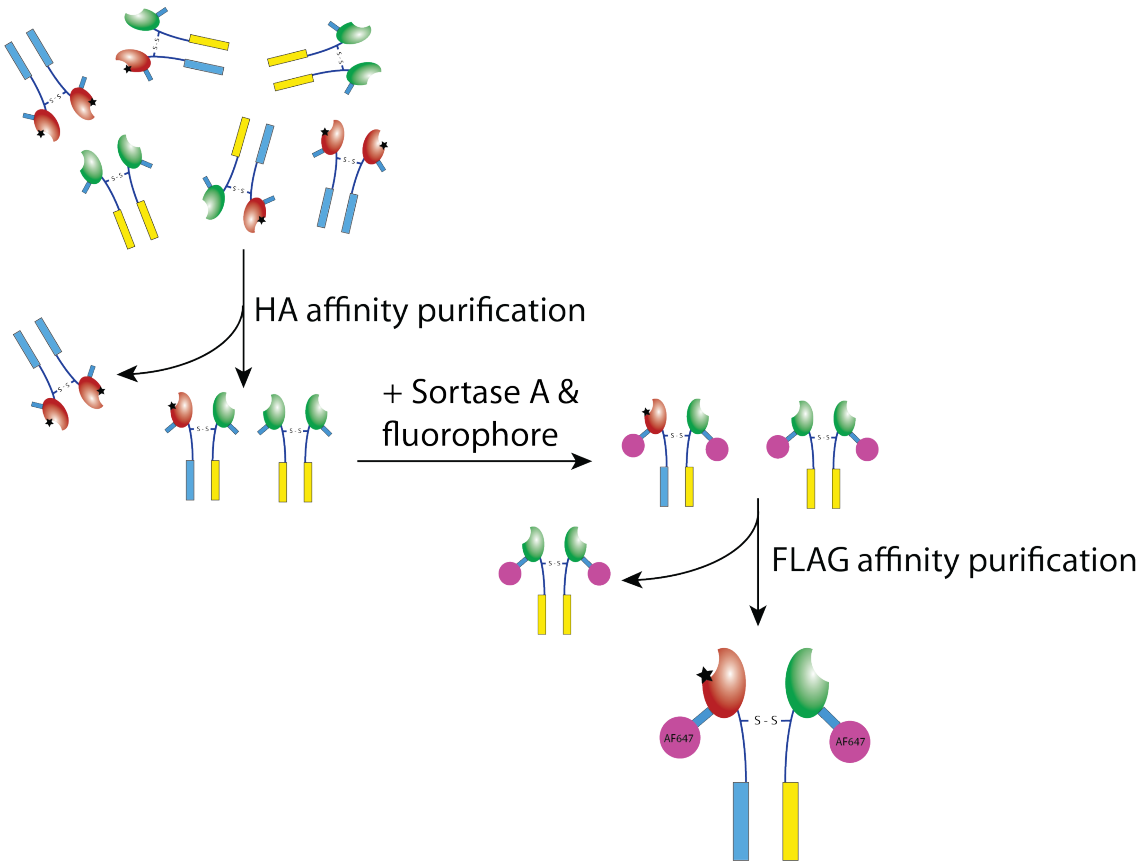

Figure 5.2 Schematic depiction of the workflow for generation of heterodimeric DNGR-1 ECD

Transient co-transfection of DNA coding for differently tagged WT and W155A W250A DNGR-1 ECD into 293F cells results in the production of a mixture of homo and heterodimeric proteins. The heterodimers can subsequently be purified by two sequential affinity purification steps. Fluorescent label is introduced by the sortagging reaction in between the affinity purification steps.

5.2.2 Validation of fluorescently labelled DNGR-1 proteins

In order to validate the fluorescently labelled DNGR-1 proteins, we tested their ability to bind to dead cells. We UV-irradiated HeLa cells, let them undergo

secondary necrosis overnight and stained the cell corpses on the following day directly with labelled WT : WT homodimer or WT : W250A W155A heterodimer. As a control, staining with unlabelled FLAG-tagged ECD (dimeric) and CTLD (monomeric) was also tested, and their binding was revealed using an anti-FLAG antibody. In both cases, the extent of binding was assessed using flow cytometry with DAPI used to discriminate dead cells. As expected, the WT : WT homodimer bound more strongly to dead cells than the WT : W155A W250A heterodimer (Fig 5.3A), suggesting an increase in the affinity of the homodimer compared to the heterodimer, due to cooperativity between the two ligand-binding domains. Encouragingly, when we compared the dimeric ECD with monomeric CTLD in the same assay, detecting DNGR-1 binding to dead cells with an anti-FLAG antibody, we observed an identical pattern where dimeric ECD bound more strongly than monomeric CTLD (Fig 5.3B). The F-actin present in dead cells is mostly in the form of actin bundles (Furukawa and Fechheimer, 1997, Claessens et al., 2006). Consequently, these results cannot give us any insight into the ability of DNGR-1 to bind to single actin filaments, but rather they demonstrate the ability of DNGR-1 to utilise both of its ligand-binding domains when interacting with bundles of F-actin, as suggested previously (Ahrens et al., 2012).

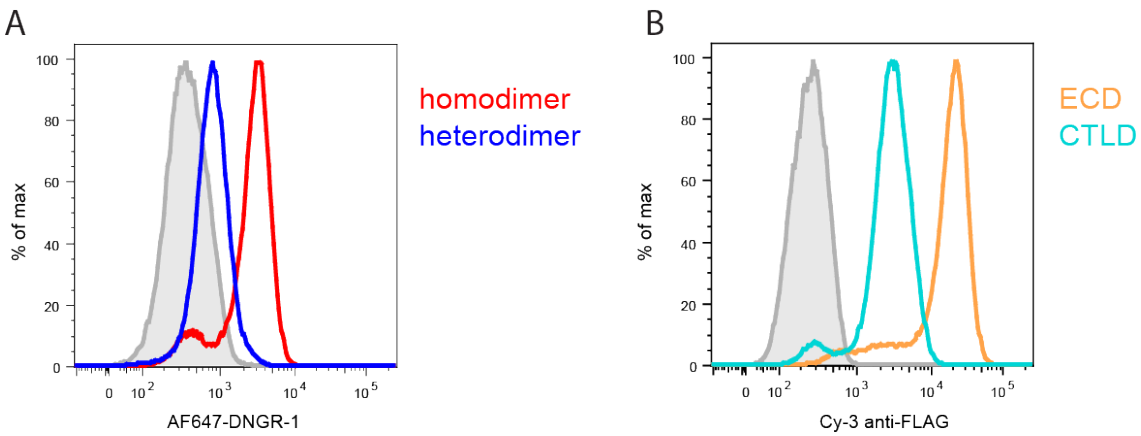

Figure 5.3 Binding of homo and heterodimeric DNGR-1 to dead cells

HeLa cells were UV-irradiated and left to undergo secondary necrosis overnight. Following the incubation, the cell corpses were stained with indicated DNGR-1 proteins and their binding was assessed using flow cytometry. Dead cells were differentiated by staining with DAPI. **A**, Binding of labelled proteins was assessed directly using the fluorescent label **B,** binding of unlabelled ECD and CTLD was assessed using Cy-3 anti-FLAG antibody.

5.2.3 Binding of heterodimeric DNGR-1 proteins to single actin filaments

Generating single actin filaments *in vitro* is complicated by the propensity of F-actin to form bundles. In order to circumvent this problem, we utilised a previously developed setup where spectrin was allowed to non-specifically adsorb onto a cover slip and the bound molecules were then used as seeds for F-actin polymerization (Jegou et al., 2011). This, together with short polymerization time (5 min), allowed us to obtain short single actin filaments anchored to the cover slip. The filaments were stained by fluorescently labelled phalloidin, decorated with the labelled homo or heterodimeric DNGR-1 proteins, and imaged using TIRF microscopy. While we observed clear binding of WT : WT protein, we could not detect any stable binding of the heterodimeric W155A W250A : WT protein (Fig 5.4), suggesting that WT DNGR-1 can bind to single actin filaments with both of its ligand-binding domains. Unexpectedly, for the WT : WT protein, we did not see uniform actin decoration, but rather a patchy staining reminiscent to that of cofilin (McGough et al., 1997). This mode of binding would suggest a previously unappreciated degree of cooperativity between DNGR-1 molecules.

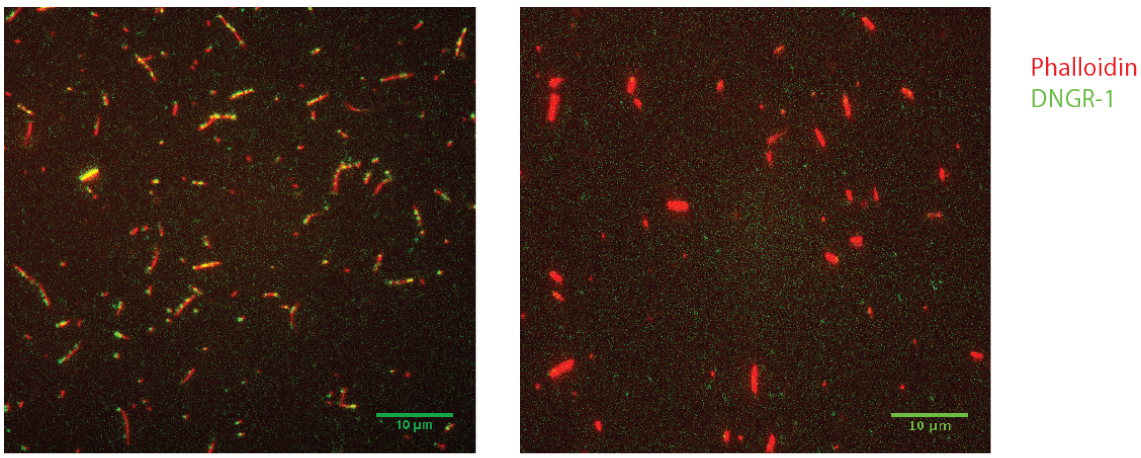

Figure 5.4 DNGR-1 homodimer and heterodimer binding to single actin filaments

Actin filaments were polymerised on spectrin seeds adsorbed onto coverslip chambers to obtain single filaments and stained with phalloidin (red). Indicated labelled DNGR-1 proteins (green) were floated into the chamber and the coverslips were imaged using TIRF microscope.

5.3 Discussion

It has previously been argued that DNGR-1 is likely to be able to bind in *trans*, crosslinking pre-bundled actin filaments (Ahrens et al., 2012). Such notion is supported by an apparent increase in the strength of binding of DNGR-1 to F-actin when the latter is complexed with actin-binding proteins that can induce its bundling (Ahrens et al., 2012, Zhang et al., 2012). This line of evidence, however, is largely indirect, and the ability of DNGR-1 to bind in *trans* is difficult to prove formally. Consequently, in this study, we set out to assess if DNGR-1 is able to bind in *cis*.

Using heterodimeric constructs, we demonstrate that WT DNGR-1 ECD has higher affinity for single actin filaments than DNGR-1 ECD molecules in which one part of the dimer has been substituted with a mutant incapable of binding to F-actin. Such protein has all the biophysical properties of WT DNGR-1, but its ligand-binding ability corresponds to that of a monomer. Consequently, taken at face value, our data suggest that both ligand-binding domains of one DNGR-1 molecule can bind to binding sites on a single actin filament in *cis*. Importantly, this observation does not mean that DNGR-1 could not bind in *trans*. The apparent ability of DNGR-1 to bind in *cis*, however, brings about a conceptual problem of how can both ligand-binding domains reach their binding sites. The binding sites for DNGR-1 on an actin filament are separated by around 6 nm, generating a repetitive pattern with largely translational symmetry (Fig 5.5A). The two neighbouring CTLDs bound to the filament share no interface, have about 2 nm of free space between them, and are both oriented in the same way, also exhibiting largely translational symmetry (Fig 5.5A). On the other hand, the symmetry that one would expect between the two parts of unbound DNGR-1 dimer is rotational, as suggested by the LOX-1-like DNGR-1 dimer model (Zhang et al., 2012) (Fig 5.5B) and seen in other C-type lectin receptors (Back et al., 2009, Park et al., 2005). The only way to reconcile these contradictory properties is to assume that there, in fact, is no rigid dimerization interface, and that the two CTLDs can exist and bind independently. Additionally, the neck region and the hinge between the neck and the CTLD have to be flexible enough for the two CTLDs to be able to twist in such a way that the rotational symmetry of unbound protein can change into a translational one upon binding to a single actin filament. Since the extra exon present in the *long* isoform of murine DNGR-1 lies in between the dimerizing cysteine and the CTLD, and

based on the structure prediction as well as our CD data appears to be largely unstructured, it is tempting to speculate that the *long* isoform of mouse DNGR-1 has evolved to give the CTLDs more flexibility than would be the case for the *short* isoform. How would such difference reflect on the functional properties of the receptors, however, is not clear, as under *in vivo* settings F-actin rarely appears in the form of single filaments, obviating the need for the ability to bind in *cis.*

Intuitively, even for the interaction in *trans*, DNGR-1 needs to be flexible enough to "reach" the two actin filaments, although, conceivably, the degree of flexibility required for such mode of interaction could be lower. Consistently, reporter cells expressing *long* or *short* murine DNGR-1 are activated by dead cells to similar extent (data not shown), and in human there is no homologue of the *long* isoform altogether, suggesting that the evolutionary pressure on higher mobility of DNGR-1 CTLDs may be limited. It would be interesting to repeat the TIRF experiment with the *short* mouse or human DNGR-1 isoforms, or mutants lacking parts of the neck region between the dimerizing cysteine and the CTLD to see if decreased mobility and/or flexibility of the neck would result in impaired binding of DNGR-1 to single actin filaments.

In summary, our data demonstrate that DNGR-1 can bind in *cis* to single actin filaments, but this is not to say that this mode of recognition is necessarily utilised *in vivo.* Importantly, however, what our data show is that even though DNGR-1 is constitutively dimeric, there appears to be no dimerization interface between the two CTLDs, and they can exist and bind independently.

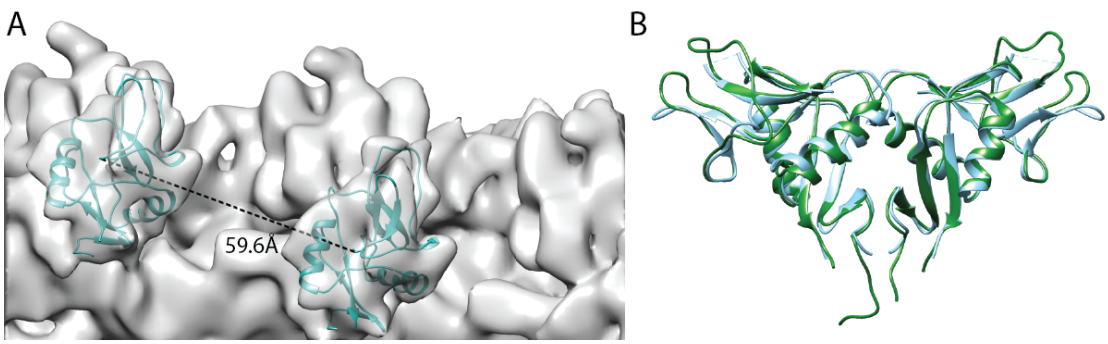

Figure 5.5 – Incompatibility between the mode of DNGR-1 binding and the LOX-1-like model of DNGR-1 dimerization

A, Crystal structure of DNGR-1 CTLD (PDB ID 3VPP; light blue)(Zhang et al., 2012) was fitted into electron density of DNGR-1-decorated actin filament as in

Fig 4.3. The distance between corresponding atoms of the two DNGR-1 CTLDs was determined in the UCSF Chimera software (black dashed line). **B,** Crystal structure of DNGR-1 CTLD (PDB ID 3VPP; (Zhang et al., 2012)) was aligned with both chains of the LOX-1 dimer (PDB ID 1YPU)(Park et al., 2005) using the MatchMaker tool in the UCSF Chimera software. RSMD for both chains was below 1 Å. DNGR-1 CTLD in light blue, LOX-1 in green.

Finally, the patchy staining pattern we observed for DNGR-1 on single actin filaments indicates a surprising cooperativity in binding between DNGR-1 molecules. Our Cryo-EM data rule out the possibility that DNGR-1, like cofilin, induces a large change in filament helicity, however, small changes that could get propagated along the filament cannot be ruled out at the resolution we achieved. Given the polymeric form of F-actin, with the binding sites appearing in regular intervals, it is conceivable that binding to F-actin positions the DNGR-1 molecules on the cell surface in the right distance from each other to induce signalling. If this were to be the case, a cooperative mode of binding, whereby occupation of one binding site potentiates binding of a second DNGR-1 molecule to the neighbouring one would be of clear advantage, allowing a “clustered” positioning of DNGR-1 molecules around one spot, rather than random distribution along the filament. As the binding sites are positioned in a helical pattern relative to one another, this would also be another reason why flexibility of DNGR-1 would be of importance, making it possible for DNGR-1 molecules to reach their binding sites on a filament even if those happen to be positioned in a way that they are not facing directly downwards towards the cell membrane.

Chapter 6. Final discussion

The field of DAMP recognition has rapidly expanded over the last years, with various endogenous molecules ranging from heat shock proteins (Asea et al., 2000) to uric acid crystals (Martinon et al., 2006, Neumann et al., 2014) now being widely accepted as putative DAMPs. Lack of detailed understanding of these interactions at molecular level has, however, hampered the advancement of the field and resulted in controversies over specificity of some of these interactions (Bausinger et al., 2002).

Currently the only way to confirm the specificity of any interaction observed within a biological system beyond any reasonable doubt is to take a step back from complex *in vivo* systems and assess the interaction and properties of all the putative interaction partners under simplified *in vitro* settings where purified reagents can be used, minimizing or completely avoiding interference from other players that might appear *in vivo*. Similarly, in order to provide a description of a protein's properties, one is best served by applying direct biophysical techniques to a purified protein or a defined mixture of those. Stemming from this rationale, in this work we attempted to provide a comprehensive description of the properties of a C-type lectin receptor, DNGR-1, and its interaction with F-actin based on *in vitro* approaches, where possible drawing conclusions about functional aspects of the protein in its biological settings.

Taken together, our structural data confirm the specificity of DNGR-1 for F-actin, unambiguously explain its exclusive binding to the polymeric form, and rule out the necessity of accessory proteins for the interaction. Additionally, we formally demonstrate the necessity of ligand-recognition for DNGR-1-mediated cross-presentation of dead cell-associated antigens by dendritic cells, and an important contribution of avidity to the interaction. Notably, we also show that DNGR-1 is able to bind with both of its ligand-binding domains to a single actin filament, demonstrating an unexpected degree of flexibility in the neck region as well as the absence of a rigid dimerization interface between the two DNGR-1 CTLDs. Finally, we note that the neck region of DNGR-1 serves as a pH- and ionic strength-specific sensor, conceivably allowing DNGR-1 to discriminate between extracellular and endosomal environments by changing its conformational state,

and suggesting a way in which DNGR-1 might modulate its function based on its subcellular localization.

Our study brings to light several questions: Firstly, do the cellular metabolism and/or infected state of a dying cell affect posttranslational modifications of actin or decoration of filaments with certain ABPs, thereby affecting DNGR-1 binding? Observations have been made for HMGB-1 where, depending on the redox state of its cysteines as well as its acetylation, different functional outcomes ensue after its extracellular recognition (Yang et al., 2013), suggesting that at least in some cases such mode of regulation of DAMP recognition has indeed evolved. Unfortunately, while a plethora of posttranslational modifications have been reported for actin, not much is known about their function or how are they regulated (Terman and Kashina, 2013). On the other hand, ABPs and their function and influence on actin have been a focus of intensive research, and involvement of some ABPs, as well as the overall status of the actin cytoskeleton in the processes of cell death have been noted both in higher eukaryotes and in yeast (Desouza et al., 2012, Gourlay et al., 2004). Of particular interest, cofilin, an ABP that changes helical twist of actin filaments and has been shown to interfere with DNGR-1 binding (Zhang et al., 2012), plays a role in programmed cell death, and its mitochondrial translocation is an early step in both apoptosis and necroptosis induction (Chua et al., 2003, Karch et al., 2015). It is, consequently, tempting to speculate that cofilin translocation from the cytoplasm could improve F-actin-recognition by DNGR-1, thus making F-actin of dead-cell origin a better ligand, even though further work will be needed to address if this is indeed relevant for DNGR-1 binding to F-actin and its function.

Second obvious question stemming from our data is, what is the advantage of DNGR-1 being able to bind with both of its ligand-binding domains to a single filament, given that under *in vivo* settings actin rarely, if ever, appears in this form? To consider this question, one first needs to take into account that, compared to other isoforms, the DNGR-1 isoform for which we observed such behaviour contains an extra stretch of twenty six amino acids between the CTLD and the dimerization cysteine, which is likely to make the flexibility of the protein even more pronounced. Consequently, it is reasonable to assume that the isoforms devoid of these extra amino acids would be less likely to exhibit the same ability, but this will need to be addressed experimentally. As a result, the answer may be that under *in vivo* settings there, in fact, is no need for DNGR-1 to be able to bind to single actin

filaments with both of its ligand-binding domains, and what we observed for the *long* DNGR-1 isoform is an isoform-specific property. Importantly, however, our observations provide a proof of principle, suggesting an absence of dimerization interface between the DNGR-1 CTLDs and their ability to exist independently, which are properties likely to be conserved between isoforms, regardless of the length of the neck region. And while the biological rationale for the ability of DNGR-1 to bind to single actin filaments in *cis* is unclear, the ability of the two domains to move and bind independently is of importance also for the ability of DNGR-1 to bind in *trans*. Most transmembrane receptors bind to ligands that have defined geometry, whether they are soluble molecules, other transmembrane proteins, or ligands arrayed in an orderly fashion on a surface. In stark contrast, DNGR-1 binds to F-actin, which in its bundled form is likely to have the DNGR-1 binding sites distributed at, more or less, random intervals (although closer together than would be the case for a single filament), making it disadvantageous for DNGR-1 to be limited to a single geometry of recognition, which would be imposed by a rigid dimerization interface. Notably, the structural similarity of DNGR-1 and LOX-1 CTLDs (Zhang et al., 2012), together with the fact that the dimerization interface of LOX-1 hinges on the presence of a single amino acid (Nakano et al., 2012), suggest an evolutionarily plausible way how such adaptation could have easily arisen.

Thirdly, we observed an ability of DNGR-1 to undergo a conformational change in a pH- and ionic strength-specific manner. Similar behaviour has been described for other C-type lectin receptors, however, the biological function of the conformational change observed in these cases does not appear to be shared with DNGR-1, begging the question, what is its function, if any? Importantly, we observed the conformational change in multiple DNGR-1 isoforms, suggesting that it is not just an isoform-specific artefact. Furthermore, the amino acid composition of the neck region is no less conserved between species than that of the ligand-binding domain, suggesting that the evolutionary pressure on the two parts of the protein is similar. This would argue in favour of a model where the neck plays an important role in DNGR-1 biology, beyond its function as a mere scaffold upholding the CTLD and connecting it to the membrane. Intuitively, for DNGR-1, regulation of its function based on its subcellular localization makes sense – on the cell surface it needs to act as an endocytic receptor, mediating internalization of dead cell-associated

material, while in the endosomes it acts through an as-of-yet incompletely understood mechanism to prevent maturation of the endosomes. It would make little sense for DNGR-1 to signal for block in endosomal maturation from cell surface, much like to signal for internalization from inside a vesicle. How exactly is this "division of labour" achieved mechanistically remains to be conclusively shown, however, the conformational change we describe provides a way for DNGR-1 to "sense" its environment and also to react to it, making it a prime candidate for such mechanism (Fig 6.1).

In summary, our study significantly broadens our knowledge of the biology and biochemistry of DNGR-1, but at the same time it alsoemphasises several new, previously unappreciated questions, answers to which will require further research.

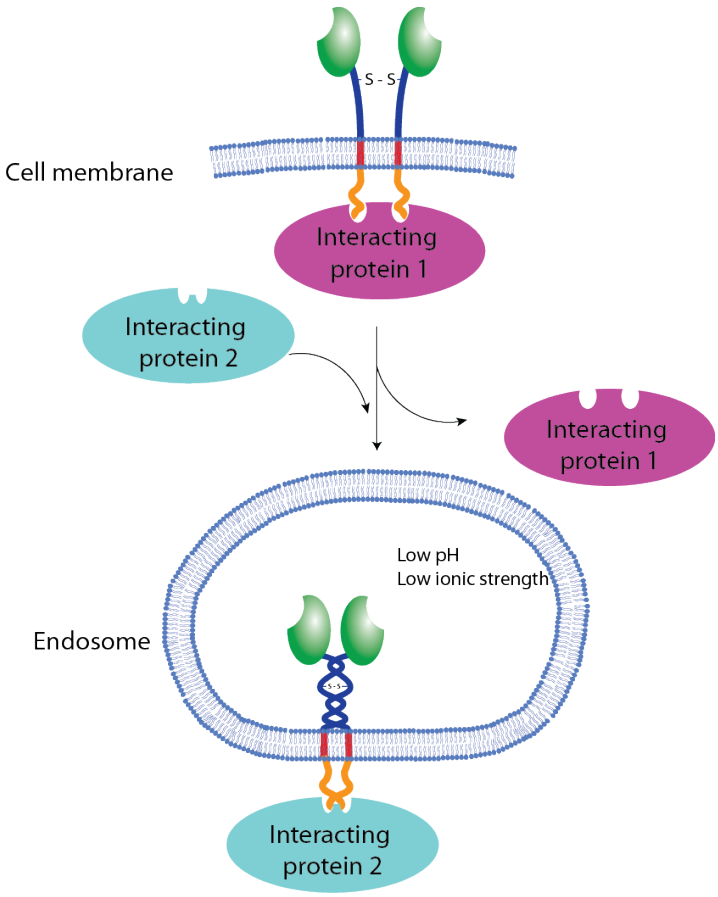

Figure 6.1 - Schematic model of how a conformational change in the neck can allow spatial regulation of DNGR-1 function

Repositioning of the neck regions can result in repositioning of the intracellular signalling motifs, thereby affecting the ability of DNGR-1 to interact with various proteins

Reference List

ABDICHE, Y., MALASHOCK, D., PINKERTON, A. & PONS, J. 2008. Determining kinetics and affinities of protein interactions using a parallel real-time label-free biosensor, the Octet. *Anal Biochem,* 377**,** 209-17.

ACKERMAN, A. L., GIODINI, A. & CRESSWELL, P. 2006. A role for the endoplasmic reticulum protein retrotranslocation machinery during crosspresentation by dendritic cells. *Immunity,* 25**,** 607-17.

ACTON, S. E., ASTARITA, J. L., MALHOTRA, D., LUKACS-KORNEK, V., FRANZ, B., HESS, P. R., JAKUS, Z., KULIGOWSKI, M., FLETCHER, A. L., ELPEK, K. G., BELLEMARE-PELLETIER, A., SCEATS, L., REYNOSO, E. D., GONZALEZ, S. F., GRAHAM, D. B., CHANG, J., PETERS, A., WOODRUFF, M., KIM, Y. A., SWAT, W., MORITA, T., KUCHROO, V., CARROLL, M. C., KAHN, M. L., WUCHERPFENNIG, K. W. & TURLEY, S. J. 2012. Podoplanin-rich stromal networks induce dendritic cell motility via activation of the C-type lectin receptor CLEC-2. *Immunity,* 37**,** 276-89.

ACTON, S. E., FARRUGIA, A. J., ASTARITA, J. L., MOURAO-SA, D., JENKINS, R. P., NYE, E., HOOPER, S., VAN BLIJSWIJK, J., ROGERS, N. C., SNELGROVE, K. J., ROSEWELL, I., MOITA, L. F., STAMP, G., TURLEY, S. J., SAHAI, E. & REIS E SOUSA, C. 2014. Dendritic cells control fibroblastic reticular network tension and lymph node expansion. *Nature,* 514**,** 498-502.

ADACHI, Y., ISHII, T., IKEDA, Y., HOSHINO, A., TAMURA, H., AKETAGAWA, J., TANAKA, S. & OHNO, N. 2004. Characterization of beta-glucan recognition site on C-type lectin, dectin 1. *Infect Immun,* 72**,** 4159-71.

AHRENS, S., ZELENAY, S., SANCHO, D., HANC, P., KJAER, S., FEEST, C., FLETCHER, G., DURKIN, C., POSTIGO, A., SKEHEL, M., BATISTA, F., THOMPSON, B., WAY, M., REIS E SOUSA, C. & SCHULZ, O. 2012. F-actin is an evolutionarily conserved damage-associated molecular pattern recognized by DNGR-1, a receptor for dead cells. *Immunity,* 36**,** 635-45.

AKIRA, S. & TAKEDA, K. 2004. Toll-like receptor signalling. *Nat Rev Immunol,* 4**,** 499-511.

AKIRA, S., UEMATSU, S. & TAKEUCHI, O. 2006. Pathogen recognition and innate immunity. *Cell,* 124**,** 783-801.

ANDERSON, S. K., ORTALDO, J. R. & MCVICAR, D. W. 2001. The ever-expanding Ly49 gene family: repertoire and signaling. *Immunol Rev,* 181**,** 79-89.

ANDERSSON, U. & TRACEY, K. J. 2011. HMGB1 is a therapeutic target for sterile inflammation and infection. *Annu Rev Immunol,* 29**,** 139-62.

ARIIZUMI, K., SHEN, G. L., SHIKANO, S., XU, S., RITTER, R., 3RD, KUMAMOTO, T., EDELBAUM, D., MORITA, A., BERGSTRESSER, P. R. & TAKASHIMA, A. 2000. Identification of a novel, dendritic cell-associated molecule, dectin-1, by subtractive cDNA cloning. *J Biol Chem,* 275**,** 20157-67.

ARSTILA, T. P., CASROUGE, A., BARON, V., EVEN, J., KANELLOPOULOS, J. & KOURILSKY, P. 1999. A direct estimate of the human alphabeta T cell receptor diversity. *Science,* 286**,** 958-61.

ASEA, A., KRAEFT, S. K., KURT-JONES, E. A., STEVENSON, M. A., CHEN, L. B., FINBERG, R. W., KOO, G. C. & CALDERWOOD, S. K. 2000. HSP70 stimulates cytokine production through a CD14-dependant pathway, demonstrating its dual role as a chaperone and cytokine. *Nat Med,* 6**,** 435-42.

BACK, J., MALCHIODI, E. L., CHO, S., SCARPELLINO, L., SCHNEIDER, P., KERZIC, M. C., MARIUZZA, R. A. & HELD, W. 2009. Distinct conformations of Ly49

natural killer cell receptors mediate MHC class I recognition in trans and cis. *Immunity,* 31**,** 598-608.
BALCH, S. G., MCKNIGHT, A. J., SELDIN, M. F. & GORDON, S. 1998. Cloning of a novel C-type lectin expressed by murine macrophages. *J Biol Chem,* 273**,** 18656-64.
BANCHEREAU, J. & STEINMAN, R. M. 1998. Dendritic cells and the control of immunity. *Nature,* 392**,** 245-52.
BARBER, G. N. 2011. Innate immune DNA sensing pathways: STING, AIMII and the regulation of interferon production and inflammatory responses. *Curr Opin Immunol,* 23**,** 10-20.
BARRANGOU, R. & MARRAFFINI, L. A. 2014. CRISPR-Cas systems: Prokaryotes upgrade to adaptive immunity. *Mol Cell,* 54**,** 234-44.
BATES, E. E., FOURNIER, N., GARCIA, E., VALLADEAU, J., DURAND, I., PIN, J. J., ZURAWSKI, S. M., PATEL, S., ABRAMS, J. S., LEBECQUE, S., GARRONE, P. & SAELAND, S. 1999. APCs express DCIR, a novel C-type lectin surface receptor containing an immunoreceptor tyrosine-based inhibitory motif. *J Immunol,* 163**,** 1973-83.
BAUSINGER, H., LIPSKER, D., ZIYLAN, U., MANIE, S., BRIAND, J. P., CAZENAVE, J. P., MULLER, S., HAEUW, J. F., RAVANAT, C., DE LA SALLE, H. & HANAU, D. 2002. Endotoxin-free heat-shock protein 70 fails to induce APC activation. *Eur J Immunol,* 32**,** 3708-13.
BENDELAC, A., BONNEVILLE, M. & KEARNEY, J. F. 2001. Autoreactivity by design: innate B and T lymphocytes. *Nat Rev Immunol,* 1**,** 177-86.
BILLADEAU, D. D. & LEIBSON, P. J. 2002. ITAMs versus ITIMs: striking a balance during cell regulation. *J Clin Invest,* 109**,** 161-8.
BILLINGHAM, R. E., BRENT, L. & MEDAWAR, P. B. 1953. Actively acquired tolerance of foreign cells. *Nature,* 172**,** 603-6.
BINSTADT, B. A., BRUMBAUGH, K. M., DICK, C. J., SCHARENBERG, A. M., WILLIAMS, B. L., COLONNA, M., LANIER, L. L., KINET, J. P., ABRAHAM, R. T. & LEIBSON, P. J. 1996. Sequential involvement of Lck and SHP-1 with MHC-recognizing receptors on NK cells inhibits FcR-initiated tyrosine kinase activation. *Immunity,* 5**,** 629-38.
BLEVINS, S. M. & BRONZE, M. S. 2010. Robert Koch and the 'golden age' of bacteriology. *Int J Infect Dis,* 14**,** e744-51.
BLUM, J. S., WEARSCH, P. A. & CRESSWELL, P. 2013. Pathways of antigen processing. *Annu Rev Immunol,* 31**,** 443-73.
BOEHM, T. 2011. Design principles of adaptive immune systems. *Nat Rev Immunol,* 11**,** 307-17.
BONILLA, W. V., FROHLICH, A., SENN, K., KALLERT, S., FERNANDEZ, M., JOHNSON, S., KREUTZFELDT, M., HEGAZY, A. N., SCHRICK, C., FALLON, P. G., KLEMENZ, R., NAKAE, S., ADLER, H., MERKLER, D., LOHNING, M. & PINSCHEWER, D. D. 2012. The alarmin interleukin-33 drives protective antiviral CD8(+) T cell responses. *Science,* 335**,** 984-9.
BORGHESI, L. & MILCAREK, C. 2007. Innate versus adaptive immunity: a paradigm past its prime? *Cancer Res,* 67**,** 3989-93.
BOULE, M. W., BROUGHTON, C., MACKAY, F., AKIRA, S., MARSHAK-ROTHSTEIN, A. & RIFKIN, I. R. 2004. Toll-like receptor 9-dependent and -independent dendritic cell activation by chromatin-immunoglobulin G complexes. *J Exp Med,* 199**,** 1631-40.
BROGDEN, K. A. 2005. Antimicrobial peptides: pore formers or metabolic inhibitors in bacteria? *Nat Rev Microbiol,* 3**,** 238-50.
BROWN, G. D. 2006. Dectin-1: a signalling non-TLR pattern-recognition receptor. *Nat Rev Immunol,* 6**,** 33-43.

BROWN, G. D. & GORDON, S. 2001. Immune recognition. A new receptor for beta-glucans. *Nature,* 413**,** 36-7.

BURNET, F. M. & FENNER, F. 1949. *The production of antibodies,* Melbourne,, Macmillan.

CAMINSCHI, I., PROIETTO, A. I., AHMET, F., KITSOULIS, S., SHIN TEH, J., LO, J. C., RIZZITELLI, A., WU, L., VREMEC, D., VAN DOMMELEN, S. L., CAMPBELL, I. K., MARASKOVSKY, E., BRALEY, H., DAVEY, G. M., MOTTRAM, P., VAN DE VELDE, N., JENSEN, K., LEW, A. M., WRIGHT, M. D., HEATH, W. R., SHORTMAN, K. & LAHOUD, M. H. 2008. The dendritic cell subtype-restricted C-type lectin Clec9A is a target for vaccine enhancement. *Blood,* 112**,** 3264-73.

CAMINSCHI, I. & SHORTMAN, K. 2012. Boosting antibody responses by targeting antigens to dendritic cells. *Trends Immunol,* 33**,** 71-7.

CAMINSCHI, I., VREMEC, D., AHMET, F., LAHOUD, M. H., VILLADANGOS, J. A., MURPHY, K. M., HEATH, W. R. & SHORTMAN, K. 2012. Antibody responses initiated by Clec9A-bearing dendritic cells in normal and Batf3(-/-) mice. *Mol Immunol,* 50**,** 9-17.

CAO, L., SHI, X., CHANG, H., ZHANG, Q. & HE, Y. 2015. pH-dependent recognition of apoptotic and necrotic cells by the human dendritic cell receptor DEC205. *Proc Natl Acad Sci U S A,* 112**,** 7237-42.

CARROLL, M. C. 2004. The complement system in regulation of adaptive immunity. *Nat Immunol,* 5**,** 981-6.

CHUA, B. T., VOLBRACHT, C., TAN, K. O., LI, R., YU, V. C. & LI, P. 2003. Mitochondrial translocation of cofilin is an early step in apoptosis induction. *Nat Cell Biol,* 5**,** 1083-9.

CHUNG, E. Y., LIU, J., HOMMA, Y., ZHANG, Y., BRENDOLAN, A., SAGGESE, M., HAN, J., SILVERSTEIN, R., SELLERI, L. & MA, X. 2007. Interleukin-10 expression in macrophages during phagocytosis of apoptotic cells is mediated by homeodomain proteins Pbx1 and Prep-1. *Immunity,* 27**,** 952-64.

CLAESSENS, M. M., BATHE, M., FREY, E. & BAUSCH, A. R. 2006. Actin-binding proteins sensitively mediate F-actin bundle stiffness. *Nat Mater,* 5**,** 748-53.

COLONNA, M., SAMARIDIS, J. & ANGMAN, L. 2000. Molecular characterization of two novel C-type lectin-like receptors, one of which is selectively expressed in human dendritic cells. *Eur J Immunol,* 30**,** 697-704.

COOPER, E. L. 1968. Transplantation immunity in annelids. I. Rejection of xenografts exchanged between Lumbricus terrestris and Eisenia foetida. *Transplantation,* 6**,** 322-7.

CROTZER, V. L. & BLUM, J. S. 2009. Autophagy and its role in MHC-mediated antigen presentation. *J Immunol,* 182**,** 3335-41.

DAI, Z., KIM, J. H., TONELLI, M., ALI, I. K. & MARKLEY, J. L. 2014. pH-induced conformational change of IscU at low pH correlates with protonation/deprotonation of two conserved histidine residues. *Biochemistry,* 53**,** 5290-7.

DAVIS, B. K., WEN, H. & TING, J. P. 2011. The inflammasome NLRs in immunity, inflammation, and associated diseases. *Annu Rev Immunol,* 29**,** 707-35.

DAVIS, M. M. & BJORKMAN, P. J. 1988. T-cell antigen receptor genes and T-cell recognition. *Nature,* 334**,** 395-402.

DEN HAAN, J. M., LEHAR, S. M. & BEVAN, M. J. 2000. CD8(+) but not CD8(-) dendritic cells cross-prime cytotoxic T cells in vivo. *J Exp Med,* 192**,** 1685-96.

DESOUZA, M., GUNNING, P. W. & STEHN, J. R. 2012. The actin cytoskeleton as a sensor and mediator of apoptosis. *Bioarchitecture,* 2**,** 75-87.

DRAKE, M. T., VIOLIN, J. D., WHALEN, E. J., WISLER, J. W., SHENOY, S. K. & LEFKOWITZ, R. J. 2008. beta-arrestin-biased agonism at the beta2-adrenergic receptor. *J Biol Chem,* 283**,** 5669-76.

DRICKAMER, K. 1988. Two distinct classes of carbohydrate-recognition domains in animal lectins. *J Biol Chem,* 263**,** 9557-60.
DRICKAMER, K. 1989. Demonstration of carbohydrate-recognition activity in diverse proteins which share a common primary structure motif. *Biochem Soc Trans,* 17**,** 13-5.
DRICKAMER, K. 1992. Engineering galactose-binding activity into a C-type mannose-binding protein. *Nature,* 360**,** 183-6.
DRICKAMER, K. 1999. C-type lectin-like domains. *Curr Opin Struct Biol,* 9**,** 585-90.
DRICKAMER, K. & DODD, R. B. 1999. C-Type lectin-like domains in Caenorhabditis elegans: predictions from the complete genome sequence. *Glycobiology,* 9**,** 1357-69.
DUDZIAK, D., KAMPHORST, A. O., HEIDKAMP, G. F., BUCHHOLZ, V. R., TRUMPFHELLER, C., YAMAZAKI, S., CHEONG, C., LIU, K., LEE, H. W., PARK, C. G., STEINMAN, R. M. & NUSSENZWEIG, M. C. 2007. Differential antigen processing by dendritic cell subsets in vivo. *Science,* 315**,** 107-11.
EAST, L. & ISACKE, C. M. 2002. The mannose receptor family. *Biochim Biophys Acta,* 1572**,** 364-86.
EGELMAN, E. H. 2000. A robust algorithm for the reconstruction of helical filaments using single-particle methods. *Ultramicroscopy,* 85**,** 225-34.
EIGENBROD, T., PARK, J. H., HARDER, J., IWAKURA, Y. & NUNEZ, G. 2008. Cutting edge: critical role for mesothelial cells in necrosis-induced inflammation through the recognition of IL-1 alpha released from dying cells. *J Immunol,* 181**,** 8194-8.
ELMORE, S. 2007. Apoptosis: a review of programmed cell death. *Toxicol Pathol,* 35**,** 495-516.
FADOK, V. A., BRATTON, D. L., KONOWAL, A., FREED, P. W., WESTCOTT, J. Y. & HENSON, P. M. 1998. Macrophages that have ingested apoptotic cells in vitro inhibit proinflammatory cytokine production through autocrine/paracrine mechanisms involving TGF-beta, PGE2, and PAF. *J Clin Invest,* 101**,** 890-8.
FANG, H., WU, Y., HUANG, X., WANG, W., ANG, B., CAO, X. & WAN, T. 2011. Toll-like receptor 4 (TLR4) is essential for Hsp70-like protein 1 (HSP70L1) to activate dendritic cells and induce Th1 response. *J Biol Chem,* 286**,** 30393-400.
FENG, J., GARRITY, D., CALL, M. E., MOFFETT, H. & WUCHERPFENNIG, K. W. 2005. Convergence on a distinctive assembly mechanism by unrelated families of activating immune receptors. *Immunity,* 22**,** 427-38.
FIALKOW, L., WANG, Y. & DOWNEY, G. P. 2007. Reactive oxygen and nitrogen species as signaling molecules regulating neutrophil function. *Free Radic Biol Med,* 42**,** 153-64.
FOGG, D. K., SIBON, C., MILED, C., JUNG, S., AUCOUTURIER, P., LITTMAN, D. R., CUMANO, A. & GEISSMANN, F. 2006. A clonogenic bone marrow progenitor specific for macrophages and dendritic cells. *Science,* 311**,** 83-7.
FRANCHI, L., MCDONALD, C., KANNEGANTI, T. D., AMER, A. & NUNEZ, G. 2006. Nucleotide-binding oligomerization domain-like receptors: intracellular pattern recognition molecules for pathogen detection and host defense. *J Immunol,* 177**,** 3507-13.
FUERTES MARRACO, S. A., GROSJEAN, F., DUVAL, A., ROSA, M., LAVANCHY, C., ASHOK, D., HALLER, S., OTTEN, L. A., STEINER, Q. G., DESCOMBES, P., LUBER, C. A., MEISSNER, F., MANN, M., SZELES, L., REITH, W. & ACHA-ORBEA, H. 2012. Novel murine dendritic cell lines: a powerful auxiliary tool for dendritic cell research. *Front Immunol,* 3**,** 331.
FUGMANN, S. D., LEE, A. I., SHOCKETT, P. E., VILLEY, I. J. & SCHATZ, D. G. 2000. The RAG proteins and V(D)J recombination: complexes, ends, and transposition. *Annu Rev Immunol,* 18**,** 495-527.

FUJII, T., IWANE, A. H., YANAGIDA, T. & NAMBA, K. 2010. Direct visualization of secondary structures of F-actin by electron cryomicroscopy. *Nature,* 467**,** 724-8.

FULLER, G. L., WILLIAMS, J. A., TOMLINSON, M. G., EBLE, J. A., HANNA, S. L., POHLMANN, S., SUZUKI-INOUE, K., OZAKI, Y., WATSON, S. P. & PEARCE, A. C. 2007. The C-type lectin receptors CLEC-2 and Dectin-1, but not DC-SIGN, signal via a novel YXXL-dependent signaling cascade. *J Biol Chem,* 282**,** 12397-409.

FURUKAWA, R. & FECHHEIMER, M. 1997. The structure, function, and assembly of actin filament bundles. *Int Rev Cytol,* 175**,** 29-90.

GALKIN, V. E., ORLOVA, A., BRIEHER, W., KUEH, H. Y., MITCHISON, T. J. & EGELMAN, E. H. 2008. Coronin-1A stabilizes F-actin by bridging adjacent actin protomers and stapling opposite strands of the actin filament. *J Mol Biol,* 376**,** 607-13.

GAVEL, Y. & VON HEIJNE, G. 1990. Sequence differences between glycosylated and non-glycosylated Asn-X-Thr/Ser acceptor sites: implications for protein engineering. *Protein Eng,* 3**,** 433-42.

GE, P., DURER, Z. A., KUDRYASHOV, D., ZHOU, Z. H. & REISLER, E. 2014. Cryo-EM reveals different coronin binding modes for ADP- and ADP-BeFx actin filaments. *Nat Struct Mol Biol,* 21**,** 1075-81.

GEIDER, S., BARONNET, A., CERINI, C., NITSCHE, S., ASTIER, J. P., MICHEL, R., BOISTELLE, R., BERLAND, Y., DAGORN, J. C. & VERDIER, J. M. 1996. Pancreatic lithostathine as a calcite habit modifier. *J Biol Chem,* 271**,** 26302-6.

GOODRIDGE, H. S., SIMMONS, R. M. & UNDERHILL, D. M. 2007. Dectin-1 stimulation by Candida albicans yeast or zymosan triggers NFAT activation in macrophages and dendritic cells. *J Immunol,* 178**,** 3107-15.

GORDON, S. 2008. Elie Metchnikoff: father of natural immunity. *Eur J Immunol,* 38**,** 3257-64.

GOUBAU, D., DEDDOUCHE, S. & REIS E SOUSA, C. 2013. Cytosolic sensing of viruses. *Immunity,* 38**,** 855-69.

GOURLAY, C. W., CARPP, L. N., TIMPSON, P., WINDER, S. J. & AYSCOUGH, K. R. 2004. A role for the actin cytoskeleton in cell death and aging in yeast. *J Cell Biol,* 164**,** 803-9.

GUERMONPREZ, P., VALLADEAU, J., ZITVOGEL, L., THERY, C. & AMIGORENA, S. 2002. Antigen presentation and T cell stimulation by dendritic cells. *Annu Rev Immunol,* 20**,** 621-67.

GUICCIARDI, M. E. & GORES, G. J. 2009. Life and death by death receptors. *FASEB J,* 23**,** 1625-37.

GUILLIAMS, M., GINHOUX, F., JAKUBZICK, C., NAIK, S. H., ONAI, N., SCHRAML, B. U., SEGURA, E., TUSSIWAND, R. & YONA, S. 2014. Dendritic cells, monocytes and macrophages: a unified nomenclature based on ontogeny. *Nat Rev Immunol,* 14**,** 571-8.

GULYAEVA, N., ZASLAVSKY, A., LECHNER, P., CHAIT, A. & ZASLAVSKY, B. 2003. pH dependence of the relative hydrophobicity and lipophilicity of amino acids and peptides measured by aqueous two-phase and octanol-buffer partitioning. *J Pept Res,* 61**,** 71-9.

GUNTURI, A., BERG, R. E. & FORMAN, J. 2004. The role of CD94/NKG2 in innate and adaptive immunity. *Immunol Res,* 30**,** 29-34.

HALLE, A., HORNUNG, V., PETZOLD, G. C., STEWART, C. R., MONKS, B. G., REINHECKEL, T., FITZGERALD, K. A., LATZ, E., MOORE, K. J. & GOLENBOCK, D. T. 2008. The NALP3 inflammasome is involved in the innate immune response to amyloid-beta. *Nat Immunol,* 9**,** 857-65.

HAN, J., ZHONG, C. Q. & ZHANG, D. W. 2011. Programmed necrosis: backup to and competitor with apoptosis in the immune system. *Nat Immunol,* 12**,** 1143-9.

HARRISON, J. S., HIGGINS, C. D., O'MEARA, M. J., KOELLHOFFER, J. F., KUHLMAN, B. A. & LAI, J. R. 2013. Role of electrostatic repulsion in controlling pH-dependent conformational changes of viral fusion proteins. *Structure,* 21**,** 1085-96.

HEATH, W. R. & CARBONE, F. R. 2009. Dendritic cell subsets in primary and secondary T cell responses at body surfaces. *Nat Immunol,* 10**,** 1237-44.

HENDSCH, Z. S. & TIDOR, B. 1994. Do salt bridges stabilize proteins? A continuum electrostatic analysis. *Protein Sci,* 3**,** 211-26.

HERNANZ-FALCON, P., JOFFRE, O., WILLIAMS, D. L. & REIS E SOUSA, C. 2009. Internalization of Dectin-1 terminates induction of inflammatory responses. *Eur J Immunol,* 39**,** 507-13.

HOCHREIN, H., SHORTMAN, K., VREMEC, D., SCOTT, B., HERTZOG, P. & O'KEEFFE, M. 2001. Differential production of IL-12, IFN-alpha, and IFN-gamma by mouse dendritic cell subsets. *J Immunol,* 166**,** 5448-55.

HOCHREITER-HUFFORD, A. & RAVICHANDRAN, K. S. 2013. Clearing the dead: apoptotic cell sensing, recognition, engulfment, and digestion. *Cold Spring Harb Perspect Biol,* 5**,** a008748.

HOFFMANN, J. A., KAFATOS, F. C., JANEWAY, C. A. & EZEKOWITZ, R. A. 1999. Phylogenetic perspectives in innate immunity. *Science,* 284**,** 1313-8.

HOFMANN, M. A., DRURY, S., FU, C., QU, W., TAGUCHI, A., LU, Y., AVILA, C., KAMBHAM, N., BIERHAUS, A., NAWROTH, P., NEURATH, M. F., SLATTERY, T., BEACH, D., MCCLARY, J., NAGASHIMA, M., MORSER, J., STERN, D. & SCHMIDT, A. M. 1999. RAGE mediates a novel proinflammatory axis: a central cell surface receptor for S100/calgranulin polypeptides. *Cell,* 97**,** 889-901.

HORNUNG, V., ABLASSER, A., CHARREL-DENNIS, M., BAUERNFEIND, F., HORVATH, G., CAFFREY, D. R., LATZ, E. & FITZGERALD, K. A. 2009. AIM2 recognizes cytosolic dsDNA and forms a caspase-1-activating inflammasome with ASC. *Nature,* 458**,** 514-8.

HORNUNG, V. & LATZ, E. 2010. Intracellular DNA recognition. *Nat Rev Immunol,* 10**,** 123-30.

HUBO, M., TRINSCHEK, B., KRYCZANOWSKY, F., TUETTENBERG, A., STEINBRINK, K. & JONULEIT, H. 2013. Costimulatory molecules on immunogenic versus tolerogenic human dendritic cells. *Front Immunol,* 4**,** 82.

HUGHES, C. E., POLLITT, A. Y., MORI, J., EBLE, J. A., TOMLINSON, M. G., HARTWIG, J. H., O'CALLAGHAN, C. A., FUTTERER, K. & WATSON, S. P. 2010. CLEC-2 activates Syk through dimerization. *Blood,* 115**,** 2947-55.

HUME, D. A. 2008. Macrophages as APC and the dendritic cell myth. *J Immunol,* 181**,** 5829-35.

HUYSAMEN, C., WILLMENT, J. A., DENNEHY, K. M. & BROWN, G. D. 2008. CLEC9A is a novel activation C-type lectin-like receptor expressed on BDCA3+ dendritic cells and a subset of monocytes. *J Biol Chem,* 283**,** 16693-701.

IBORRA, S., IZQUIERDO, H. M., MARTINEZ-LOPEZ, M., BLANCO-MENENDEZ, N., REIS E SOUSA, C. & SANCHO, D. 2012. The DC receptor DNGR-1 mediates cross-priming of CTLs during vaccinia virus infection in mice. *J Clin Invest,* 122**,** 1628-43.

IWASAKI, A. & MEDZHITOV, R. 2015. Control of adaptive immunity by the innate immune system. *Nat Immunol,* 16**,** 343-53.

JANEWAY, C. A., JR. 1989. Approaching the asymptote? Evolution and revolution in immunology. *Cold Spring Harb Symp Quant Biol,* 54 Pt 1**,** 1-13.

JANEWAY, C. A., JR. & MEDZHITOV, R. 2002. Innate immune recognition. *Annu Rev Immunol,* 20**,** 197-216.

JARVIS, M. F. & KHAKH, B. S. 2009. ATP-gated P2X cation-channels. *Neuropharmacology,* 56**,** 208-15.

JEGOU, A., NIEDERMAYER, T., ORBAN, J., DIDRY, D., LIPOWSKY, R., CARLIER, M. F. & ROMET-LEMONNE, G. 2011. Individual actin filaments in a microfluidic flow reveal the mechanism of ATP hydrolysis and give insight into the properties of profilin. *PLoS Biol,* 9**,** e1001161.

JIANG, D., LIANG, J., FAN, J., YU, S., CHEN, S., LUO, Y., PRESTWICH, G. D., MASCARENHAS, M. M., GARG, H. G., QUINN, D. A., HOMER, R. J., GOLDSTEIN, D. R., BUCALA, R., LEE, P. J., MEDZHITOV, R. & NOBLE, P. W. 2005. Regulation of lung injury and repair by Toll-like receptors and hyaluronan. *Nat Med,* 11**,** 1173-9.

JOFFRE, O. P., SANCHO, D., ZELENAY, S., KELLER, A. M. & REIS E SOUSA, C. 2010. Efficient and versatile manipulation of the peripheral CD4+ T-cell compartment by antigen targeting to DNGR-1/CLEC9A. *Eur J Immunol,* 40**,** 1255-65.

JOFFRE, O. P., SEGURA, E., SAVINA, A. & AMIGORENA, S. 2012. Cross-presentation by dendritic cells. *Nat Rev Immunol,* 12**,** 557-69.

JOHNSON, G. B., BRUNN, G. J., KODAIRA, Y. & PLATT, J. L. 2002. Receptor-mediated monitoring of tissue well-being via detection of soluble heparan sulfate by Toll-like receptor 4. *J Immunol,* 168**,** 5233-9.

KACZMAREK, A., VANDENABEELE, P. & KRYSKO, D. V. 2013. Necroptosis: the release of damage-associated molecular patterns and its physiological relevance. *Immunity,* 38**,** 209-23.

KALANI, M. R., MORADI, A., MORADI, M. & TAJKHORSHID, E. 2013. Characterizing a histidine switch controlling pH-dependent conformational changes of the influenza virus hemagglutinin. *Biophys J,* 105**,** 993-1003.

KARCH, J., KANISICAK, O., BRODY, M. J., SARGENT, M. A., MICHAEL, D. M. & MOLKENTIN, J. D. 2015. Necroptosis Interfaces with MOMP and the MPTP in Mediating Cell Death. *PLoS One,* 10**,** e0130520.

KERRIGAN, A. M. & BROWN, G. D. 2010. Syk-coupled C-type lectin receptors that mediate cellular activation via single tyrosine based activation motifs. *Immunol Rev,* 234**,** 335-52.

KILPATRICK, D. C. 2002. Animal lectins: a historical introduction and overview. *Biochim Biophys Acta,* 1572**,** 187-97.

KOFOED, E. M. & VANCE, R. E. 2011. Innate immune recognition of bacterial ligands by NAIPs determines inflammasome specificity. *Nature,* 477**,** 592-5.

KOL, A., LICHTMAN, A. H., FINBERG, R. W., LIBBY, P. & KURT-JONES, E. A. 2000. Cutting edge: heat shock protein (HSP) 60 activates the innate immune response: CD14 is an essential receptor for HSP60 activation of mononuclear cells. *J Immunol,* 164**,** 13-7.

KRUKENBERG, K. A., SOUTHWORTH, D. R., STREET, T. O. & AGARD, D. A. 2009. pH-dependent conformational changes in bacterial Hsp90 reveal a Grp94-like conformation at pH 6 that is highly active in suppression of citrate synthase aggregation. *J Mol Biol,* 390**,** 278-91.

KRYSKO, D. V., VANDEN BERGHE, T., PARTHOENS, E., D'HERDE, K. & VANDENABEELE, P. 2008. Methods for distinguishing apoptotic from necrotic cells and measuring their clearance. *Methods Enzymol,* 442**,** 307-41.

KUMARAN, S., GRUCZA, R. A. & WAKSMAN, G. 2003. The tandem Src homology 2 domain of the Syk kinase: a molecular device that adapts to interphosphotyrosine distances. *Proc Natl Acad Sci U S A,* 100**,** 14828-33.

LAFFERTY, K. J. & CUNNINGHAM, A. J. 1975. A new analysis of allogeneic interactions. *Aust J Exp Biol Med Sci,* 53**,** 27-42.

LATZ, E. 2010. The inflammasomes: mechanisms of activation and function. *Curr Opin Immunol,* 22**,** 28-33.

LEIBUNDGUT-LANDMANN, S., GROSS, O., ROBINSON, M. J., OSORIO, F., SLACK, E. C., TSONI, S. V., SCHWEIGHOFFER, E., TYBULEWICZ, V., BROWN, G. D., RULAND, J. & REIS E SOUSA, C. 2007. Syk- and CARD9-dependent coupling of innate immunity to the induction of T helper cells that produce interleukin 17. *Nat Immunol,* 8**,** 630-8.

LEIBUNDGUT-LANDMANN, S., OSORIO, F., BROWN, G. D. & REIS E SOUSA, C. 2008. Stimulation of dendritic cells via the dectin-1/Syk pathway allows priming of cytotoxic T-cell responses. *Blood,* 112**,** 4971-80.

LEMAITRE, B., NICOLAS, E., MICHAUT, L., REICHHART, J. M. & HOFFMANN, J. A. 1996. The dorsoventral regulatory gene cassette spatzle/Toll/cactus controls the potent antifungal response in Drosophila adults. *Cell,* 86**,** 973-83.

LI, J., AHMET, F., SULLIVAN, L. C., BROOKS, A. G., KENT, S. J., DE ROSE, R., SALAZAR, A. M., REIS, E. S. C., SHORTMAN, K., LAHOUD, M. H., HEATH, W. R. & CAMINSCHI, I. 2015. Antibodies targeting Clec9A promote strong humoral immunity without adjuvant in mice and non-human primates. *Eur J Immunol,* 45**,** 854-64.

LILIC, M., GALKIN, V. E., ORLOVA, A., VANLOOCK, M. S., EGELMAN, E. H. & STEBBINS, C. E. 2003. Salmonella SipA polymerizes actin by stapling filaments with nonglobular protein arms. *Science,* 301**,** 1918-21.

LIU, Y., CHEN, G. Y. & ZHENG, P. 2009. CD24-Siglec G/10 discriminates danger- from pathogen-associated molecular patterns. *Trends Immunol,* 30**,** 557-61.

MANNE, B. K., BADOLIA, R., DANGELMAIER, C., EBLE, J. A., ELLMEIER, W., KAHN, M. & KUNAPULI, S. P. 2015. Distinct Pathways Regulate Syk Protein Activation Downstream of Immune Tyrosine Activation Motif (ITAM) and hemITAM Receptors in Platelets. *J Biol Chem,* 290**,** 11557-68.

MARSHALL, A. S., WILLMENT, J. A., LIN, H. H., WILLIAMS, D. L., GORDON, S. & BROWN, G. D. 2004. Identification and characterization of a novel human myeloid inhibitory C-type lectin-like receptor (MICL) that is predominantly expressed on granulocytes and monocytes. *J Biol Chem,* 279**,** 14792-802.

MARTIN, S. R. & SCHILSTRA, M. J. 2008. Circular dichroism and its application to the study of biomolecules. *Methods Cell Biol,* 84**,** 263-93.

MARTINON, F., BURNS, K. & TSCHOPP, J. 2002. The inflammasome: a molecular platform triggering activation of inflammatory caspases and processing of proIL-beta. *Mol Cell,* 10**,** 417-26.

MARTINON, F., PETRILLI, V., MAYOR, A., TARDIVEL, A. & TSCHOPP, J. 2006. Gout-associated uric acid crystals activate the NALP3 inflammasome. *Nature,* 440**,** 237-41.

MASOPUST, D. & SCHENKEL, J. M. 2013. The integration of T cell migration, differentiation and function. *Nat Rev Immunol,* 13**,** 309-20.

MATSUMOTO, M., TANAKA, T., KAISHO, T., SANJO, H., COPELAND, N. G., GILBERT, D. J., JENKINS, N. A. & AKIRA, S. 1999. A novel LPS-inducible C-type lectin is a transcriptional target of NF-IL6 in macrophages. *J Immunol,* 163**,** 5039-48.

MATTEI, F., SCHIAVONI, G., BELARDELLI, F. & TOUGH, D. F. 2001. IL-15 is expressed by dendritic cells in response to type I IFN, double-stranded RNA, or lipopolysaccharide and promotes dendritic cell activation. *J Immunol,* 167**,** 1179-87.

MATZINGER, P. 1994. Tolerance, danger, and the extended family. *Annu Rev Immunol,* 12**,** 991-1045.

MCGOUGH, A., POPE, B., CHIU, W. & WEEDS, A. 1997. Cofilin changes the twist of F-actin: implications for actin filament dynamics and cellular function. *J Cell Biol,* 138**,** 771-81.

MEDZHITOV, R., PRESTON-HURLBURT, P. & JANEWAY, C. A., JR. 1997. A human homologue of the Drosophila Toll protein signals activation of adaptive immunity. *Nature,* 388**,** 394-7.

MERAD, M., SATHE, P., HELFT, J., MILLER, J. & MORTHA, A. 2013. The dendritic cell lineage: ontogeny and function of dendritic cells and their subsets in the steady state and the inflamed setting. *Annu Rev Immunol,* 31**,** 563-604.

METLAY, J. P., WITMER-PACK, M. D., AGGER, R., CROWLEY, M. T., LAWLESS, D. & STEINMAN, R. M. 1990. The distinct leukocyte integrins of mouse spleen dendritic cells as identified with new hamster monoclonal antibodies. *J Exp Med,* 171**,** 1753-71.

MILLER, J. C., BROWN, B. D., SHAY, T., GAUTIER, E. L., JOJIC, V., COHAIN, A., PANDEY, G., LEBOEUF, M., ELPEK, K. G., HELFT, J., HASHIMOTO, D., CHOW, A., PRICE, J., GRETER, M., BOGUNOVIC, M., BELLEMARE-PELLETIER, A., FRENETTE, P. S., RANDOLPH, G. J., TURLEY, S. J., MERAD, M. & IMMUNOLOGICAL GENOME, C. 2012. Deciphering the transcriptional network of the dendritic cell lineage. *Nat Immunol,* 13**,** 888-99.

MILNER, J. D. & HOLLAND, S. M. 2013. The cup runneth over: lessons from the ever-expanding pool of primary immunodeficiency diseases. *Nat Rev Immunol,* 13**,** 635-48.

MOCSAI, A., RULAND, J. & TYBULEWICZ, V. L. 2010. The SYK tyrosine kinase: a crucial player in diverse biological functions. *Nat Rev Immunol,* 10**,** 387-402.

MORAGA, I., WERNIG, G., WILMES, S., GRYSHKOVA, V., RICHTER, C. P., HONG, W. J., SINHA, R., GUO, F., FABIONAR, H., WEHRMAN, T. S., KRUTZIK, P., DEMHARTER, S., PLO, I., WEISSMAN, I. L., MINARY, P., MAJETI, R., CONSTANTINESCU, S. N., PIEHLER, J. & GARCIA, K. C. 2015. Tuning cytokine receptor signaling by re-orienting dimer geometry with surrogate ligands. *Cell,* 160**,** 1196-208.

MORIWAKI, K. & CHAN, F. K. 2013. RIP3: a molecular switch for necrosis and inflammation. *Genes Dev,* 27**,** 1640-9.

MOURAO-SA, D., ROBINSON, M. J., ZELENAY, S., SANCHO, D., CHAKRAVARTY, P., LARSEN, R., PLANTINGA, M., VAN ROOIJEN, N., SOARES, M. P., LAMBRECHT, B. & REIS E SOUSA, C. 2011. CLEC-2 signaling via Syk in myeloid cells can regulate inflammatory responses. *Eur J Immunol,* 41**,** 3040-53.

NAKANO, S., SUGIHARA, M., YAMADA, R., KATAYANAGI, K. & TATE, S. 2012. Structural implication for the impaired binding of W150A mutant LOX-1 to oxidized low density lipoprotein, OxLDL. *Biochim Biophys Acta,* 1824**,** 739-49.

NATARAJAN, K., DIMASI, N., WANG, J., MARIUZZA, R. A. & MARGULIES, D. H. 2002. Structure and function of natural killer cell receptors: multiple molecular solutions to self, nonself discrimination. *Annu Rev Immunol,* 20**,** 853-85.

NEMAZEE, D., KOUSKOFF, V., HERTZ, M., LANG, J., MELAMED, D., PAPE, K. & RETTER, M. 2000. B-cell-receptor-dependent positive and negative selection in immature B cells. *Curr Top Microbiol Immunol,* 245**,** 57-71.

NEUMANN, K., CASTINEIRAS-VILARINO, M., HOCKENDORF, U., HANNESSCHLAGER, N., LEMEER, S., KUPKA, D., MEYERMANN, S., LECH, M., ANDERS, H. J., KUSTER, B., BUSCH, D. H., GEWIES, A., NAUMANN, R., GROSS, O. & RULAND, J. 2014. Clec12a is an inhibitory receptor for uric acid crystals that regulates inflammation in response to cell death. *Immunity,* 40**,** 389-99.

NG, K. K., KOLATKAR, A. R., PARK-SNYDER, S., FEINBERG, H., CLARK, D. A., DRICKAMER, K. & WEIS, W. I. 2002. Orientation of bound ligands in mannose-binding proteins. Implications for multivalent ligand recognition. *J Biol Chem,* 277**,** 16088-95.

NIKOLICH-ZUGICH, J., SLIFKA, M. K. & MESSAOUDI, I. 2004. The many important facets of T-cell repertoire diversity. *Nat Rev Immunol,* 4**,** 123-32.

NUSSENZWEIG, M. C., STEINMAN, R. M., UNKELESS, J. C., WITMER, M. D., GUTCHINOV, B. & COHN, Z. A. 1981. Studies of the cell surface of mouse dendritic cells and other leukocytes. *J Exp Med,* 154**,** 168-87.

O'LEARY, J. G., GOODARZI, M., DRAYTON, D. L. & VON ANDRIAN, U. H. 2006. T cell- and B cell-independent adaptive immunity mediated by natural killer cells. *Nat Immunol,* 7**,** 507-16.

O'NEILL, L. A., GOLENBOCK, D. & BOWIE, A. G. 2013. The history of Toll-like receptors - redefining innate immunity. *Nat Rev Immunol,* 13**,** 453-60.

OBEID, M., TESNIERE, A., GHIRINGHELLI, F., FIMIA, G. M., APETOH, L., PERFETTINI, J. L., CASTEDO, M., MIGNOT, G., PANARETAKIS, T., CASARES, N., METIVIER, D., LAROCHETTE, N., VAN ENDERT, P., CICCOSANTI, F., PIACENTINI, M., ZITVOGEL, L. & KROEMER, G. 2007. Calreticulin exposure dictates the immunogenicity of cancer cell death. *Nat Med,* 13**,** 54-61.

ONAI, N., OBATA-ONAI, A., SCHMID, M. A., OHTEKI, T., JARROSSAY, D. & MANZ, M. G. 2007. Identification of clonogenic common Flt3+M-CSFR+ plasmacytoid and conventional dendritic cell progenitors in mouse bone marrow. *Nat Immunol,* 8**,** 1207-16.

PALMA, A. S., FEIZI, T., ZHANG, Y., STOLL, M. S., LAWSON, A. M., DIAZ-RODRIGUEZ, E., CAMPANERO-RHODES, M. A., COSTA, J., GORDON, S., BROWN, G. D. & CHAI, W. 2006. Ligands for the beta-glucan receptor, Dectin-1, assigned using "designer" microarrays of oligosaccharide probes (neoglycolipids) generated from glucan polysaccharides. *J Biol Chem,* 281**,** 5771-9.

PARK, C. G., TAKAHARA, K., UMEMOTO, E., YASHIMA, Y., MATSUBARA, K., MATSUDA, Y., CLAUSEN, B. E., INABA, K. & STEINMAN, R. M. 2001. Five mouse homologues of the human dendritic cell C-type lectin, DC-SIGN. *Int Immunol,* 13**,** 1283-90.

PARK, H., ADSIT, F. G. & BOYINGTON, J. C. 2005. The 1.4 angstrom crystal structure of the human oxidized low density lipoprotein receptor lox-1. *J Biol Chem,* 280**,** 13593-9.

PICCIRILLO, C. A. & SHEVACH, E. M. 2004. Naturally-occurring CD4+CD25+ immunoregulatory T cells: central players in the arena of peripheral tolerance. *Semin Immunol,* 16**,** 81-8.

PLOUGASTEL, B. F. & YOKOYAMA, W. M. 2006. Extending missing-self? Functional interactions between lectin-like NKrp1 receptors on NK cells with lectin-like ligands. *Curr Top Microbiol Immunol,* 298**,** 77-89.

POLLARD, T. D. 1986. Rate constants for the reactions of ATP- and ADP-actin with the ends of actin filaments. *J Cell Biol,* 103**,** 2747-54.

POLTORAK, A., HE, X., SMIRNOVA, I., LIU, M. Y., VAN HUFFEL, C., DU, X., BIRDWELL, D., ALEJOS, E., SILVA, M., GALANOS, C., FREUDENBERG, M., RICCIARDI-CASTAGNOLI, P., LAYTON, B. & BEUTLER, B. 1998. Defective LPS signaling in C3H/HeJ and C57BL/10ScCr mice: mutations in Tlr4 gene. *Science,* 282**,** 2085-8.

POPP, M. W., ANTOS, J. M. & PLOEGH, H. L. 2009. Site-specific protein labeling via sortase-mediated transpeptidation. *Curr Protoc Protein Sci,* Chapter 15**,** Unit 15 3.

POULIN, L. F., REYAL, Y., URONEN-HANSSON, H., SCHRAML, B. U., SANCHO, D., MURPHY, K. M., HAKANSSON, U. K., MOITA, L. F., AGACE, W. W., BONNET, D. & REIS E SOUSA, C. 2012. DNGR-1 is a specific and universal marker of

mouse and human Batf3-dependent dendritic cells in lymphoid and nonlymphoid tissues. *Blood,* 119**,** 6052-62.

POULIN, L. F., SALIO, M., GRIESSINGER, E., ANJOS-AFONSO, F., CRACIUN, L., CHEN, J. L., KELLER, A. M., JOFFRE, O., ZELENAY, S., NYE, E., LE MOINE, A., FAURE, F., DONCKIER, V., SANCHO, D., CERUNDOLO, V., BONNET, D. & REIS E SOUSA, C. 2010. Characterization of human DNGR-1+ BDCA3+ leukocytes as putative equivalents of mouse CD8alpha+ dendritic cells. *J Exp Med,* 207**,** 1261-71.

PULENDRAN, B. & AHMED, R. 2006. Translating innate immunity into immunological memory: implications for vaccine development. *Cell,* 124**,** 849-63.

QUINTANA, F. J. & COHEN, I. R. 2005. Heat shock proteins as endogenous adjuvants in sterile and septic inflammation. *J Immunol,* 175**,** 2777-82.

RADBRUCH, A., MUEHLINGHAUS, G., LUGER, E. O., INAMINE, A., SMITH, K. G., DORNER, T. & HIEPE, F. 2006. Competence and competition: the challenge of becoming a long-lived plasma cell. *Nat Rev Immunol,* 6**,** 741-50.

RAST, J. P., SMITH, L. C., LOZA-COLL, M., HIBINO, T. & LITMAN, G. W. 2006. Genomic insights into the immune system of the sea urchin. *Science,* 314**,** 952-6.

RATHINAM, V. A., VANAJA, S. K. & FITZGERALD, K. A. 2012. Regulation of inflammasome signaling. *Nat Immunol,* 13**,** 333-42.

RAVETCH, J. V. & LANIER, L. L. 2000. Immune inhibitory receptors. *Science,* 290**,** 84-9.

REID, D. M., GOW, N. A. & BROWN, G. D. 2009. Pattern recognition: recent insights from Dectin-1. *Curr Opin Immunol,* 21**,** 30-7.

REIZIS, B., BUNIN, A., GHOSH, H. S., LEWIS, K. L. & SISIRAK, V. 2011. Plasmacytoid dendritic cells: recent progress and open questions. *Annu Rev Immunol,* 29**,** 163-83.

RIEDEL, S. 2005. Edward Jenner and the history of smallpox and vaccination. *Proc (Bayl Univ Med Cent),* 18**,** 21-5.

ROCK, K. L. & SHEN, L. 2005. Cross-presentation: underlying mechanisms and role in immune surveillance. *Immunol Rev,* 207**,** 166-83.

ROGERS, N. C., SLACK, E. C., EDWARDS, A. D., NOLTE, M. A., SCHULZ, O., SCHWEIGHOFFER, E., WILLIAMS, D. L., GORDON, S., TYBULEWICZ, V. L., BROWN, G. D. & REIS E SOUSA, C. 2005. Syk-dependent cytokine induction by Dectin-1 reveals a novel pattern recognition pathway for C type lectins. *Immunity,* 22**,** 507-17.

ROUILLER, I., XU, X. P., AMANN, K. J., EGILE, C., NICKELL, S., NICASTRO, D., LI, R., POLLARD, T. D., VOLKMANN, N. & HANEIN, D. 2008. The structural basis of actin filament branching by the Arp2/3 complex. *J Cell Biol,* 180**,** 887-95.

ROWLINSON, S. W., YOSHIZATO, H., BARCLAY, J. L., BROOKS, A. J., BEHNCKEN, S. N., KERR, L. M., MILLARD, K., PALETHORPE, K., NIELSEN, K., CLYDE-SMITH, J., HANCOCK, J. F. & WATERS, M. J. 2008. An agonist-induced conformational change in the growth hormone receptor determines the choice of signalling pathway. *Nat Cell Biol,* 10**,** 740-7.

SAIJO, S., FUJIKADO, N., FURUTA, T., CHUNG, S. H., KOTAKI, H., SEKI, K., SUDO, K., AKIRA, S., ADACHI, Y., OHNO, N., KINJO, T., NAKAMURA, K., KAWAKAMI, K. & IWAKURA, Y. 2007. Dectin-1 is required for host defense against Pneumocystis carinii but not against Candida albicans. *Nat Immunol,* 8**,** 39-46.

SANCHO, D., JOFFRE, O. P., KELLER, A. M., ROGERS, N. C., MARTINEZ, D., HERNANZ-FALCON, P., ROSEWELL, I. & REIS E SOUSA, C. 2009. Identification of a dendritic cell receptor that couples sensing of necrosis to immunity. *Nature,* 458**,** 899-903.

SANCHO, D., MOURAO-SA, D., JOFFRE, O. P., SCHULZ, O., ROGERS, N. C., PENNINGTON, D. J., CARLYLE, J. R. & REIS E SOUSA, C. 2008. Tumor therapy in mice via antigen targeting to a novel, DC-restricted C-type lectin. *J Clin Invest,* 118**,** 2098-110.

SANCHO, D. & REIS E SOUSA, C. 2012. Signaling by myeloid C-type lectin receptors in immunity and homeostasis. *Annu Rev Immunol,* 30**,** 491-529.

SANO, H., KUROKI, Y., HONMA, T., OGASAWARA, Y., SOHMA, H., VOELKER, D. R. & AKINO, T. 1998. Analysis of chimeric proteins identifies the regions in the carbohydrate recognition domains of rat lung collectins that are essential for interactions with phospholipids, glycolipids, and alveolar type II cells. *J Biol Chem,* 273**,** 4783-9.

SCHAEFER, L., BABELOVA, A., KISS, E., HAUSSER, H. J., BALIOVA, M., KRZYZANKOVA, M., MARSCHE, G., YOUNG, M. F., MIHALIK, D., GOTTE, M., MALLE, E., SCHAEFER, R. M. & GRONE, H. J. 2005. The matrix component biglycan is proinflammatory and signals through Toll-like receptors 4 and 2 in macrophages. *J Clin Invest,* 115**,** 2223-33.

SCHRAML, B. U. & REIS E SOUSA, C. 2015. Defining dendritic cells. *Curr Opin Immunol,* 32**,** 13-20.

SCHRAML, B. U., VAN BLIJSWIJK, J., ZELENAY, S., WHITNEY, P. G., FILBY, A., ACTON, S. E., ROGERS, N. C., MONCAUT, N., CARVAJAL, J. J. & REIS E SOUSA, C. 2013. Genetic tracing via DNGR-1 expression history defines dendritic cells as a hematopoietic lineage. *Cell,* 154**,** 843-58.

SCHWARTZ-ALBIEZ, R., MONTEIRO, R. C., RODRIGUEZ, M., BINDER, C. J. & SHOENFELD, Y. 2009. Natural antibodies, intravenous immunoglobulin and their role in autoimmunity, cancer and inflammation. *Clin Exp Immunol,* 158 Suppl 1**,** 43-50.

SCOTT, C. C. & GRUENBERG, J. 2011. Ion flux and the function of endosomes and lysosomes: pH is just the start: the flux of ions across endosomal membranes influences endosome function not only through regulation of the luminal pH. *Bioessays,* 33**,** 103-10.

SHEN, L., SIGAL, L. J., BOES, M. & ROCK, K. L. 2004. Important role of cathepsin S in generating peptides for TAP-independent MHC class I crosspresentation in vivo. *Immunity,* 21**,** 155-65.

SHIMAOKA, M., TAKAGI, J. & SPRINGER, T. A. 2002. Conformational regulation of integrin structure and function. *Annu Rev Biophys Biomol Struct,* 31**,** 485-516.

SHIN, C., HAN, J. A., KOH, H., CHOI, B., CHO, Y., JEONG, H., RA, J. S., SUNG, P. S., SHIN, E. C., RYU, S. & DO, Y. 2015. CD8alpha(-) Dendritic Cells Induce Antigen-Specific T Follicular Helper Cells Generating Efficient Humoral Immune Responses. *Cell Rep,* 11**,** 1929-40.

SILVA, M. T. 2010. Secondary necrosis: the natural outcome of the complete apoptotic program. *FEBS Lett,* 584**,** 4491-9.

SILVERSTEIN, A. M. 1999. Paul Ehrlich's passion: the origins of his receptor immunology. *Cell Immunol,* 194**,** 213-21.

SOBANOV, Y., BERNREITER, A., DERDAK, S., MECHTCHERIAKOVA, D., SCHWEIGHOFER, B., DUCHLER, M., KALTHOFF, F. & HOFER, E. 2001. A novel cluster of lectin-like receptor genes expressed in monocytic, dendritic and endothelial cells maps close to the NK receptor genes in the human NK gene complex. *Eur J Immunol,* 31**,** 3493-503.

SOMERS, W. S., TANG, J., SHAW, G. D. & CAMPHAUSEN, R. T. 2000. Insights into the molecular basis of leukocyte tethering and rolling revealed by structures of P- and E-selectin bound to SLe(X) and PSGL-1. *Cell,* 103**,** 467-79.

STARR, T. K., JAMESON, S. C. & HOGQUIST, K. A. 2003. Positive and negative selection of T cells. *Annu Rev Immunol,* 21**,** 139-76.

STEINMAN, R. M. & BANCHEREAU, J. 2007. Taking dendritic cells into medicine. *Nature,* 449**,** 419-26.

STEINMAN, R. M. & COHN, Z. A. 1973. Identification of a novel cell type in peripheral lymphoid organs of mice. I. Morphology, quantitation, tissue distribution. *J Exp Med,* 137**,** 1142-62.

STEINMAN, R. M. & COHN, Z. A. 1974. Identification of a novel cell type in peripheral lymphoid organs of mice. II. Functional properties in vitro. *J Exp Med,* 139**,** 380-97.

STEINMAN, R. M. & HEMMI, H. 2006. Dendritic cells: translating innate to adaptive immunity. *Curr Top Microbiol Immunol,* 311**,** 17-58.

STEINMAN, R. M. & IDOYAGA, J. 2010. Features of the dendritic cell lineage. *Immunol Rev,* 234**,** 5-17.

STEWART, C. R., STUART, L. M., WILKINSON, K., VAN GILS, J. M., DENG, J., HALLE, A., RAYNER, K. J., BOYER, L., ZHONG, R., FRAZIER, W. A., LACY-HULBERT, A., EL KHOURY, J., GOLENBOCK, D. T. & MOORE, K. J. 2010. CD36 ligands promote sterile inflammation through assembly of a Toll-like receptor 4 and 6 heterodimer. *Nat Immunol,* 11**,** 155-61.

STOCKWIN, L. H., MCGONAGLE, D., MARTIN, I. G. & BLAIR, G. E. 2000. Dendritic cells: immunological sentinels with a central role in health and disease. *Immunol Cell Biol,* 78**,** 91-102.

SUZUKI, S., HONMA, K., MATSUYAMA, T., SUZUKI, K., TORIYAMA, K., AKITOYO, I., YAMAMOTO, K., SUEMATSU, T., NAKAMURA, M., YUI, K. & KUMATORI, A. 2004. Critical roles of interferon regulatory factor 4 in CD11bhighCD8alpha-dendritic cell development. *Proc Natl Acad Sci U S A,* 101**,** 8981-6.

SUZUKI-INOUE, K., FULLER, G. L., GARCIA, A., EBLE, J. A., POHLMANN, S., INOUE, O., GARTNER, T. K., HUGHAN, S. C., PEARCE, A. C., LAING, G. D., THEAKSTON, R. D., SCHWEIGHOFFER, E., ZITZMANN, N., MORITA, T., TYBULEWICZ, V. L., OZAKI, Y. & WATSON, S. P. 2006. A novel Syk-dependent mechanism of platelet activation by the C-type lectin receptor CLEC-2. *Blood,* 107**,** 542-9.

SWAMINATHAN, G. J., WEAVER, A. J., LOEGERING, D. A., CHECKEL, J. L., LEONIDAS, D. D., GLEICH, G. J. & ACHARYA, K. R. 2001. Crystal structure of the eosinophil major basic protein at 1.8 A. An atypical lectin with a paradigm shift in specificity. *J Biol Chem,* 276**,** 26197-203.

TABARANI, G., THEPAUT, M., STROEBEL, D., EBEL, C., VIVES, C., VACHETTE, P., DURAND, D. & FIESCHI, F. 2009. DC-SIGN neck domain is a pH-sensor controlling oligomerization: SAXS and hydrodynamic studies of extracellular domain. *J Biol Chem,* 284**,** 21229-40.

TAKEUCHI, O. & AKIRA, S. 2010. Pattern recognition receptors and inflammation. *Cell,* 140**,** 805-20.

TANNE, A., MA, B., BOUDOU, F., TAILLEUX, L., BOTELLA, H., BADELL, E., LEVILLAIN, F., TAYLOR, M. E., DRICKAMER, K., NIGOU, J., DOBOS, K. M., PUZO, G., VESTWEBER, D., WILD, M. K., MARCINKO, M., SOBIESZCZUK, P., STEWART, L., LEBUS, D., GICQUEL, B. & NEYROLLES, O. 2009. A murine DC-SIGN homologue contributes to early host defense against Mycobacterium tuberculosis. *J Exp Med,* 206**,** 2205-20.

TAYLOR, P. R., TSONI, S. V., WILLMENT, J. A., DENNEHY, K. M., ROSAS, M., FINDON, H., HAYNES, K., STEELE, C., BOTTO, M., GORDON, S. & BROWN, G. D. 2007. Dectin-1 is required for beta-glucan recognition and control of fungal infection. *Nat Immunol,* 8**,** 31-8.

TERMAN, J. R. & KASHINA, A. 2013. Post-translational modification and regulation of actin. *Curr Opin Cell Biol,* 25**,** 30-8.

TEWARY, P., YANG, D., DE LA ROSA, G., LI, Y., FINN, M. W., KRENSKY, A. M., CLAYBERGER, C. & OPPENHEIM, J. J. 2010. Granulysin activates antigen-presenting cells through TLR4 and acts as an immune alarmin. *Blood,* 116**,** 3465-74.

TIAN, W., NUNEZ, R., CHENG, S., DING, Y., TUMANG, J., LYDDANE, C., ROMAN, C. & LIOU, H. C. 2005. C-type lectin OCILRP2/Clr-g and its ligand NKRP1f costimulate T cell proliferation and IL-2 production. *Cell Immunol,* 234**,** 39-53.

TING, J. P., LOVERING, R. C., ALNEMRI, E. S., BERTIN, J., BOSS, J. M., DAVIS, B. K., FLAVELL, R. A., GIRARDIN, S. E., GODZIK, A., HARTON, J. A., HOFFMAN, H. M., HUGOT, J. P., INOHARA, N., MACKENZIE, A., MALTAIS, L. J., NUNEZ, G., OGURA, Y., OTTEN, L. A., PHILPOTT, D., REED, J. C., REITH, W., SCHREIBER, S., STEIMLE, V. & WARD, P. A. 2008. The NLR gene family: a standard nomenclature. *Immunity,* 28**,** 285-7.

TONEGAWA, S. 1983. Somatic generation of antibody diversity. *Nature,* 302**,** 575-81.

TOPF, M., LASKER, K., WEBB, B., WOLFSON, H., CHIU, W. & SALI, A. 2008. Protein structure fitting and refinement guided by cryo-EM density. *Structure,* 16**,** 295-307.

TRUMPFHELLER, C., LONGHI, M. P., CASKEY, M., IDOYAGA, J., BOZZACCO, L., KELER, T., SCHLESINGER, S. J. & STEINMAN, R. M. 2012. Dendritic cell-targeted protein vaccines: a novel approach to induce T-cell immunity. *J Intern Med,* 271**,** 183-92.

VABULAS, R. M., AHMAD-NEJAD, P., DA COSTA, C., MIETHKE, T., KIRSCHNING, C. J., HACKER, H. & WAGNER, H. 2001. Endocytosed HSP60s use toll-like receptor 2 (TLR2) and TLR4 to activate the toll/interleukin-1 receptor signaling pathway in innate immune cells. *J Biol Chem,* 276**,** 31332-9.

VAN DE WETERING, J. K., VAN GOLDE, L. M. & BATENBURG, J. J. 2004. Collectins: players of the innate immune system. *Eur J Biochem,* 271**,** 1229-49.

VANCE, R. E. 2000. Cutting edge: cutting edge commentary: a Copernican revolution? Doubts about the danger theory. *J Immunol,* 165**,** 1725-8.

VOEHRINGER, D., KOSCHELLA, M. & PIRCHER, H. 2002. Lack of proliferative capacity of human effector and memory T cells expressing killer cell lectinlike receptor G1 (KLRG1). *Blood,* 100**,** 3698-702.

VOLLMER, J., TLUK, S., SCHMITZ, C., HAMM, S., JURK, M., FORSBACH, A., AKIRA, S., KELLY, K. M., REEVES, W. H., BAUER, S. & KRIEG, A. M. 2005. Immune stimulation mediated by autoantigen binding sites within small nuclear RNAs involves Toll-like receptors 7 and 8. *J Exp Med,* 202**,** 1575-85.

VU MANH, T. P., BERTHO, N., HOSMALIN, A., SCHWARTZ-CORNIL, I. & DALOD, M. 2015. Investigating Evolutionary Conservation of Dendritic Cell Subset Identity and Functions. *Front Immunol,* 6**,** 260.

WACHSSTOCK, D. H., SCHWARTZ, W. H. & POLLARD, T. D. 1993. Affinity of alpha-actinin for actin determines the structure and mechanical properties of actin filament gels. *Biophys J,* 65**,** 205-14.

WAGNER, S. D. & NEUBERGER, M. S. 1996. Somatic hypermutation of immunoglobulin genes. *Annu Rev Immunol,* 14**,** 441-57.

WALDNER, H. 2009. The role of innate immune responses in autoimmune disease development. *Autoimmun Rev,* 8**,** 400-4.

WALKER, J. A., BARLOW, J. L. & MCKENZIE, A. N. 2013. Innate lymphoid cells--how did we miss them? *Nat Rev Immunol,* 13**,** 75-87.

WEIS, W. I., DRICKAMER, K. & HENDRICKSON, W. A. 1992. Structure of a C-type mannose-binding protein complexed with an oligosaccharide. *Nature,* 360**,** 127-34.

WEIS, W. I., KAHN, R., FOURME, R., DRICKAMER, K. & HENDRICKSON, W. A. 1991. Structure of the calcium-dependent lectin domain from a rat mannose-binding protein determined by MAD phasing. *Science,* 254**,** 1608-15.

WLODAWER, A., MINOR, W., DAUTER, Z. & JASKOLSKI, M. 2013. Protein crystallography for aspiring crystallographers or how to avoid pitfalls and traps in macromolecular structure determination. *FEBS J,* 280**,** 5705-36.

WOOD, J. L. 1974. pH-controlled hydrogen-bonding. *Biochem J,* 143**,** 775-7.

WRIGHT, J. R. 2004. Host defense functions of pulmonary surfactant. *Biol Neonate,* 85**,** 326-32.

XU, S., HUO, J., GUNAWAN, M., SU, I. H. & LAM, K. P. 2009. Activated dectin-1 localizes to lipid raft microdomains for signaling and activation of phagocytosis and cytokine production in dendritic cells. *J Biol Chem,* 284**,** 22005-11.

YAMASAKI, S., ISHIKAWA, E., SAKUMA, M., HARA, H., OGATA, K. & SAITO, T. 2008. Mincle is an ITAM-coupled activating receptor that senses damaged cells. *Nat Immunol,* 9**,** 1179-88.

YAN, S. D., CHEN, X., FU, J., CHEN, M., ZHU, H., ROHER, A., SLATTERY, T., ZHAO, L., NAGASHIMA, M., MORSER, J., MIGHELI, A., NAWROTH, P., STERN, D. & SCHMIDT, A. M. 1996. RAGE and amyloid-beta peptide neurotoxicity in Alzheimer's disease. *Nature,* 382**,** 685-91.

YANG, D., POSTNIKOV, Y. V., LI, Y., TEWARY, P., DE LA ROSA, G., WEI, F., KLINMAN, D., GIOANNINI, T., WEISS, J. P., FURUSAWA, T., BUSTIN, M. & OPPENHEIM, J. J. 2012. High-mobility group nucleosome-binding protein 1 acts as an alarmin and is critical for lipopolysaccharide-induced immune responses. *J Exp Med,* 209**,** 157-71.

YANG, H., ANTOINE, D. J., ANDERSSON, U. & TRACEY, K. J. 2013. The many faces of HMGB1: molecular structure-functional activity in inflammation, apoptosis, and chemotaxis. *J Leukoc Biol,* 93**,** 865-73.

YEO, K. J., HONG, Y. S., JEE, J. G., LEE, J. K., KIM, H. J., PARK, J. W., KIM, E. H., HWANG, E., KIM, S. Y., LEE, E. G., KWON, O. & CHEONG, H. K. 2014. Mechanism of the pH-induced conformational change in the sensor domain of the DraK Histidine kinase via the E83, E105, and E107 residues. *PLoS One,* 9**,** e107168.

YOO, S. K., STARNES, T. W., DENG, Q. & HUTTENLOCHER, A. 2011. Lyn is a redox sensor that mediates leukocyte wound attraction in vivo. *Nature,* 480**,** 109-12.

ZEHNER, M., MARSCHALL, A. L., BOS, E., SCHLOETEL, J. G., KREER, C., FEHRENSCHILD, D., LIMMER, A., OSSENDORP, F., LANG, T., KOSTER, A. J., DUBEL, S. & BURGDORF, S. 2015. The translocon protein sec61 mediates antigen transport from endosomes in the cytosol for cross-presentation to CD8(+) T cells. *Immunity,* 42**,** 850-63.

ZELENAY, S., KELLER, A. M., WHITNEY, P. G., SCHRAML, B. U., DEDDOUCHE, S., ROGERS, N. C., SCHULZ, O., SANCHO, D. & REIS E SOUSA, C. 2012. The dendritic cell receptor DNGR-1 controls endocytic handling of necrotic cell antigens to favor cross-priming of CTLs in virus-infected mice. *J Clin Invest,* 122**,** 1615-27.

ZELENAY, S. & REIS E SOUSA, C. 2013. Adaptive immunity after cell death. *Trends Immunol,* 34**,** 329-35.

ZELENSKY, A. N. & GREADY, J. E. 2003. Comparative analysis of structural properties of the C-type-lectin-like domain (CTLD). *Proteins,* 52**,** 466-77.

ZELENSKY, A. N. & GREADY, J. E. 2005. The C-type lectin-like domain superfamily. *FEBS J,* 272**,** 6179-217.

ZHANG, J. G., CZABOTAR, P. E., POLICHENI, A. N., CAMINSCHI, I., WAN, S. S., KITSOULIS, S., TULLETT, K. M., ROBIN, A. Y., BRAMMANANTH, R., VAN DELFT, M. F., LU, J., O'REILLY, L. A., JOSEFSSON, E. C., KILE, B. T., CHIN,

W. J., MINTERN, J. D., OLSHINA, M. A., WONG, W., BAUM, J., WRIGHT, M. D., HUANG, D. C., MOHANDAS, N., COPPEL, R. L., COLMAN, P. M., NICOLA, N. A., SHORTMAN, K. & LAHOUD, M. H. 2012. The dendritic cell receptor Clec9A binds damaged cells via exposed actin filaments. *Immunity,* 36**,** 646-57.

ZHANG, S. M., ADEMA, C. M., KEPLER, T. B. & LOKER, E. S. 2004. Diversification of Ig superfamily genes in an invertebrate. *Science,* 305**,** 251-4.

Appendix

Hanč et al., 2015. Structure of the Complex of F-Actin and DNGR-1, a C-Type Lectin Receptor Involved in Dendritic Cell Cross-Presentation of Dead Cell-Associated Antigens. *Immunity,* 42(5), 839–49